CHEMICAL REVIEWS

Review

pubs.acs.org/CR

Dispersion-Corrected Mean-Field Electronic Structure Methods

Stefan Grimme,* Andreas Hansen, Jan Gerit Brandenburg, and Christoph Bannwarth

Mulliken Center for Theoretical Chemistry, Universität Bonn, 53113 Bonn, Germany

ABSTRACT: Mean-field electronic structure methods like Hartree−Fock, semilocal density functional approximations, or semiempirical molecular orbital (MO) theories do not account for long-range electron correlation (London dispersion interaction). Inclusion of these effects is mandatory for realistic calculations on large or condensed chemical systems and for various intramolecular phenomena (thermochemistry). This Review describes the recent developments (including some historical aspects) of dispersion corrections with an emphasis on methods that can be employed routinely with reasonable accuracy in large-scale applications. The most prominent correction schemes are classified into three groups: (i) nonlocal, density-based functionals, (ii) semiclassical C_6-based, and (iii) one-electron effective potentials. The properties as well as pros and cons of these methods are critically discussed, and typical examples and benchmarks on molecular complexes and crystals are provided. Although there are some areas for further improvement (robustness, many-body and short-range effects), the situation regarding the overall accuracy is clear. Various approaches yield long-range dispersion energies with a typical relative error of 5%. For many chemical problems, this accuracy is higher compared to that of the underlying mean-field method (i.e., a typical semilocal (hybrid) functional like B3LYP).

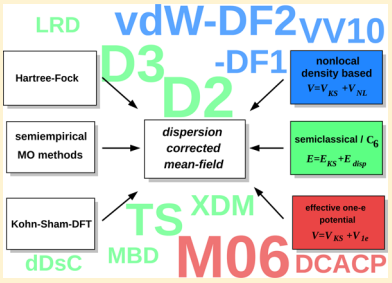

CONTENTS

1. INTRODUCTION

Mean-field (MF) electronic structure methods like Hartree−Fock (HF), approximate, semilocal Kohn−Sham density functional theory (KS-DFT), and semiempirical molecular orbital (SE-MO) theory are widely used in chemistry and physics, particularly for large systems. These methods do not describe long-range electronic correlation effects, and hence they cannot account for so-called London dispersion interactions.[1−5] The development of appropriate dispersion corrections to cure this deficiency is a very active and practically relevant field of theoretical research. The increased attention to this topic in the past few years is directly reflected in the growing number of citations found in the field of *dispersion correction* or *van der Waals + density functional theory* (see Figure 1). This Review shall report

Special Issue: Noncovalent Interactions

Received: September 11, 2015

DOI: 10.1021/acs.chemrev.5b00533
Chem. Rev. XXXX, XXX, XXX−XXX

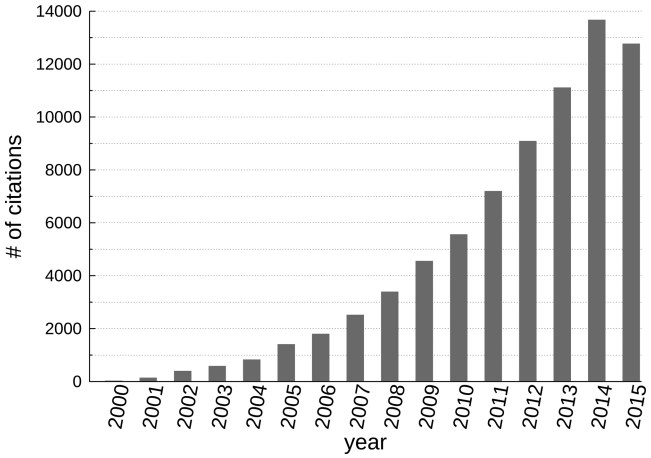

Figure 1. Number of citations found on the Web of Science[6] in the time period from 2000 through 2015 for papers on "dispersion correction" or "density functional theory" + "van der Waals".

on dispersion corrections for MF approaches that have been developed and applied in the last few years. For related works with some review character, see refs 7−16.

Dispersion interactions can be empirically defined as the attractive part of a van der Waals (vdW)-type interaction potential between atoms or molecules that are not directly (covalent or ionic) bonded to each other. They are prominently mentioned in the very first quantum chemistry textbook by Hellmann.[17] In the current literature, the terms "dispersion" and "vdW" are often used synonymously. The attribute dispersive should be avoided in this context because it has various other meanings in science. According to a more precise definition, London dispersion interactions result from relatively long-ranged electron correlation effects in any many-electron system that neither requires "polarity" nor wave function (WF) overlap (see section 5 for a discussion on the distance regime relevant for London dispersion). They involve coupled local components and can be explained in a stationary, time-independent electronic state picture. Already in 1930,[1] from the simplest perturbation theory Eisenschitz and London have derived the famous asymptotic formula for the dispersion energy between two atoms A and B at large distance R

$$E_{\mathrm{disp}}^{AB} \approx -\frac{3}{2}\frac{I_A I_B}{I_A + I_B}\alpha_A^0 \alpha_B^0 R^{-6} = -C_{6,\mathrm{approx}}^{AB} R^{-6} \quad (1)$$

where α^0 is the static dipole polarizability and I is the atomic ionization potential. The atomic constants can be condensed to the pair-specific C_6 dispersion coefficient, which determines the strength of the interaction. Note that E_{disp} is attractive for any distance and hence stabilizes molecules with respect to their constituting atoms, condensed phases over the (diluted) gas phase, and in general more dense structures and materials. The well-established London formula represents a central element in the correction schemes discussed herein. Quantum chemical methods to compute the C_6 and higher-order dispersion coefficients are briefly discussed in section 4. Note that there is no consensus in the literature if the sign in the above equation should be stated explicitly (and hence the C_6 would be positive) or if it is included in the coefficients. In any case, the long-range dispersion energy as an electron correlation effect is always an energy-lowering (negative) quantity. In this Review, we adopt the former variant, i.e., with C_6 being a positive quantity.

It has now become very clear, especially for the chemistry and physics of large or condensed-phase systems, e.g., in bio- or nanoarchitectures, that inclusion of these interactions in theoretical simulations is indispensable in order to reach chemical accuracy (∼1 kcal/mol). Classical, atomistic force-fields have treated these interactions from the very beginning, for example, by interatomic Lennard-Jones type 6−12 potentials. For a recent overview on various calculation methods for large systems, see ref 18. Because dispersion effects are due to ubiquitous electron correlation, they also influence the accuracy of theoretical (reaction) thermodynamics.[19] See ref 20 for a recent review on dispersion effects from a chemical/catalysis point of view. They are, of course, most important when aiming at a good description of intermolecular, noncovalent interactions (NCIs), and this is also historically the origin of the field. However, here we will pursue a more general picture of dispersion effects as outlined in the next section and illustrated with examples in section 5.

If perturbation theory is applied to the electrons of interacting atoms,[4,21] two distance regimes can be identified (Figure 2). At

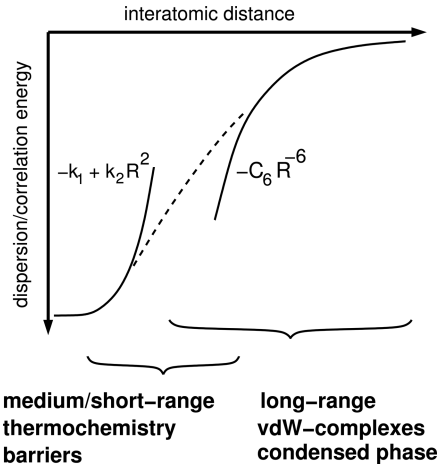

Figure 2. Qualitative behavior of the correlation energy at short distances R (unified atom limit) and asymptotically for large distances, where it is termed interatomic (molecular) London dispersion energy (k_1, k_2, and C_6 are system-specific constants). The dashed line depicts the interpolation that is used in many correction methods and indicates the medium-range correlation/dispersion range of ∼2.5−3.5 Å. Reprinted with permission from ref 14. Copyright 2014 Wiley-VCH.

large distances, the dispersion energy is given by the well-known $-1/R^6$ dependence on the interaction distance. Note that the C_6 dispersion coefficient can refer to atoms as well as entire systems (molecules) because it is derived from a centered multipole expansion. In this long-distance region, London dispersion can be considered as the attractive part of a typical Lennard-Jones (model) potential. According to a less well-known analysis,[21] at small distances, the dispersion energy becomes constant and part of the normal correlation energy (as first used in a correction scheme by Becke and Johnson[22]). The currently established notion is that the dispersion energy is a continuous quantity representing a meaningful concept for all values of R (i.e., including the dashed line in Figure 2). It can be expected that in intermediate regions it influences the electronic energy of molecules significantly and hence has to be considered in computational thermochemistry. Note that it is defined not only for the intermolecular/interatomic situation but also for the interaction of intramolecular fragments (functional groups)

DOI: 10.1021/acs.chemrev.5b00533
Chem. Rev. XXXX, XXX, XXX−XXX

because of the locality of electronic structure for most chemical systems (i.e., large gap systems with a sparse one-particle density matrix).[23] This leads to the concept of intramolecular dispersion energy. A more concrete chemical example for the different correlation length scales is given in section 5, for a discussion of dispersion effects on molecular structure where the short-range part is also relevant; see ref 24.

The scope of this Review is methods that introduce dispersion interactions into MF methods (see Figure 3), their historical

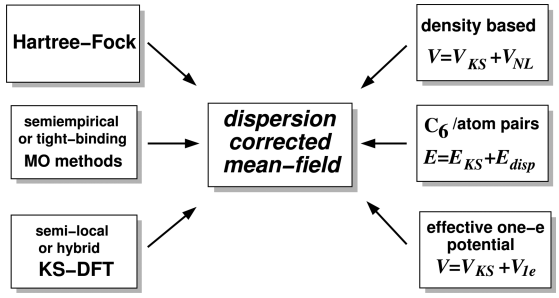

Figure 3. Overview about dispersion-correction strategies to mean-field quantum chemical methods.

development, and their physical/theoretical context. The currently more widely used, practical, and robust approaches are in the focus here. Dispersion corrections are nowadays mostly applied in the framework of KS-DFT. For a more general discussion about status, accuracy, and further problems of KS-DFT in chemistry, see refs 25−28. Although KS-DFT is, in principle, an exact theory that of course includes dispersion (electron correlation), in its current approximate state it behaves more like Hartree−Fock in this respect. We use the term "DFT" synonymously for approximate KS-DFT in this work as it is common in the current literature. Because KS-DFT is a single-determinant, orbital-based scheme, it is considered here as a MF method even though a considerable amount of electron correlation effects are covered. DFT-related virtual orbital-dependent methods such as the random phase approximation (RPA)[29] or fragment-based methods like symmetry-adapted (intermolecular) perturbation theory DFT-SAPT[30,31] (see ref 32 for a related approach) are, however, only mentioned shortly in section 2 but are mostly excluded from the discussion. They either are not completely general (not applicable to the intramolecular case), are still at some kind of preliminary development stage (e.g., no analytical gradients are available), or are currently not applicable to very large systems (roughly defined by >1000 atoms to which MF methods are applicable). The applicability to very large systems is actually one of the key advantages of MF approaches: the scaling behavior of the computation time with the system size is much better (formally $O(N^4)$, practically $O(N^2)$ to $O(N^3)$, where N is the number of electrons) compared to correlated WF theory (WFT) methods. Furthermore, MF approaches converge significantly faster to the complete basis set (CBS) limit,[33] and basis set superposition and incompleteness errors are generally smaller. This allows for calculations already close to the CBS limit with polarized quadruple-ζ (QZ) basis sets or allows one to employ smaller basis sets in combination, e.g., with empirical basis set superposition error (BSSE) absorbing potentials (atom pair-wise[34] as well as effective core potentials (ECP)[35] are available). Remarkable steps toward (near) linear scaling variants of correlated WF methods have been taken in recent years;[23,36−39] however, their slow convergence to the CBS limit still persists. The correlated WF method with lowest scaling (formally $O(N^5)$) is second-order Møller−Plesset perturbation theory (MP2).[40] A modified variant (scaled opposite-spin MP2)[41] exists that scales with $O(N^4)$. Even at the CBS limit, however, MP2 performs badly for dispersion-dominated interactions,[42−44] in particular for chemically unsaturated systems. The reason for this is that the dispersion energy contribution to the supermolecular MP2 energy lacks intramolecular correlation effects and therefore describes the long-range correlation energy on the so-called uncoupled level (see below). For association reactions of two separate species (eq 9), this situation could be remedied by replacing the MP2 dispersion contribution with coupling-inclusive terms from time-dependent HF[42] or time-dependent DFT (the latter yielding the MP2C approach[45]). These methods unfortunately require the definition of separate fragments and are consequently not generally applicable. To arrive at a generally applicable MP2-based approach, range separation of the correlation energy into short- and long-range parts is possible (similar to Figure 2).[46] Another workable approach is to introduce different scalings of the same-spin and opposite-spin components in MP2[47] including further developed variants thereof.[48] Recently, MP2 correlation at short range has been combined with a dispersion correction originally developed for MF approaches, which then describes the correlation at long range.[49,50] Such methods are beyond the focus of this Review. However, one should be aware of the fact that, for an accurate description of dispersion interactions, cost-efficient correlated WF methods require modifications at long range as well, notwithstanding the mentioned slower convergence to the CBS limit. Consequently, in the foreseeable future, MF approaches (in particular sophisticated DFT methods) will be the only reasonable choice to routinely conduct gradient calculations on large systems with >100 atoms.

According to Figure 3, the corrections considered herein can be classified into three groups: nonlocal density-based (which mostly include a correction to the electronic potential V), semiclassical (C_6-based) schemes (which often apply corrections only to the total energy E), and effective one-electron potentials. Almost all of the current dispersion corrections include empirical elements in various ways. Hence, solid benchmarking on reliable experimental or high-level theoretical reference data is mandatory. For the inter- and intramolecular interactions and mostly main-group thermochemistry considered here, the current gold standard in quantum chemistry is the WF-based singles and doubles coupled-cluster method with perturbative triples (CCSD(T)), which yields accurate results of benchmark quality (<1 kcal/mol error for typical chemical reactions or <1% relative error, respectively, for molecules of up to ∼50 atoms whose electronic structure is dominated by a single Slater determinant in the wave function).[51,52] The use of theoretical benchmark values has the advantage that dynamic, thermal, and solvation effects are excluded, and direct comparisons for the same fixed (or equilibrium, respectively) structure are made. Therefore, this is the preferred approach pursued here.

The Review is organized as follows: the next section provides basic information about the theory and properties of the considered MF methods and their behavior in the field of noncovalent interactions. Section 3 gives a historical overview about the development of dispersion corrections spanning ∼30 years from the 1970s to the early 2000s. Section 4 provides a

DOI: 10.1021/acs.chemrev.5b00533
Chem. Rev. XXXX, XXX, XXX−XXX

comprehensive picture of all types of modern dispersion corrections including recent uncorrected density functionals. This part emphasizes recommended methods for typical applications. We furthermore make some remarks on treatments for periodic (solid) systems, although our overall focus is clearly on molecules. In section 5 we will illustrate the achievable accuracy for intermolecular interactions in small- to large-sized complexes, intramolecular dispersion effects on conformational energies, and some prototypical chemical reaction energies.

2. SETTING THE STAGE

As already mentioned, this Review considers only a selection of important and widely used quantum chemical methods. They have in common that they are based on a single-determinant wave function Ψ composed of single-particle functions (orbitals) φ_i (electron spin indices are neglected in the following). In the case of KS-DFT, this object has some auxiliary character and is called Kohn−Sham (KS) determinant, while in WF theory it is termed Slater determinant. The unknown orbitals are obtained by solving

$$\left[-\frac{1}{2}\nabla_i^2 + \sum_A \frac{Z_A}{|\mathbf{R}_A - \mathbf{r}_1|} + \int \frac{\rho(\mathbf{r}_2)}{|\mathbf{r}_1 - \mathbf{r}_2|} + V_{\mathrm{XC}}[\rho]\right]\varphi_i(\mathbf{r}_1) = \hat{h}_{\mathrm{KS}}\varphi_i(\mathbf{r}_1) = \epsilon_i\varphi_i(\mathbf{r}_1) \quad (2)$$

with the kinetic energy operator, nuclear-electron interaction and Coulomb (Hartree), and exchange-correlation (XC) potentials. Semiempirical (also called tight-binding) molecular orbital (SE-MO) theories discussed herein employ, instead of the formally exact effective one-electron Kohn−Sham operator $\hat{h}_{\mathrm{KS}}$, an appropriately modified semiempirical approximation $\hat{h}_{\mathrm{SE}}$, although they basically solve the same one-particle equation (eq 2). The SE-MO approaches typically apply drastic simplifications in the linear combination of atomic orbitals (LCAO) expansion of the orbitals φ (minimal AO basis set) and electronic potentials appearing in $\hat{h}_{\mathrm{SE}}$. From here on we will denote electron coordinates by small r while interatomic or interfragment distances will be represented by capitalized R. If not stated otherwise, atomic units are used throughout this Review.

The crucial term in KS-DFT is the XC potential given as the functional derivative of the exchange-correlation energy

$$V_{\mathrm{XC}}[\rho] = \delta E_{\mathrm{XC}}[\rho]/\delta\rho \quad (3)$$

with respect to the electron density ρ. Various approximations for E_{XC} have been proposed over the years; see ref 28 for a recent review. In the case of HF, the electron-correlation part is missing and the exchange term is given by the nonlocal exchange-operator $\hat{K}$ (termed Fock exchange here)

$$\hat{K}_j(\mathbf{r}_1)\varphi_i(\mathbf{r}_1) = \int \mathrm{d}\mathbf{r}_2 \frac{\varphi_j(\mathbf{r}_2)\varphi_i(\mathbf{r}_2)}{|\mathbf{r}_1 - \mathbf{r}_2|}\varphi_j(\mathbf{r}_1) \quad (4)$$

Hybrid functionals (global hybrids like B3LYP,[53,54] local hybrids,[55,56] or range-separated hybrids[57]) mix in various ways semilocal density functional (DF) approximations with nonlocal Fock exchange. The most common way is the global approach introduced by Becke,[58]

$$E_{\mathrm{XC}} = (1 - a_x)E_X^{\mathrm{GGA}} + a_x E_X^{\mathrm{Fock}} + E_C^{\mathrm{GGA}} \quad (5)$$

where a_x is an empirical mixing parameter with $0 < a_x < 1$, E_X^{GGA} represents a semilocal DF approximation, and E_X^{Fock} is the Fock exchange energy obtained by applying $\hat{K}$ to the KS (but not HF) orbitals. If the correlation part is neglected (which is a reasonable first approximation because the exchange energy is an order of magnitude larger than the correlation energy on an absolute scale), eq 5 allows one to linearly interpolate between HF and KS-DFT. Numerical calculations indeed show that many molecular properties as well as electronic and geometric structures often depend linearly on the amount of nonlocal Fock exchange mixing.[59]

All methods mentioned above (HF, KS-DFT, SE-MO) have in common that a set of N one-particle functions (or $N/2$ in the restricted closed-shell case) for the considered N electrons are optimized and that the total energy depends exclusively on the so-called occupied orbitals. The functions that are left over in the variational optimization are usually called virtual orbitals. They contain information about excitation energies and the response of the system with respect to external (electromagnetic in our case) perturbations. This is exploited in WF theories of electron correlation where virtual orbitals are used to construct an improved WF by inclusion of excited determinants.[33] However, neither virtual orbitals nor nonlocal density information is used in any MF approach considered here, and hence long-range London dispersion interactions are missing.

This failure is easily understood by considering the true wave function based origin of the dispersion energy. For example, in second-order Møller−Plesset (MP) perturbation theory (PT),[40] the correlation energy is given by the Coulomb and exchange interactions of single-electron transition densities centered on interacting fragments A and B,

$$E_{\mathrm{corr}}^{AB} = -\sum_{ia}\sum_{jb} \frac{(ia|jb)[(ia|jb) - (ib|ja)]}{\epsilon_a + \epsilon_b - \epsilon_i - \epsilon_j} \quad (6)$$

where the sum is over all possible single particle-hole excitations between orbitals $i \rightarrow a$ (localized on A) and $j \rightarrow b$ (on B), $(ia|jb)$ is a two-electron integral, and ϵ are the corresponding orbital energies. The superscript AB denotes a second-order or two-body treatment, which provides only pairwise additive dispersion energies (see below). This is also illustrated schematically in Figure 4. Note that A and B do not necessarily refer to clearly separated atoms or molecules but can also be molecular fragments leading to intramolecular dispersion effects. The induced dipole moment on one of the fragments has its origin in charge fluctuations on the other, but this simultaneous process is better viewed as instantaneous electron correlation. In a more precise picture, electromagnetic zero-point energy fluctuations in the vacuum lead to virtual excitations to atomic or molecular electronic states. The corresponding transition densities interact electrostatically with exchange-type modifications at smaller distances. They are not represented by HF or conventional (hybrid) functionals that only consider electron exchange but do not employ virtual orbitals (i.e., use electronic charge and occupied orbitals but no transition density). It is noted that dispersion is transmitted by electromagnetic radiation at the finite speed of light while the interacting electrons move. This leads to small so-called retardation effects that appear for very distant fragments.[60] However, due to their insignificance in molecular systems, these are not discussed further.

Dispersion interactions are most important for a quantitative description and qualitative understanding of noncovalent interactions (NCIs). To put the properties of the MF electronic structure methods into a broader perspective, we briefly describe the symmetry-adapted perturbation theory (SAPT[30,31]) picture

DOI: 10.1021/acs.chemrev.5b00533
Chem. Rev. XXXX, XXX, XXX−XXX

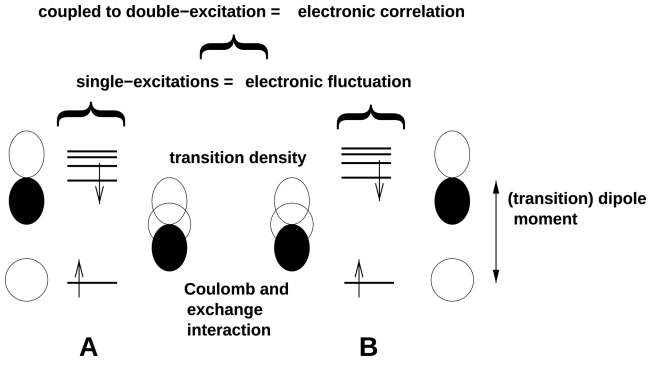

Figure 4. Schematic description of the dispersion interaction for two interacting fragments *A* and *B* (e.g., helium atoms with a ground state doubly occupied 1s orbital and virtual 2p3p4p··· orbitals) at large distance. Transitions from the 1s orbital to the *n*p orbitals lead to nonvanishing transition dipoles if the transition densities are expressed in a multipole expansion. Hence, this simplified picture is only valid in the latter case. Excitations to *n*d orbitals would lead to higher-order dipole−quadruple, quadrupole−quadrupole, etc. dispersion interactions while s−*n*s transitions are electrically forbidden and do not appear in the dispersion-energy expressions. Reprinted with permission from ref 11. Copyright 2011 Wiley-VCH.

of noncovalent interactions. Normally, MF methods employ a supermolecular computation of the interaction energy ΔE_{AB},

$$\Delta E_{AB} = E(AB) - E(A) - E(B) \tag{7}$$

where $E(AB)$ and $E(A)/E(B)$ refer to the complex and noninteracting fragment total energies, respectively. This approach is rather general but has the disadvantage that the result can be contaminated by the basis set superposition error (BSSE) and that no insight into the nature of the interaction is obtained.[61] On the other hand, SAPT applies PT starting with unperturbed monomer WFs (HF or KS-DFT) and a double-perturbation scheme in the monomer correlation and the intermolecular interaction $\hat{V}$,

$$\hat{H} = \hat{F} + \hat{W} + \hat{V} \tag{8}$$

where $\hat{F}$ is the (KS-)Fock operator and $\hat{W}$ is the MP perturbation in the case of HF. Note that the standard Rayleigh−Schrödinger PT cannot be applied at short distances because of non-negligible exchange interactions, i.e., the (antisymmetrized) fragment product states are not eigenstates of the zeroth order Hamiltonian. These difficulties are well-documented in the literature.[1,62−67] Although ignoring the antisymmetry at short range can lead to unphysical states that do not satisfy the Pauli principle, one can carry out a nonstandard perturbation treatment working with both the antisymmetric and unsymmetric product functions.[1] The above double perturbation on the basis of MF models has been proposed and refined by several groups.[68−74]

The result of SAPT are the components of the interaction (denoted normally without Δ symbol) in various orders $E_{es}^{(1j)}$, $E_{EXR}^{(1j)}$, $E_{ind}^{(2j)}$, and $E_{disp}^{(2j)}$ with coupling terms $E_{EXR-ind}^{(2j)}$, $E_{EXR-disp}^{(2j)}$, and $E_{ind-disp}^{(3j)}$, where the indices denote the order in the corresponding perturbation (*j* refers to the intramolecular perturbation). This is often condensed to the following working equation:

$$\Delta E_{AB} = E_{EXR} + E_{es} + E_{ind} + E_{disp} \tag{9}$$

Here, "EXR" refers to the Pauli-exchange repulsion term, "es" denotes the electrostatic interaction of unperturbed monomers, "ind" indicates their induction (polarization) contribution, and "disp" is the London dispersion energy. The last two terms are of second-order type and hence involve the response of at least one fragment. Note that similarly to the MP2 dispersion energy (eq 6), all orders in the SAPT expansion have a charge penetration as well as an exchange counterpart. The corresponding exchange-dispersion contribution is not explicitly treated by any of the methods presented here, but it decays exponentially with the fragment separation and the error is assumed to be small. Detailed analysis of MF methods with this theory shows that HF includes $E_{EXR} + E_{es} + E_{ind}$ terms for uncorrelated monomers to infinite order but completely lacks the second (and higher)-order E_{disp} terms.[75,76] A similar behavior can be expected for approximate semilocal or hybrid DFT with the difference being that the monomer description is partially "correlated" (mainly affecting the $E_{es} + E_{ind}$ terms) and that the electron density decay is slightly different (influencing mainly E_{EXR}). Due to the approximate character of currently used XC functionals, particularly the short-range repulsive behavior (and its interplay with the attractive components) is considerably different for HF and various typical DFs. This is illustrated for the simple case of two argon atoms in Figure 5a.

As can be seen from comparison to the reference CCSD(T) curve (Figure 5a), all dispersion-devoid MF methods (HF, B3LYP, and PBE) are over-repulsive and the energy ordering is HF > B3LYP > PBE > CCSD(T). Dispersion corrections should properly correct this behavior not only in the equilibrium and large-distance regime (here >3.5 Å) but also for short interatomic

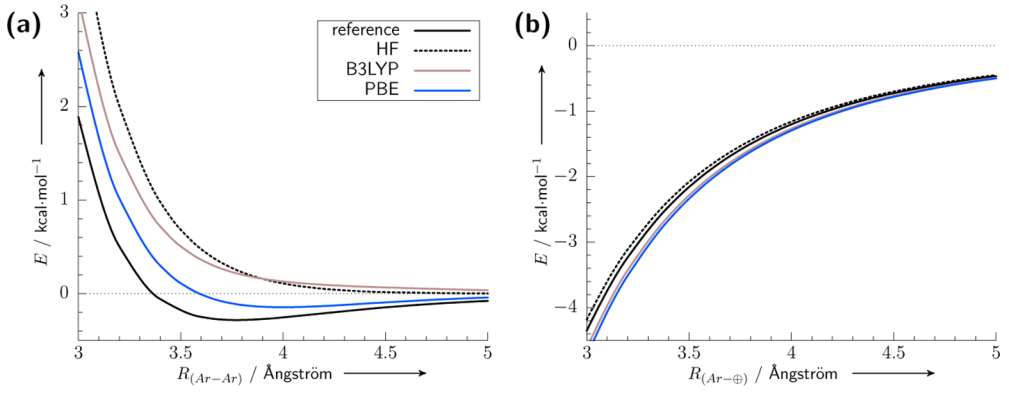

Figure 5. Computed (aug-cc-pV5Z AO basis) potential energy curves for (a) two interacting Ar atoms and (b) an Ar atom interacting with a positive point charge.

DOI: 10.1021/acs.chemrev.5b00533
Chem. Rev. XXXX, XXX, XXX−XXX

distances that occur in "real" systems, for example, in strained molecular systems or under high-pressure conditions. In fact, HF and B3LYP yield a completely unbound Ar_2 complex contrary to what is obtained at the reference level (R_e = 3.78 Å with a D_e of 0.28 kcal/mol).

Part b of the figure shows the induction energies of the same methods when an Ar atom is perturbed by a point charge. As a stabilizing, second-order property, the induction energy E_{ind} is also considerably influenced by the monomer electronic excitation energies. These are generally lower for DF than for HF,[77] which explains the observed order for E_{ind}: HF > CCSD(T) > B3LYP > PBE. Note the overestimated polarizability for both DFs, which in fact perform worse than HF. However, the too low induction energy with approximate DFs partially cancels the too repulsive E_{EXR} part so that, at least for polar systems, relatively good NCIs can result (if dispersion is properly accounted for by additional corrections). This is in fact a fundamental reason for the relatively accurate NCI energies computed by dispersion-corrected DFT, which is documented in more detail in section 5. The above picture is consistent with the results of a recent study of three-body (nonadditive) effects on NCIs in typical organic complexes.[78]

DFT-SAPT is an ideal tool for distinguishing the different types of interactions contributing to the noncovalent binding. Another related approach that allows for a similar decomposition is the effective fragment potential (EFP) method.[79] In Figure 6,

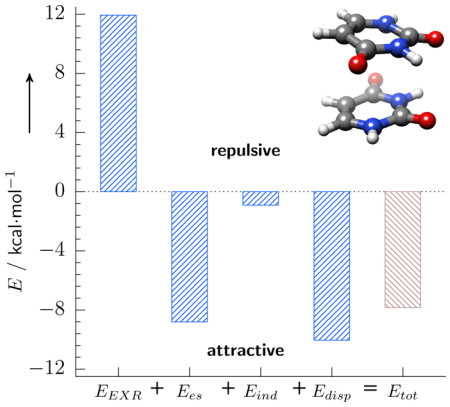

Figure 6. Contributions to the binding of a π-stacked uracil dimer calculated with DFT-SAPT via the asymptotically corrected AC-PBE0 functional. Here, the PBE0 potential is shifted to reproduce the correct ionization potential of the uracil monomer. The first-order contributions are the exchange repulsion E_{EXR} and the electrostatic E_{es}; the second-order induction E_{ind} and dispersion E_{disp} include the mixed exchange type contributions as well.

we exemplify this decomposition for DFT-SAPT on the π-stacked uracil dimer for which the corresponding first-order exchange repulsion E_{EXR} and electrostatic E_{es} and the second-order induction E_{ind} and dispersion E_{disp} interactions are shown. As usual, the exchange repulsion is the largest (and often the only) repulsive contribution. The electrostatic and dispersion terms are of similar magnitude. Apparently, the London dispersion is a very important interaction in this system, and its accurate description is mandatory for accurate quantum chemical predictions.

The dispersion energy (like the other NCI energy components in eq 9) has many-body nonadditive components that are not covered by the purely atomic or molecular pairwise treatments as in eq 1. This means, in the simplest example, that an atomic or molecular trimer *ABC* does not have the interaction energy as given by the sum of the three dimer energies *AB*, *AC*, and *BC*. We give a summary of this topic following the clear and comprehensive description by Dobson.[80] In his work he introduced three types of dispersion nonadditivity, defined in general as the departure of the dispersion interaction from a sum of gas-phase based C_n terms between pairs of previously selected "centers" (usually atoms). These categories are termed type-A, type-B, and type-C nonadditivity, respectively.

The type-A case refers to the change of the pairwise dispersion coefficient for the free atoms C_n^{AB} when they are bound in a molecule to other atoms. This change (typically a decrease) in the corresponding "atom-in-molecule" dispersion coefficient is caused by bonding (increase in atomic excitation energies); crowding of orbitals, which effectively causes a reduction of atomic volume, and, consequently, the atomic polarizability (see ref 14 for a numerical overview for almost all atoms in the periodic table). This type-A category was ignored in all early dispersion-correction schemes (see section 3) and was often dealt with semiempirically, for example, by choosing the optimal coefficients through minimization of the error of the pairwise calculation relative to accurate molecular-binding energies of a dispersion-bonded training set.[81,82] All modern pairwise corrections like the XDM model,[22,83,84] the D3 scheme,[85] or Tkatchenko and Scheffler's (TS) approach[86] include type-A effects by making the coefficients dependent on atom-in-molecule multipole moments (XDM), geometric coordination number (D3), or an atomic volume (TS), respectively.

In contrast to the type-A case, type-B effects are nonadditive in a strict sense. They occur because an additional polarizable center *C* can effectively screen the Coulomb interaction between a given pair of centers *AB*, thus altering their pairwise correlation energy and the total dispersion energy of the trimeric system. The lowest-order triple-dipole term leads, in the isotropic case, to a three-center angularly and $R_{AB}^{-3}R_{AC}^{-3}R_{BC}^{-3}$ dependent interaction energy often dubbed the Axilrod−Teller−Muto interaction (see section 4.1 for more details). In a diagrammatic representation, an infinite number of further terms (ring diagrams) like this arise from multiple response function insertions into all possible Coulomb interaction lines, leading to *N*-center contributions. Note that the terminology in the literature regarding nonadditivity is not fully consistent. Dobson defines the type-B nonpairwise interaction as present between more than two atomic centers, and this definition is adopted in the many-body-dispersion (MBD) scheme of Tkatchenko and co-workers.[87] It could, however, also refer to the number of Coulomb-lines, i.e., correlating electrons. In WF theory description, type-B effects are *not* captured by pairwise theories like MP2 or SAPT2 but require at least coupling of first-order perturbed WF as in MP3, or to infinite order as in RPA or CCSD. Nonlocal density-dependent dispersion corrections like vdW-DF2[88] or VV10[89] described in section 4.2 also do *not* account for type-B effects. Semilocal density functional approximations (DFAs) provide short-range many-body XC effects, but their magnitude and even their sign strongly depend on the particular functional. The general agreement with CCSD(T) reference data for rare gas (RG) triatomics is found to be insufficient.[90,91]

Atom or fragment-based approaches assume an inherently localized electronic structure, i.e., that electrons can be ascribed to centers of fragments. On the contrary, type-C nonadditivity is an intrinsically quantum phenomenon that occurs in cases of (near) degeneracy and strong electronic delocalization. This causes zero-energy denominators in perturbation theory and

DOI: 10.1021/acs.chemrev.5b00533
Chem. Rev. XXXX, XXX, XXX−XXX

favors large electronic response and electron density fluctuations. Such situations occur in metals, and perhaps the most striking consequence of type-C effects is the quite different and slower spatial decay of the asymptotic interaction energy between gapless objects separated by a distance D (e.g., $E \propto D^{-3}$ for parallel graphene sheets[92]), which cannot be obtained by any atom pairwise scheme. The nonlinear size-dependence of the interaction energy of differently sized fullerenes, which have a highly delocalized electronic structure, is also a consequence of type-C dispersion effects. Note, however, that they are only really significant for conjugated system of substantial size (e.g., a few hundred carbon atoms) and that, for example, C_{60} containing vdW complexes are relatively well (but not very accurately)[93] described by pairwise approaches.[95] The nonadditivity of vdW interactions in nanostructures has been analyzed by models that recover the exact zero- and high-frequency limits. The resulting size dependencies of the nonadditive contributions can both increase and decrease the interaction depending on the system.[96,97]

In Figure 7, we sketch the long-range perturbation theory of intermolecular interactions as used in all modern London

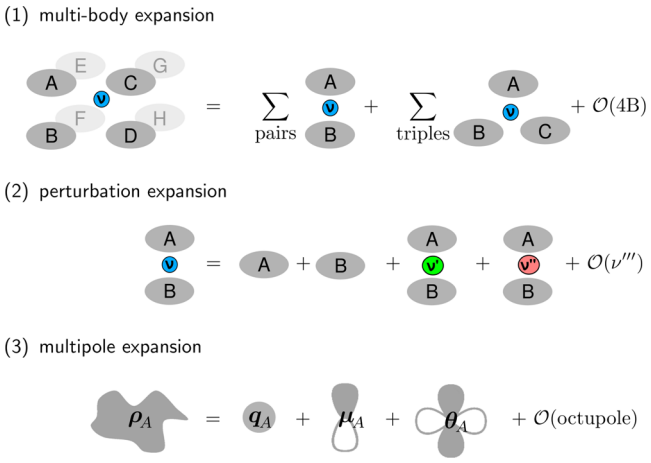

Figure 7. Three main approximations used in the long-range perturbation theory of interfragment interactions. This is the foundation of all modern London dispersion corrections, which treat the expansions to various orders. Here, the blue ν represents the noncategorized perturbation, while the green ν' and the red ν'' correspond to induction (excitations only within one fragment) and dispersion (excitations within both fragments) interactions, respectively. ρ_A is the electron density on fragment A, q_A is the monopole, μ_A the dipole, and θ_A is the quadrupole term arising from the multipole expansion of the Coulomb potential due to the electrons on A.

dispersion approximations. For a system of interacting fragments (A, B, C, ...) with nonoverlapping electron densities, these approximations are (1) the interaction is decomposed into additive multibody interactions, (2) the interaction is treated perturbatively (London dispersion terms arising in second and higher order), and (3) the perturbing Coulomb potential is approximated by its multipole components. Due to the orthogonality of the excited states with respect to the ground state (the integral of the charge transition density is zero), the leading order corresponds to a dipole−dipole second-order perturbation of the two-fragment interaction.

3. OLDER DISPERSION CORRECTIONS

The fact that standard local density approximations (LDAs) and generalized gradient approximations (GGAs) yield an inconsistent or even unbound description of small vdW complexes was discovered by three groups in the mid-1990s.[98−100] RG dimers were suggested even earlier as difficult test cases for density functional approximations,[101] although in this work the DFT failure was not that clearly documented. In 1996, Meijer and Sprik[102] presented the first clear analysis of the strong density functional dependence of the problem (i.e., LDA vs GGA functionals) for the "canonical" case of the benzene dimer and, furthermore, made the connection to errors in computed solid-phase properties like mass density or lattice energy. General claims that semilocal functionals cannot describe long-range correlation forces were occasionally made,[102,103] but without clear reference or theoretical explanation. Even in 2002 the situation was not clear as indicated by the summary of van Mourik and Gdanitz[104] of DFT studies on RG dimers, which identified over-repulsive as well as overbinding approximations that were further found to be strongly dependent on the actual system.

Those days also have been dominated by the simple and actually incomplete picture that dispersion forces are only relevant for the *intermolecular* situation, i.e., vdW complexes and condensed phases. The modern notion that *intramolecular* dispersion effects are especially important in large systems[19] was undeveloped, at least in the theoretical chemistry community. Note, however, that such intramolecular effects were occasionally mentioned in the experimental literature; see refs 105 and 106 for very early notes.

Dispersion corrections to DFT and HF were scarcely applied prior to the year 2000, and if so, mostly in various nonstandardized ways. These precursors to more modern approaches are reviewed in this section. A common feature of the methods described herein is that they do not target a general solution of the problem but present ad hoc solutions for a few systems at most, or sometimes even for one specific vdW complex only.

All methods reviewed here approximate the total molecular energy as a sum of a quantum mechanical (QM) energy from a mean-field approach E_{MF} and a dispersion-energy contribution E_{disp}.

$$E_{tot} = E_{MF} + E_{disp} \tag{10}$$

where MF (i.e., mean-field approach) stands for Hartree−Fock (HF), a density functional approximation (DFA), or a SE-MO method. The E_{MF} can be obtained even in a very approximate, nonself-consistent way. The dispersion coefficients (see below) in these early methods were not varied (geometry or electronic structure dependent) or computed specifically but were mostly taken as fixed parameters with numerical values often obtained in experiments. In the terminology of Dobson (see previous section), type-A (as well as type-B and type-C) nonadditivity effects were neglected.

3.1. Dispersion-corrected DFT

Cohen and Pack were likely the first who applied an atom pairwise dispersion correction to a density functional type interatomic potential.[107] The authors used the so-called Gordon−Kim (GK)[108] model as an approximation to HF and applied a dispersion correction of the form

DOI: 10.1021/acs.chemrev.5b00533
Chem. Rev. XXXX, XXX, XXX−XXX

$$E_{\mathrm{disp}}(R) = -\frac{C_6}{R^6} - \frac{C_8}{R^8} - \frac{C_{10}}{R^{10}} \tag{11}$$

where R denotes an interatomic distance. The GK method uses the simple sum of atomic electron densities ρ_A and ρ_B to express the total molecular density $\rho = \rho_A + \rho_B$ for a diatomic AB and employs various density functionals to compute electronic Coulomb, exchange, and correlation energies nonself-consistently. For the pair-dispersion coefficients $C_n(A,B)$, general combination rules of the form

$$C_{4+2^l}(A, B) = \sum_{n,m}{}' \frac{f_{ml}(A) f_{nl}(B)}{\epsilon_m(A)\epsilon_n(B)(\epsilon_m(A) + \epsilon_n(B))} \tag{12}$$

were proposed, where the $\epsilon_m = E_m - E_0$ are atomic excitation energies, the prime implies summation over all states of the atoms except the ground (0) states, and the $f_{ml}(A)$ are the 2^l-pole oscillator strengths of the atoms. This GK + dispersion approach was shown to give a reasonable estimate of the whole potential curve for both like and unlike pairs of RG atoms. Simple but seemingly reliable combinatorial rules were also proposed and tested for the higher-order dispersion coefficients. An additional exchange correction according to Rae[109] (termed GKR method) was found to improve the agreement with HF data. Because the above dispersion energy was used in an undamped, thus wrong short-range form, parts of the interatomic potential were not considered and the entire work was focused on the long-range interactions. As was common in all these early works, only diatomic RG complexes were investigated.

In a series of papers published in the late 1990s,[110−113] the group of Gianturco applied a special version of dispersion-corrected DFT to RG(He, Ne, Ar)−CO vdW complexes. The treatment involved a so-called half-and-half density functional of global hybrid type ($E_{\mathrm{xc}} = \frac{1}{2}E_X^{\mathrm{Fock}} + \frac{1}{2}E_{XC}^{\mathrm{LDA}}$), a large standard Gaussian AO basis set, and a dispersion term of the form as given in eq 11. The dispersion coefficients were dependent on the bending angle θ in the triatomic complex. Two approaches to merge the DFT and dispersion parts were considered. The first was multiplication of the dispersion potential by a damping function of the Tang−Toennies (TT) type[114]

$$f_{\mathrm{damp,TT}}^{(n)}(bR) = 1 - \exp(-bR)\sum_{k=0}^{n}\frac{(bR)^k}{k!} \tag{13}$$

where b is an empirical parameter and n defines the order of the dispersion expansion (usually n = 6, 8). This is similar to the treatment in the HFD model of Ahlrichs and Scoles (see below). In modern notation this form of the damping function that asymptotically approaches zero for $R \to 0$ is called "zero-damping" (see section 4 for further discussion). The second approach was somewhat less empirical and involves the short- and medium-range (SMR) correlation energy estimated from the difference of DFT and HF interatomic potentials, i.e.,

$$E_{\mathrm{corr,SMR}}(R) = E_{\mathrm{DFT}}(R) - E_{\mathrm{HF}}(R) \tag{14}$$

which was then used to define a total correlation correction,

$$E_{\mathrm{corr,tot}}(R) = D_\lambda E_{\mathrm{corr,SMR}}(R) + E_{\mathrm{disp}}(R) \tag{15}$$

where D_λ is a scaling parameter obtained by matching the two regions at the points R_λ where the logarithmic derivatives of the dispersion and correlation branches are equal. The final energy was then given by

$$E_{\mathrm{tot}} = \begin{cases} E_{\mathrm{DFT}}(R) & R < R_\lambda \\ E_{\mathrm{HF}}(R) + E_{\mathrm{corr,tot}}(R) & R > R_\lambda \end{cases} \tag{16}$$

The resulting two-dimensional potentials compared well with the best known data from SAPT calculations, and derived thermal transport properties of RG/CO mixtures were in good agreement with corresponding measurements. Although the method was quite successful, it has never been applied to more complicated systems. Presumably, this is because the complexity of the problem when aiming at very high accuracy is hidden in the angle-dependent dispersion coefficients $C_n(\theta)$, which were taken from literature data but not actually computed specifically for the considered system.

The common, textbook-prevalent view that dispersion forces are relatively unimportant for polar or hydrogen-bonded systems (where electrostatic and induction terms dominate) while they are decisive for, e.g., hydrocarbon or rare gas complexes was questioned for the first time in the years 2001−2002. It is attributed to the growing interest in accurate quantum chemistry based biomolecular simulations for proteins and DNA fragments at that time.[115−117] In that time the groups of Yang, Elstner/Hobza, and Scoles more or less independently published dispersion-corrected DFT approaches (or tight-binding versions) aiming at a more general description of noncovalent interactions in bio-organic systems.[118−120] These works did not add anything particularly new from the methodological standpoint because they just applied a damped-dispersion scheme with typical density functionals (nowadays known as DFT-D). However, they marked a turning point in the rediscovery of the problem in DFT and motivated all further more general and widely used DFT-D schemes.

The work of Scoles et al.[118] made the most general statements regarding the applicability of DFT-D (although this modern term was in fact not used). They tested various functionals and applied it even to transition metal carbonyls. Standard atomic dispersion coefficients, combinatorial rules, and special damping functions were employed, and the use of a three-body dispersion term was already mentioned in this work.

Wu and Yang[120] considered organic systems and used atomic hybridization state dependent (but not system-specific) dispersion coefficients. Different combinatorial rules and damping functions as well as three typical GGA and one hybrid (B3LYP) functional were tested for RG dimers, for DNA base stacking situations, and even for the intramolecular case of polyalanine conformations. The same basic approach was used two years later by Zimmerli et al.[121] to describe water−benzene complexes with B3LYP.

The paper of Elstner et al.[119] is probably the first where a dispersion correction is employed in a modern semiempirical context. They combined it with the self-consistent-charge, density-functional tight-binding (SCC-DFTB) approach, which represents a minimal-basis set, second-order approximation to a GGA calculation.[122] The form of the dispersion correction is very similar to the one used by Wu and Yang. DNA base complexes of stacked and hydrogen-bonded type were investigated in this first publication, and a very good agreement with corresponding MP2 results was reported.

3.2. Dispersion-corrected HF

Scoles and co-workers[123] started from the pure dispersion interaction in the H_2 $^3\Sigma_u^+$ two-electron system, which is known to a high degree of accuracy, and compared it to the corresponding, entirely repulsive HF potential. It is noted that triplet H_2 (not

DOI: 10.1021/acs.chemrev.5b00533
Chem. Rev. XXXX, XXX, XXX−XXX

He_2) is actually the simplest chemical system showing clear dispersion interactions. From this comparison the authors derived the correction potential needed for the dispersion. They obtained the following relation for the total energy of the dispersion-corrected HF method (often termed HFD) as a function of interatomic distance R,

$$E_{\mathrm{HFD}}(R) = E_{\mathrm{HF}} - \left(\frac{C_6}{R^6} + \frac{C_8}{R^8} + \frac{C_{10}}{R^{10}}\right) \times \exp\left[-\left(\frac{5}{4}R_m/R - 1\right)^{1.9}\right] \quad (17)$$

Here, the dispersion coefficients C_6−C_{10} for hydrogen and the RG gas atom pairs (to which the method was applied first) were taken from the literature, and the exponential term represents a short-range damping with appropriate atomic or pair-specific radii R_m. The method was later used by the same group with a modified damping term and medium-sized Gaussian AO basis sets, and was even applied to H_2−He mixtures.[124] For such polyatomic systems, a standard atom pairwise additive approximation

$$E_{\mathrm{disp}} = \sum_{AB} E_{\mathrm{disp}}(R_{AB}) \quad (18)$$

was employed where the sum is over all unique atom pairs in the system and $E_{\mathrm{disp}}(R_{AB})$ is the corresponding damped pairwise dispersion energy. As noted before, this approach neglects dispersion-energy nonadditivity (type-B effects).

An undamped HF + dispersion approach including terms up to C_{10} was solely applied to the potential energy curve of the neon dimer in 1973 by Conway and Murrell[125] (which was one year earlier than the HFD paper of Hepburn and Scoles). This work, although being rather special by focusing on the exchange-interaction energy and only mentioning the applied dispersion correction in a small paragraph, is to the best of our knowledge the very first HF + dispersion work.

The various HF-based methods mentioned could have easily been extended and generalized to arbitrary polyatomic molecules. In particular, this holds for HF compared to DFT because the former was widely used in chemistry and various computer codes were commonly available already in the 1970s and 1980s. However, HFD methods have been used only occasionally to compute small aggregates of aromatic molecules in later decades.[126−128] The good accuracy of HF with a general (e.g., D3) dispersion correction for almost arbitrary noncovalent interactions was mentioned for the first time by Grimme et al.[129] The very reasonable performance of HF-D3 was later documented by the same group for various complexes[34,130] and was recently reconfirmed by Conrad and Gordon.[131] These authors furthermore coupled their so-called EFP dispersion model to HF and DFT, leading to the HF-D(EFP) and DFT-D(EFP) methods, which seem to perform similar to the corresponding HF-D3 or DFT-D3 methods on a limited number of smaller test complexes.[132] To some extent related to HFD is the Hartree−Fock−Clementi−Corongiu method, which scales the two-electron repulsion integrals to include correlation effects and includes an additional long-range dispersion term.[133] This reference describes corresponding potential energy curves for naphthalene−RG complexes.

4. MODERN DISPERSION CORRECTIONS

4.1. Semiclassical treatments of the dispersion interaction

In semiclassical treatments, the dispersion energy evaluated between atom pairs is simply added to the electronic energy of the mean-field approach (MF; e.g., DFT, HF, or SE-MO) as shown in eq 10. The term "semiclassical" originates from the fact that the dispersion interaction is evaluated as the *effective* classical interaction between atoms (or molecules), commonly known as London or vdW interaction, although it is intrinsically a purely quantum mechanical interaction. The most widely used semiclassical methods are the exchange-dipole moment (XDM) method by Becke and Johnson,[22,83,84] the Tkatchenko−Scheffler[86] method, and the D3 approach[85,129] (as well as its precursor D2)[81] by Grimme and co-workers. Extensions accounting for many-body effects in different flavors have been reported as well.[85,87,134]

Note that in the current literature some (but not all) of the atom pairwise methods are denoted with the attribute "empirical", which is inappropriate. In fact, all dispersion-correction schemes to MF quantum chemical methods described in this Review except vdW-DF contain empirical elements and fitting to external (theoretical or experimental) reference data. The term empirical may suggest inaccuracy, but a simple quality−empiricism relation does not exist here. Hence, the term "empirical" is misleading and should be avoided in this context. We recommend to replace it by a short attribute denoting the basic physical/theoretical foundation of the applied correction (e.g., semiclassical (or, more specifically, atom pairwise), nonlocal density based, effective one-electron based, etc.).

All of the semiclassical approaches share more or less the same theoretical foundation, which can be derived from perturbation theory (PT). The approaches then differ in the truncations and approximations introduced. We will briefly demonstrate this by deriving the $-C_6/R^6$ term from second-order perturbation theory (PT2). The electron correlation energy up to second-order in the perturbation after application of the Slater−Condon rules is given by (cf. eq 6)

$$E_{\mathrm{corr}}^{\mathrm{PT2}} = -\sum_{ij}^{n_{\mathrm{occ}}} \sum_{ab}^{n_{\mathrm{virt}}} \frac{[(ia|jb) - (ib|ja)]^2}{\omega_{ai} + \omega_{bj}} \quad (19)$$

where ij/ab denote occupied/virtual orbitals, respectively. Here and in all following summations, we sum over unique pairs, triples, etc. without explicitly restricting the sum. We use the Mulliken notation for two electron integrals, i.e., $(ia|jb) = \int \mathrm{d}\mathbf{r}_1\, \mathrm{d}\mathbf{r}_2 \varphi_i(\mathbf{r}_1)\varphi_a(\mathbf{r}_1)\frac{1}{|\mathbf{r}_1 - \mathbf{r}_2|}\varphi_j(\mathbf{r}_2)\varphi_b(\mathbf{r}_2)$. ω_{ai} is the excitation energy corresponding to an electronic excitation from orbital i to a. At this order in the perturbation, two-body correlation effects, leading to pairwise dispersion, are captured. Many-body dispersion effects are obtained if the perturbation series is extended to higher orders in the interelectronic perturbation parameter. It should be mentioned that in the uncoupled approximation the denominator reduces to the respective orbital energy differences, resulting in the MP2 expression for the correlation energy (see eq 6).

When the orbitals i and a are localized on fragment A and orbitals j and b are localized on fragment B (eq 19, compare Figure 4), the second (exchange) term in the numerator $(ib|ja)$ will vanish faster (exponentially) in the asymptotic limit ($R \to \infty$). The first term, however, decays slower, and after rearranging

DOI: 10.1021/acs.chemrev.5b00533
Chem. Rev. XXXX, XXX, XXX−XXX

the sums, we can express the PT2 correlation energy in the asymptotic limit as

$$\lim_{R\to\infty} E_{\mathrm{corr}}^{\mathrm{PT2}} = E_{\mathrm{disp}}^{AB} = -\sum_{i,a\in A}\sum_{j,b\in B}\frac{(ia|jb)^2}{\omega_{ai}+\omega_{bj}} \tag{20}$$

Thus, in the asymptotic regime, the PT2 correlation energy reduces to the square of Coulomb interactions between the transition densities *ia* and *jb* localized on each fragment *A* and *B*, respectively. Describing the Coulomb potential in a multipole expansion, the nonvanishing term of lowest order is the dipole−dipole term

$$E_{\mathrm{disp}}^{AB} \approx -\sum_{i,a\in A}\sum_{j,b\in B}\frac{1}{\omega_{ai}+\omega_{bj}}\left(\frac{\vec{\mu}_{ia}\cdot\vec{\mu}_{jb}-3(\vec{\mu}_{ia}\cdot\vec{e}_R)(\vec{\mu}_{jb}\cdot\vec{e}_R)}{R^3}\right)^2 \tag{21}$$

Here, $\vec{\mu}_{ia}$ is the electric transition dipole moment $(i\to a)$ and $\vec{e}_R$ is a unit vector along the interfragment axis. For spherically symmetric fragments *A* and *B*—which is true, e.g., for the free atoms—averaging over all possible orientations of the transition dipole moments on *A* and *B* leads to the following formula for the dispersion energy

$$E_{\mathrm{disp}}^{(6)} = -\frac{3}{2}\sum_{i,a\in A}\sum_{j,b\in B}\frac{|\mu_{ia}|^2|\mu_{jb}|^2}{(\omega_{ai}+\omega_{bj})R^6} \tag{22}$$

As originally demonstrated by Mavroyannis and Stephen,[135] the following integral identity can be introduced,

$$\frac{1}{\omega_{ai}+\omega_{bj}} = \frac{2}{\pi}\int_0^\infty \frac{\omega_{ai}\omega_{bj}}{[\omega_{ai}^2+\omega^2][\omega_{bj}^2+\omega^2]}\,\mathrm{d}\omega \tag{23}$$

which is used to factorize the energy denominator:

$$E_{\mathrm{disp}}^{(6)} = -\frac{3}{\pi R^6}\int_0^\infty\left[\sum_{i,a\in A}\frac{\omega_{ai}|\mu_{ia}|^2}{\omega_{ai}^2+\omega^2}\right]\left[\sum_{j,b\in B}\frac{\omega_{bj}|\mu_{jb}|^2}{\omega_{bj}^2+\omega^2}\right]\mathrm{d}\omega \tag{24}$$

Using the identity $\omega_{ai}^2+\omega^2 = \omega_{ai}^2-(i\omega)^2$, we can express the dispersion energy via the averaged, isotropic dynamical dipole−dipole polarizability $\alpha_{A,B}(i\omega)$ of the fragments *A*,*B* at imaginary frequency ω:

$$E_{\mathrm{disp}}^{(6)} = -\frac{3}{\pi R^6}\int_0^\infty \alpha_A(i\omega)\alpha_B(i\omega)\,\mathrm{d}\omega = -\frac{C_6^{AB}}{R^6} \tag{25}$$

Here, we have used the Casimir−Polder expression of the dispersion coefficient[60]

$$C_6^{AB} = \frac{3}{\pi}\int_0^\infty \alpha_A(i\omega)\alpha_B(i\omega)\,\mathrm{d}\omega \tag{26}$$

The dispersion energy, which is intrinsically an electron-correlation effect, is reduced to local dynamical properties of the individual fragments. While the poles of the dynamical polarizability arise at real excitation frequencies, the polarizability at an imaginary frequency is a mathematically much simpler object. It decays monotonically from the static value $\alpha(0)$ and vanishes at high frequencies $\alpha(i\omega\to\infty)$. This is of high practical relevance as it significantly reduces the required number of grid points in the numerical frequency integration (in eq 26).

If higher multipoles are considered in eqs 19−21, similar expressions for $E_{\mathrm{disp}}^{(8)}$, $E_{\mathrm{disp}}^{(10)}$, etc. are obtained. The integer numbers 6, 8, and 10 denote the power by which the respective interactions collected within C_6^{AB}, C_8^{AB}, and C_{10}^{AB} decay with increasing separation *R* (compare with eq 11). As demonstrated above, the C_6^{AB} contains all terms arising from dipole−dipole interactions, C_8^{AB} arises from dipole−quadrupole interactions, and C_{10}^{AB} arises from dipole−octupole as well as quadrupole−quadrupole interactions. Due to its slower decay, the dipole−dipole term is asymptotically dominating and most important in the long-range regime. For nonspherically symmetric fragments, the expression of the dispersion energy (eq 20) in a multipole expansion also leads to a C_7^{AB} dispersion coefficient (and higher orders). The C_7^{AB} arises from a Casimir−Polder integral (see eq 26) with the dipole−quadrupole polarizability on one fragment, either *A* or *B*. Its contribution is typically small and an average of the C_7 contribution over all equal-weighted orientations is zero, so that it can be omitted in atom−atom models or effectively absorbed into the symmetric higher-order terms (see section 4.4).

If the C_n^{AB} for fragments *A* and *B* are known, the pairwise dispersion energy can easily be calculated. As discussed in section 3, early approaches made use of C_n^{AB} coefficients that were specifically obtained for the systems of interest (typically rare gas atoms). In general, however, the C_n^{AB} coefficients are unknown for arbitrary fragments, and particularly in the intramolecular case, the definition of such fragments is nontrivial and may become highly artificial. The most straightforward and natural scheme is the fragmentation into atoms.[136] Thereby, the coefficient C_n^{IJ} for interaction between (molecular) fragments *I* and *J* can be decomposed into a sum of atom pairwise terms as

$$C_n^{IJ} = \sum_{A\in I}\sum_{B\in J} C_n^{AB} \tag{27}$$

This allows the formulation of methods that are in principle applicable to any system (inter- as well as intramolecular) as long as the atom pairwise dispersion coefficients are known. However, the polarizabilities and consequently the dispersion coefficients of atoms in a molecular environment differ from free-atom ones (type-A effects). Therefore, the dependence of the atomic dispersion coefficients on the molecular environment needs to be taken into account in some way, for which various schemes are in use (see below). Note that the above pairwise additivity assumption is physically motivated by the approximate additivity of polarizability, which has the dimension of volume. The decomposition in eq 27 is valid as long as type-B and type-C nonadditivity effects are not pronounced (see section 2). This is true for most cases in organic or main group chemistry. Nevertheless, it should be mentioned that, e.g., fullerene dimers already exhibit C_6 dispersion coefficients, which are larger in magnitude than the plain sum of atom pairwise contributions.[137,138]

The expression for the dispersion energy (see eq 25 for $E_{\mathrm{disp}}^{(6)}$) is only defined at long range and will lead to singularities when *R* approaches zero. Consequently, it must be damped at short interatomic distances to avoid artificial overbinding in typical covalent-bonding regimes. The damped atom pairwise dispersion energy is given by

$$E_{\mathrm{disp}}^{AB} = \sum_{n=6,8,10,\ldots} E_{\mathrm{disp}}^{(n)} = -\sum_{AB}\sum_{n=6,8,10,\ldots}\frac{C_n^{AB}}{R^n} f_{\mathrm{damp}}^{(n)} \tag{28}$$

where $f_{\mathrm{damp}}^{(n)}$ denotes a typical damping function that normally decays to zero for $R\to 0$. The different damping models will be discussed separately for each dispersion-correction scheme.

Before we present these in some detail, we summarize the key points of the semiclassical treatment of E_{disp} (compare with Figure 7):

DOI: 10.1021/acs.chemrev.5b00533
Chem. Rev. XXXX, XXX, XXX−XXX

(1) Within many-body perturbation theory, the order in the perturbation defines the maximum order of fragments considered in the dispersion energy (i.e., how many fragments are at most involved): E_{disp}^{AB} first arises at second order in PT, E_{disp}^{ABC} appears first at third order, etc. However, it should be noted that higher-order terms involving intrafragment coupling may implicitly be contained within the pairwise, triplewise terms (e.g., E_{corr}^{ABBA} effects are included within E_{disp}^{AB}) if the fragment polarizability captures these couplings.

(2) Within each order in the perturbation, the truncation of the multipole expansion of the Coulomb potential defines the considered dispersion terms with different decay behaviors in R, i.e., C_6^{AB}, C_8^{AB}, etc.

(3) The way in which the atom-in-molecules (or solid) dispersion coefficients are obtained (e.g., incorporation of the molecular environment, type-A effects) significantly affects their accuracy.

(4) The shape of the damping function is important for a balanced treatment of both the short/medium range correlation (within the chosen MF) and the long-range dispersion.

The latter point requires an additional comment: Ideally, the damping function seamlessly interpolates between the two correlation regimes depicted in Figure 2. However, in reality its contribution goes beyond that as it implicitly absorbs errors of the MF approach in that region as well (e.g., in the description of exchange dispersion). In principle, this is true for all dispersion approaches where the dispersion energy is added to the MF energy (see eq 10), i.e., for semiclassical (section 4.1) and similarly for nonlocal density based (section 4.2) corrections. For a dispersion-free functional specifically designed to avoid the double-counting, see ref 139.

In the following, only workable, i.e., generally applicable, semiclassical dispersion corrections are presented that have found application in recent years. Therefore, approaches that solely focus on the calculation of dispersion coefficients without coupling them to a MF method will not be considered in the following (some examples can be found in refs 140−145).

Although the multipole expansion is the most intuitive way to describe the perturbing Coulomb field, it is ill-defined at short distances, where it formally diverges. Note that the reduction of the dispersion energy to local fragment properties does not necessarily depend on this expansion. It may be expressed in a more general form via the charge density susceptibility $\chi(\mathbf{r},\mathbf{r}',\omega)$, which describes the response of the charge density at $\mathbf{r}$ due to perturbation at $\mathbf{r}'$ with frequency ω,

$$E_{\mathrm{disp}}^{AB} = -\frac{1}{2\pi}\int \mathrm{d}\omega \times \int \mathrm{d}\mathbf{r}_a\, \mathrm{d}\mathbf{r}'_a\, \mathrm{d}\mathbf{r}_b\, \mathrm{d}\mathbf{r}'_b \frac{\chi(\mathbf{r}_a, \mathbf{r}'_a, i\omega)\chi(\mathbf{r}_b, \mathbf{r}'_b, i\omega)}{|\mathbf{r}_a - \mathbf{r}_b||\mathbf{r}'_a - \mathbf{r}'_b|} \tag{29}$$

where the integration over $\mathbf{r}_a$ and $\mathbf{r}_b$ is restricted to fragments A and B, respectively. From this expression, one can build a bridge to the nonlocal density functionals presented later in section 4.2 as they make local approximations to the charge-density susceptibility $\chi(\mathbf{r},\mathbf{r}',\omega)$ and thus recover the dispersion interaction by a more complicated Casimir−Polder-type expression.

4.1.1. D2 approach. The D2 method was presented by Grimme in 2006[81] as a successor of the D1 approach from 2004, which was limited regarding the covered chemical elements.[146] Even though the D2 method (often abbreviated as "-D") is not considered to be state-of-the-art anymore, it is discussed here as it still is widely in use[147] and constitutes a comprehensible starting point for developing other approaches. In D2, only the two-body, dipole−dipole dispersion energy $E_{\mathrm{disp}}^{(6)}$ is evaluated

$$E_{\mathrm{disp}}^{D2} = -s_6 \sum_{AB} \frac{C_6^{AB}}{R^6} f_{\mathrm{damp}}^{\mathrm{Fermi}}(R) \tag{30}$$

where s_6 is a functional-specific scaling parameter. $f_{\mathrm{damp}}^{\mathrm{Fermi}}(R)$ is a Fermi-type damping function that reduces the dispersion energy to zero at small interatomic separations[120]

$$f_{\mathrm{damp}}^{\mathrm{Fermi}}(R) = \frac{1}{1 + \mathrm{e}^{20[R/(s_R R_{\mathrm{vdW}})-1]}} \tag{31}$$

where R_{vdW} is the sum of the vdW radii of the two atoms and s_R is a scaling parameter. These are estimated from the electron density obtained by restricted-open-shell HF calculations of the free atoms. The C_6^{AB} dispersion coefficients in eq 30 are obtained as the geometric mean of the respective homoatomic value C_6^{AA}

$$C_6^{AB} = \sqrt{C_6^{AA} C_6^{BB}} \tag{32}$$

The C_6^{AA} coefficients are computed using the empirical relationship

$$C_6^{AA} = 0.05 N I_A \alpha_A^0 \tag{33}$$

The scaling factor N increases with the row in the periodic table of elements. The static dipole polarizability α_A^0 and first ionization potentials I_A are computed with the PBE0[148−150] functional. Because D2 does not use dispersion coefficients from the correct Casimir−Polder expression (eq 26), it is regarded as a fully empirical correction. The C_6^{AA} are element-specific parameters and are available for all elements up to xenon. They do not, however, contain any dependence on the molecular environment, but instead the atomic dispersion coefficients are averaged for different hybridization states of the atom. This "force-field"-like character makes it computationally very efficient. Only the geometry of a molecule is required, and the dispersion energy as well as its gradients are easily calculated. However, for example, the C_6^{AA} for carbons in ethene and ethane are identical, which limits the accuracy of the method.

Originally, the method was proposed together with a reparametrized, nonhybrid variant of the B97[151] functional (called B97-D).[81] It represents the first DFA that has been specifically designed to include a dispersion correction from the very beginning. This mostly avoids electron correlation double-counting effects, which sometimes appear with standard DFAs (which already describe correlation effects) when they are augmented with dispersion models that additionally describe correlation.

As such, the method is still applied. Neglecting the higher-order atom pairwise dispersion coefficients (C_n^{AB}, $n \geq 8$) works quite well in B97-D because the flexible B97 functional implicitly captures these effects to some extent. The good interplay between D2 and B97 has also been exploited by Chai and Head-Gordon in the development of the range-separated hybrid functional ωB97X-D.[147]

The D2 method represents one of the first semiclassical approaches available for a large part of the periodic table. However, its major deficiency is the missing dependence of the dispersion energy on the molecular environment. Nevertheless, being one of the first dispersion methods that was widely available for (almost) arbitrary systems, this method became extremely popular, with the original paper[81] being cited more

DOI: 10.1021/acs.chemrev.5b00533
Chem. Rev. XXXX, XXX, XXX−XXX

than 5000 times.[6] D2 has been combined with several MFs like semiempirical methods[152−156] and density functionals.[157,158] Furthermore, it has been included as an integral component into some newly developed density functionals.[147,159] Because of its very simple and manually tunable character, D2 can easily be modified and special variants have been presented.[160] In combination with the B3LYP functional,[53,54,58,161,162] Civalleri et al. proposed the B3LYP-D* scheme in which the scaling factor s_6 is set equal to 1 (originally 1.05)[81] and by rescaling R_{vdW} in the damping function (eq 31).[163] This modification improved the performance for structures and cohesive energies of molecular crystals. Steinmann, Csonka, and Corminboeuf[164] have presented a variant (known as "dD10" in the literature) that employs the TT damping function and includes higher-order multipole terms (i.e., C_8^{AB} and C_{10}^{AB}) via recursion relations. A recent approach related to D2, i.e., use of fixed dispersion coefficients, is the spherical atom model by Austin et al.,[165] which has been proposed together with the so-called APF-D functional. Here, the dispersion coefficients are obtained from the London formula (eq 1) employing precomputed atomic polarizabilities and ionization energies.

4.1.2. D3 approach. In 2010, Grimme and co-workers proposed the D3 approach.[85] In contrast to D2, the molecular environment is explicitly taken into account by the empirical concept of fractional coordination numbers (CNs). The coordination number of an atom A in a molecule (or crystal) is given by

$$\mathrm{CN}^A = \sum_{B\neq A}^{N_{\mathrm{atoms}}} \frac{1}{1 + \mathrm{e}^{-16(4(R_{A,\mathrm{cov}}+R_{B,\mathrm{cov}})/(3R_{AB})-1)}} \tag{34}$$

where the covalent radii $R_{A,\mathrm{cov}}/R_{B,\mathrm{cov}}$ for each element are taken from ref 166. Atoms in different bonding/hybridization situations have different coordination numbers, which is in agreement with chemical intuition. This is illustrated in Figure 8 for carbon, which has a coordination number of roughly 4 in ethane, 3 in ethene, and about 2 in ethyne. This way, the chemical environment (type-A effect) is taken into account only in terms of the molecular geometry.

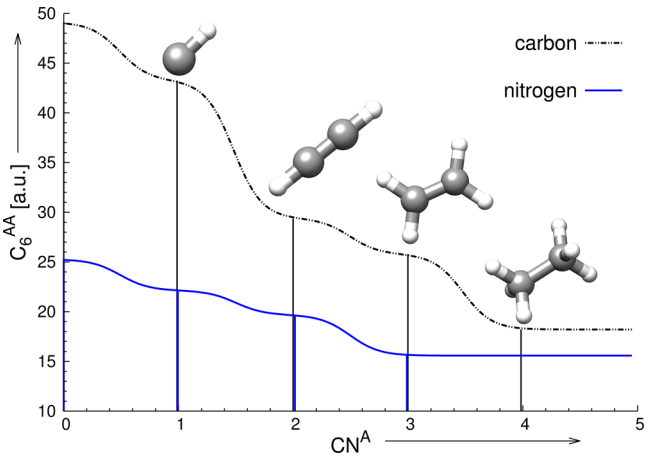

Figure 8. CN-dependent atom pairwise dispersion coefficient for homoatomic pairs C_6^{AA} as a function of the coordination number CN^A. The reference points $C_{6,\mathrm{ref}}^{AA}$ are drawn as vertical sticks in the respective colors (black for carbon, blue for nitrogen). For carbon, the structures of CH, ethyne, ethene, and ethane (corresponding to the coordination numbers 1−4) are depicted as well.

To derive system-specific dispersion coefficients, the electric dipole polarizability $\alpha^A(i\omega)$ of the free atom as well as for the atom in differently coordinated hydrides as model systems (A_mH_n and B_kH_l in eq 35) was computed. All elements ($Z \leq 94$) were treated nonempirically by calculations at different imaginary frequencies via time-dependent density functional theory (TD-DFT).[141,142,167] A variant of the PBE0 hybrid functional with a modified amount of Fock exchange $a_x = 3/8$ (called PBE38) in an augmented quadruple-ζ (triple-ζ for $Z \geq 87$) basis set has been employed. The PBE38 hybrid functional provides accurate dynamic polarizabilities for rare gas atoms and small molecules. It may be less accurate for electronically complicated systems, but all reference calculations were done on relatively simple and small model molecules. A modified Casimir−Polder expression has been used to compute the atom pairwise dispersion coefficients $C_{6,\mathrm{ref}}^{AB}(\mathrm{CN}^A,\mathrm{CN}^B)$ for atoms A and B in these reference molecules

$$C_{6,\mathrm{ref}}^{AB}(\mathrm{CN}^A, \mathrm{CN}^B) = \frac{3}{\pi}\int_0^\infty \frac{1}{m}\left[\alpha^{A_mH_n}(i\omega) - \frac{n}{2}\alpha^{H_2}(i\omega)\right] \times \frac{1}{k}\left[\alpha^{B_kH_l}(i\omega) - \frac{l}{2}\alpha^{H_2}(i\omega)\right] \mathrm{d}\omega \tag{35}$$

Here, A_mH_n and B_kH_l are the reference compounds with atoms A/B having a specific coordination number CN. The contribution of the hydrogen atoms in the reference molecules is subtracted. These reference compounds reflect typical bonding situations for each element and are distinguished by their CN^A. In D3, the $C_{6,\mathrm{ref}}^{AB}(\mathrm{CN}^A,\mathrm{CN}^B)$ values are precomputed for every possible pair combination (both element and CN) and stored. In the actual D3 calculation for a target system, the atom pairwise C_6^{AB} dispersion coefficient is evaluated as the Gaussian average of the precomputed reference values,

$$C_6^{AB}(\mathrm{CN}^A, \mathrm{CN}^B) = \frac{\sum_i^{N_A}\sum_j^{N_B} C_{6,\mathrm{ref}}^{AB}(\mathrm{CN}_i^A, \mathrm{CN}_j^B)L_{ij}}{\sum_i^{N_A}\sum_j^{N_B} L_{ij}} \tag{36}$$

with

$$L_{ij} = \mathrm{e}^{-4[(\mathrm{CN}^A-\mathrm{CN}_i^A)^2+(\mathrm{CN}^B-\mathrm{CN}_j^B)^2]} \tag{37}$$

Therefore, the D3 method requires only the molecular geometry to obtain CN^A and CN^B as input. For carbon and nitrogen, the dispersion coefficient for homoatomic pairs C_6^{AA} is plotted as a function of the coordination number in Figure 8. For clarity, we will drop the lengthy notation $C_6^{AB}(\mathrm{CN}^A,\mathrm{CN}^B)$ in favor of C_6^{AB}, implying that this is the system-specific dispersion coefficient obtained via eq 36. In D3, dispersion contributions beyond the lowest dipole−dipole order $E_{\mathrm{disp}}^{(6)}$ are taken into account as well. The atom pairwise dipole−quadrupole contribution $E_{\mathrm{disp}}^{(8)}$ is included with the respective C_8^{AB} dispersion coefficient, which is computed recursively from

$$C_8^{AB} = 3C_6^{AB}\sqrt{Q_AQ_B} \tag{38}$$

with

$$Q_A = \sqrt{Z_A}\frac{\langle r_A^4\rangle}{\langle r_A^2\rangle} \tag{39}$$

Here, $\langle r_A^4\rangle$ and $\langle r_A^2\rangle$ are multipole-type expectation values derived from atomic densities and Z_A is the atomic number of element A. The ratio is thus an element-specific parameter that yields good estimates of C_8^{AB} based on C_6^{AB}. These established

DOI: 10.1021/acs.chemrev.5b00533
Chem. Rev. XXXX, XXX, XXX−XXX

recursion formulas[168] give values for the dispersion coefficients of hydrogen with only a few percent errors.[169] Explicit higher multipolar terms (e.g., $E_{\mathrm{disp}}^{(10)}$) are neglected in D3 but absorbed through the s_8 scaling factor into the R^{-8} term. The atom pairwise, two-body dispersion energy in D3 is then given as

$$E_{\mathrm{disp}}^{D3} = -\sum_{AB}\sum_{n=6,8} s_n \frac{C_n^{AB}}{R^n} f_{\mathrm{damp}}^{(n)}(R) \tag{40}$$

The factors s_n scale the individual multipolar contributions. The leading term is set to unity ($s_6 = 1$) for most functionals (except for double-hybrid functionals, which already comprise some MP2 correlation). This is mandatory for the correct asymptotic decay of the dispersion energy. The higher order term s_8, however, is a parameter that is fitted (along with the parameters in the damping function $f_{\mathrm{damp}}^{(n)}(R)$, see below) for each density functional to avoid double counting at the short and medium ranges (see Figure 2).

Two variants of D3 exist that employ different damping schemes. The original D3 approach employs a damping function proposed by Chai and Head-Gordon in the context of the ωB97X-D functional[147] by which the dispersion energy is damped to zero at short distances,

$$f_{\mathrm{damp,zero}}^{(n)}(R) = \frac{1}{1 + 6(R/(s_{r,n}R_0^{AB}))^{a_n}} \tag{41}$$

where $a_6 = 14$, $a_8 = 16$, and $s_{r,6}$ and $s_{r,8}$ are functional-specific parameters. This original D3 scheme will be dubbed D3(0) in the further context.

Inspired by the work of Johnson and Becke,[83] the rational (Becke–Johnson) damping scheme was combined with the atom pairwise D3 method.[129] Here, the dispersion energy is damped to a finite value at short distances

$$f_{\mathrm{damp,BJ}}^{(n)}(R) = \frac{R^n}{R^n + (a_1R_0 + a_2)^n} \tag{42}$$

where the functional-specific parameters a_1 and a_2 and the radii $R_0 = \sqrt{C_8^{AB}/C_6^{AB}}$ are introduced in the denominator. Because of its physically more reasonable behavior at short interatomic distances, this variant (dubbed D3(BJ) in the following) has become the default D3 scheme in the past years.[19] The different damping behaviors of D3(BJ) and D3(0) are visualized for the $E_{\mathrm{disp}}^{(6)}$ part in Figure 9. Both damping schemes do not affect the long-range decay of the dispersion energy. However, in the short-range part, the D3(0) dispersion energy decays to zero. This introduces an artificial repulsive dispersion force in some practically relevant cases, where D3(0) might thus lead to longer bond lengths than dispersion-uncorrected DFT. Such a behavior would be purely artificial and solely due to the damping function as dispersion should always be attractive. Hence, D3(BJ) is generally preferred over D3(0). Today, parameters for >40 functionals are available for either the D3(0) or the D3(BJ) approach. The D3(0) variant remains in use only for DFA, which already includes medium-range dispersion and in this way avoids double-counting effects better than D3(BJ).

In the original publication,[85] it was already proposed to additionally compute the three-body dipole–dipole–dipole dispersion energy (also called Axilrod–Teller–Muto term, ATM):[170,171]

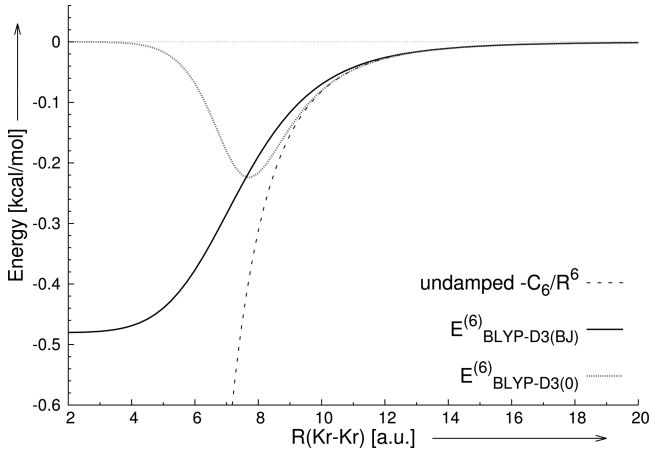

Figure 9. Different D3 damping schemes for the $E_{\mathrm{disp}}^{(6)}$ contribution of the Kr–Kr dispersion energy. For D3(BJ) (solid black) and D3(0) (dotted gray), the curves are given using the damping parameters for the BLYP functional. The undamped $-C_6/R^6$ contribution is given for comparison (dashed black).

$$E_{\mathrm{disp}}^{(9),\mathrm{D3}} = -\sum_{ABC} \frac{C_9^{ABC}(3\cos\theta_a\cos\theta_b\cos\theta_c + 1)}{(R_{AB}R_{AC}R_{BC})^3} \times f_{\mathrm{damp}}^{(9)}(\bar{R}_{ABC}) \tag{43}$$

Here, the damping scheme in $f_{\mathrm{damp}}^{(9)}(\bar{R}_{ABC})$ is that of D3(0) (see eq 41) with $\bar{R}_{\mathrm{ABC}}$ being the geometric mean of the atom pairwise distances R_{AB}, R_{AC}, and R_{BC}. It should be noted that the ATM energy in D3 is always computed with the zero-damping function. Because of the faster decay with R, the ATM energy is smaller in magnitude, and hence the potentially nonphysical effect of the zero-damping function is expected to be less important. The dispersion coefficient C_9^{ABC} is approximated as

$$C_9^{ABC} \approx -\sqrt{C_6^{AB}C_6^{AC}C_6^{BC}} \tag{44}$$

Initially, it was not clear whether it is reasonable to include the ATM term. Its contribution to the dispersion energy is typically <5%. Recent work,[95,172,173] however, showed that its inclusion in the D3 context is important for accurate binding energies in large noncovalently bound complexes and molecular crystals. The importance of many-body effects for such systems has furthermore been highlighted in the context of the Tkatchenko–Scheffler method (see below).[91,174,175] The total atom pairwise and triplewise dispersion energy in D3 (dubbed D3$^{\mathrm{ATM}}$) is then given by

$$E_{\mathrm{disp}}^{\mathrm{D3^{ATM}}} = -\sum_{AB}\sum_{n=6,8} s_n \frac{C_n^{AB}}{R^n} f_{\mathrm{damp}}^{(n)}(R) - \sum_{ABC} s_9 \frac{C_9^{ABC}(3\cos\theta_a\cos\theta_b\cos\theta_c + 1)}{(R_{AB}R_{AC}R_{BC})^3} \times f_{\mathrm{damp}}^{(9)}(\bar{R}_{ABC}) \tag{45}$$

Apart from its accuracy (C_6 values are, on average, accurate to ~5%),[11] the major advantage of the D3 approach is the computational efficiency. The dispersion energy is evaluated as a sum over all atom pairs (triples). This makes it much more efficient compared to XDM or TS models, particularly in geometry optimizations and harmonic frequency calculations.

DOI: 10.1021/acs.chemrev.5b00533
Chem. Rev. XXXX, XXX, XXX–XXX

Furthermore, no information about the electronic structure is required, and only the molecular geometry is needed as input. This is different from other "true" post-self-consistent-field (SCF) approaches, where a quantum chemical calculation must precede the dispersion energy calculation. Hence, D3 is easily applicable together with semiempirical approaches[130,176−179] without sacrificing either the speed of these approaches or the accuracy of the dispersion treatment. Recently, the D3(BJ) approach has been applied together with a quantum mechanically derived force field as well.[180] The degree of empiricism is low (three functional dependent parameters), and it is the only atom pairwise method in which the effect of the chemical environment is explicitly taken into account (at least for the model compounds) in the computation of the dynamic polarizabilities. Recently, Schwabe and co-workers[181] have modified the D3(BJ) approach (called D3(CSO) for "C-Six Only"), reducing the number of functional specific parameters to just one while retaining roughly the same accuracy.

The atom pairwise D3 (independent of the damping function) as well as D3^{ATM} are consistent methods in the sense that all dispersion contributions up to a certain order in the distance dependence (R^{-8} for D3, R^{-9} for D3^{ATM}) are taken into account (see section 4.4). The exclusion of the underlying density (or WF) is, however, a disadvantage. Whenever the electron density around an atom in a molecule or solid is significantly different from the one present in the reference compound, larger errors for the dispersion coefficients can be expected. This occurs, for example, in metal complexes where the metal centers often carry significant partial positive charge, i.e., change their oxidation state relative to the reference molecule. In principle, one can increase the space of reference molecules in the C_6 calculations for a specific application. In an investigation of ionic surfaces, electrostatically embedded clusters were used for the calculations of dynamic dipole polarizabilities[182] for Na and Mg. Likewise, positively charged model compounds were employed as references for organometallic Pd complexes.[183] In a study by Saue and co-workers,[184] it was shown that, for C_6 coefficients, spin−orbit effects are not relevant for most elements. Because scalar relativistic effects are included within the effective core potentials and corresponding basis sets employed in the computation of the D3 C_6 coefficients, the atomic dispersion coefficients compare well with four-component relativistic Kohn−Sham results.

4.1.3. Tkatchenko−Scheffler model. In 2009, Tkatchenko and Scheffler presented a density-dependent, atom pairwise dispersion-correction scheme.[86] This model (dubbed TS in the following) is restricted to the lowest-order two-body dispersion energy $E_{disp}^{(6)}$ and takes into account the molecular environment via the electron density (see below). The dispersion energy in TS is given as

$$E_{disp}^{TS} = -\sum_{AB} \frac{C_6^{AB}}{R^6} f_{damp}^{Fermi}(R) \tag{46}$$

The damping function $f_{damp}^{Fermi}(R)$ is similar to the one of Wu and Yang[120] and in D2 (see eq 31). Within the TS model, the so-called "average-energy" or "Unsöld" approximation is used.[2,3,185] That is, the sum over all excitation energies in eq 24 is replaced by an average excitation energy. This way the C_6^{AB} are approximated from the homoatomic ones via the Slater−Kirkwood formula,[4]

$$C_6^{AB} = \frac{2C_6^{AA}C_6^{BB}}{(\alpha_B^0/\alpha_A^0)C_6^{AA} + (\alpha_A^0/\alpha_B^0)C_6^{BB}} \tag{47}$$

with the static polarizability α_A^0 of atom A (in its molecular environment) and where C_6^{AA} is the respective homoatomic dispersion coefficient. For the free atoms, the static polarizabilities $\alpha_{A,free}^0$ and dispersion coefficients $C_{6,free}^{AA}$ are taken from the literature.[186] The homoatomic dispersion coefficients for an atom in a molecule C_6^{AA}, as well as the corresponding static polarizability, are computed via an empirical relationship to the atomic volume,[187]

$$C_6^{AA} = v_A{}^2 C_{6,free}^{AA} \tag{48}$$

$$\alpha_A^0 = v_A \alpha_{A,free}^0 \tag{49}$$

where v_A is the ratio between the *effective* volume of atom A in a molecule and the volume of the free atom. This ratio is obtained by a Hirshfeld partitioning,[188]

$$v_A = \frac{\int d\mathbf{r}\, w_A(\mathbf{r})\rho(\mathbf{r})r^3}{\int d\mathbf{r}\, \rho_A^{free}(\mathbf{r})r^3} \tag{50}$$

$$w_A(\mathbf{r}) = \frac{\rho_A^{free}(\mathbf{r})}{\sum_B \rho_B^{free}(\mathbf{r})} \tag{51}$$

where $w_A(\mathbf{r})$ is the atomic Hirshfeld partitioning weight for atom A. In the TS method, changes in the polarizability of an atom A due to the molecular environment are estimated by changes in the atomic volume. Once the (homo)atomic data for the atoms in the molecular environment are calculated, the C_6^{AB} dispersion coefficients between all atoms in the system can be evaluated using eq 47. For the damping function, the vdW radii are modified in a similar way

$$R_A = v_A{}^{1/3} R_A^{free} \tag{52}$$

The free atom vdW radii are taken from the literature,[189] and for the damping function $R_{vdW} = R_A + R_B$ is used. The dispersion energy is typically overestimated[172,174] by the TS model, particularly for highly ionic species.[190] This can be alleviated, e.g., by an iterative adjustment of the Hirshfeld partitioning weights.[191] The first approach in this direction is the iterative Hirshfeld I scheme[191], which was proposed in this context by Bučko et al.[190] Here, the total density of the system ($\rho(\mathbf{r})$ in the numerator of eq 50) remains unchanged, and instead, the reference densities $\rho_A^{free}(\mathbf{r})$ of the free atoms that enter the Hirshfeld partitioning are iteratively adjusted. In contrast to a free atom, the reference densities $\rho_A^{free}(\mathbf{r})$ may then resemble the density of a free ion (with noninteger electron number). This causes changes only in $w_A(\mathbf{r})$ (eq 51), however, due to charge preservation not in the denominator of eq 50. These reference densities seem to be more appropriate in highly polar systems than neutral atomic ones.[190] Recently, Tkatchenko and co-workers[192] presented an alternative approach to this problem. Here the total TS dispersion inclusive energy is computed self-consistently with respect to changes in the electron density, i.e., the Hirshfeld partition weights $w_A(\mathbf{r})$ are kept constrained. The induced changes in the total density $\rho(\mathbf{r})$ in eq 50 improve the unsatisfactory performance for highly polar and ionic systems.[192]

Overall, the degree of empiricism is comparable to the one in D3. On the one hand, information on the electronic structure is captured by means of the Hirshfeld partitioning. On the other hand, the use of precomputed reference polarizabilities α_A^0 and $C_{6,free}^{AA}$ keeps the computation of dispersion coefficients simple. These precomputed entities and their mapping to the target system (via Hirshfeld) define the accuracy of the method.

DOI: 10.1021/acs.chemrev.5b00533
Chem. Rev. XXXX, XXX, XXX−XXX

Molecular C_6 coefficients from TS show a mean absolute relative deviation of 5.5%.[86]

4.1.4. TS-based many-body dispersion scheme. In 2012, two extensions of the original, nonself-consistent TS method were introduced by Tkatchenko et al.[87] The first one is to account for screening of the dispersion interaction due to the chemical environment, termed self-consistent-screening (SCS) approach. Note that the term "screening" here is somewhat different from its normal use in the context of electrostatics because the dispersion interaction does not involve a static Coulomb potential. The screening by the environment is dependent on the frequency of the electromagnetic radiation that transmits the induced electric field (see above) and is reflected in the dynamic polarizability of an atom A. In TS, instead of the exact dynamic dipole polarizability, the Padé approximation[193] for the dynamic dipole polarizability is used,

$$\alpha_A(i\omega) \approx \frac{\alpha_A^0}{1 + (\omega/\bar{\omega}_A)^2} \tag{53}$$

where $\bar{\omega}_A$ is an *effective* frequency defined as

$$\bar{\omega}_A = \frac{4}{3}\frac{C_6^{AA}}{(\alpha_A^0)^2} \tag{54}$$

For this purpose, all atoms are represented as a collection of spherical quantum harmonic oscillators (QHOs). Their coupling influences the dynamic polarizability of each atom at a given imaginary frequency $i\omega$. The screened polarizability $\alpha_A^{\mathrm{TS+SCS}}(i\omega)$ is then obtained by self-consistently solving

$$\alpha_A^{\mathrm{TS+SCS}}(i\omega) = \alpha_A^{\mathrm{TS}}(i\omega) + \alpha_A^{\mathrm{TS}}(i\omega)\sum_{B\neq A} \tau_{AB}^{\mathrm{SR}}\alpha_B^{\mathrm{TS+SCS}}(i\omega) \tag{55}$$

with τ_{AB}^{SR} being the short-ranged[175,194] dipole−dipole interaction and $\alpha_A^{\mathrm{TS}}(i\omega)$ being the unscreened dynamic polarizability in TS from eq 53. This is done for several imaginary frequencies $i\omega$, and the resulting $\alpha_A^{\mathrm{TS+SCS}}(i\omega)$ are used to compute the screened $C_{6,\mathrm{SCS}}^{AA}$ for homoatomic pairs by numerical integration of the Casimir−Polder expression (see eq 26). The screened static polarizability $\alpha_A^{0,\mathrm{SCS}}$ is obtained similarly, and both are used to calculate $C_{6,\mathrm{SCS}}^{AB}$ via eq 47.

To compute the many-body dispersion (MBD) energy, a coupled fluctuating dipole model (CFDM)[195] is applied. The atoms in the system of interest are represented as a collection of three-dimensional, isotropic quantum harmonic oscillators with eigenfrequencies $\bar{\omega}_A^{\mathrm{SCS}}$, i.e., the "effective" frequency, which is obtained via eq 54 by employing both the screened $C_{6,\mathrm{SCS}}^{AA}$ and $\alpha_A^{0,\mathrm{SCS}}$. Then, the coupling term in the Hamiltonian for the coupled oscillators is given as

$$V_{\mathrm{CFDM}} = \sum_{A<B}^{N}\sum_{p\in A}^{3}\sum_{q\in B}^{3} \chi_p \tau_{pq}^{\mathrm{LR}} \chi_q \tag{56}$$

In total $3N$ oscillators are set up as the basis and coupled with the displacement χ_p of oscillator p from the equilibrium. However, initially (i.e., no coupling) they are isotropic and all Cartesian directions p or q are identical for atom A and B, respectively. τ_{pq}^{LR} is the dipole−dipole interaction tensor at long range (c.f. eq 55). In the most recent version,[175] a smooth separation into short and long range is achieved by damping the full dipole−dipole interaction tensor τ_{AB} (see ref 136 for the full expression):[194]

$$\tau_{AB} = \underbrace{(1 - f_{\mathrm{damp}})\tau_{AB}}_{\tau_{AB}^{\mathrm{SR}}} + \underbrace{f_{\mathrm{damp}}\tau_{AB}}_{\tau_{AB}^{\mathrm{LR}}} \tag{57}$$

This way, double-counting of dipole interactions is avoided in the dispersion energy. In MBD, a Fermi-type damping function is used for f_{damp} (see eq 31).[196] Diagonalizing the $3N \times 3N$ coupling matrix yields the many-body dispersion energy as the difference between the zero-point energies of the coupled and uncoupled oscillators,

$$E_{\mathrm{disp}}^{\mathrm{MBD}} = \frac{1}{2}\sum_{p=1}^{3N}\sqrt{\lambda_p} - \frac{3}{2}\sum_{A}^{N}\omega_A^{\mathrm{TS+SCS}} \tag{58}$$

where λ_p is the pth eigenvalue of the coupling matrix. Note that the second term in eq 58 is a summation over all atoms, because the uncoupled oscillators are isotropic, and, consequently, has a prefactor of three. This expression has some similarities to the random-phase-approximation (RPA) correlation energy,[197] which was pointed out by Tkatchenko et al. in 2013.[136] The overall procedure is sketched in Figure 10.

The MBD model significantly alleviates the TS problem of overestimating the dispersion energy. Excellent performance was reported for lattice energies of organic crystals[174] as well as for

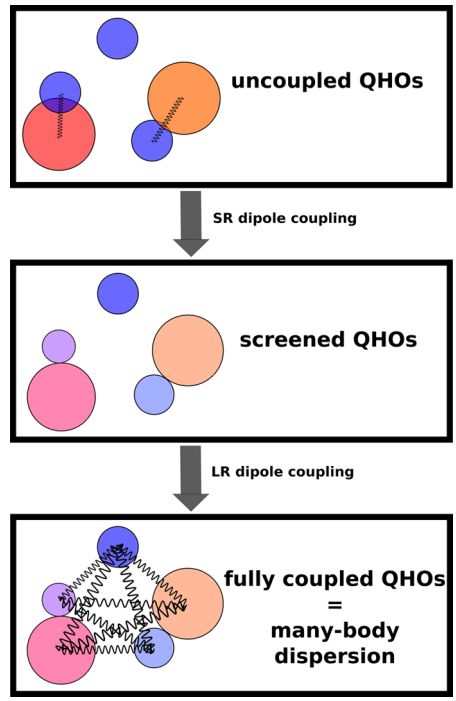

Figure 10. Schematic illustration of how to arrive at the many-body dispersion (MBD) energy based on the Tkatchenko−Scheffler (TS) method. The starting points are the oscillators (eq 54) from the TS model, which are depicted as differently sized and colored circles. First, these are coupled at short range via dipole−dipole interactions. Self-consistent solution of these coupled oscillators yields a new set of screened oscillators. This is schematically depicted as a change in size and color of initially "overlapping" circles. Note that the isolated oscillator (depicted as the "non-overlapping" circle) is not affected by short-range dipole−dipole coupling and remains unchanged. In the last step, the screened oscillators interact through dipole−dipole coupling at long range, which yields the final many-body dispersion energy. The same scheme is also valid for the related Wannier function based approach (vdW-QHO-WF-SCS-SR).

DOI: 10.1021/acs.chemrev.5b00533
Chem. Rev. XXXX, XXX, XXX−XXX

the association energies of large supramolecular complexes (a selection from the S12L[198] test set).[175] In the latter study, the authors pointed out the importance of including many-body terms beyond the three-body contribution. It was found that the truncation at the three-body level lead to errors of ∼10% with respect to the all-order MBD dispersion energy. The three-body dispersion energy amounts to 10−20% of the two-body dispersion energy in MBD, which is different from D3^{ATM} (and XDM; see below) where the three-body energy is typically <5%. Good results for the S12L test set[198] are already obtained at the atom pairwise D3 level, and adding the ATM contribution leads only to small improvements.[172] It is difficult to judge the general importance of multicenter terms in different semiclassical dispersion corrections. Short-ranged (i.e., intrafragment) terms arising from higher orders in the PT series may implicitly be included, e.g., within the underlying atomic polarizabilities in the latter approaches. Because this is an ongoing debate in the literature,[80,134,172,175] we abstain from giving a final conclusion on this topic, but instead we like to point out that the results on benchmark sets for noncovalent interactions in large organic complexes and organic crystals (see, e.g., Table 9) show that MBD (as a semiclassical variant of RPA) as well as D3 and XDM (which can be considered as semiclassical decomposition schemes of the PT series into two- and three-center terms) yield comparable results. The atom pairwise TS scheme tends to overbind van der Waals complexes,[174] which is overcome within the MBD scheme (and the comprised TS + SCS procedure). Approaches that already yield reasonable atom pairwise dispersion coefficients (D3 or XDM) benefit to a much smaller degree from higher multicenter terms.

MBD can be regarded as a semiclassical approximation to the long-range, direct RPA (dRPA) correlation energy.[29,136] The latter is equivalent to the direct ring coupled-cluster doubles (drCCD) correlation energy[199,200] (the term "direct" in this context refers to the neglect of exchange contributions). In dRPA, many-body dispersion effects arising from multiple excitations beyond doubles are consequently captured as the products of so-called disconnected double excitations. Connected multiple excitations beyond doubles, however, are missing. While the correlation from dRPA arises from coupling of excited electronic configurations in the entire system, in MBD the long-range correlation is approximated by setting up a model system of QHOs (one per atom and each Cartesian direction) that interact via a dipole−dipole coupling model. This approximation can be considered to be in line with the Unsöld approximation, and the average frequency of the uncoupled oscillator is estimated from $\alpha_A^{0,SCS}$ and $C_{6,SCS}^{AA}$. Although the ATM term $E_{disp}^{(9)} \propto R^{-9}$ and faster decaying dipole many-body contributions are included, the slightly slower decaying, pairwise dipole−quadrupole term $E_{disp}^{(8)} \propto R^{-8}$ (cf. D3^{ATM} in eq 43) is neglected (see section 4.4). The same is true for corresponding higher-order many-body terms and higher-order multipolar terms. Nevertheless, the MBD yields a much better description of the dispersion energy than pure TS. Due to its comparably simple structure and good performance, it has become one of the most popular dispersion corrections in recent years.[201] Recently, analytic nuclear gradients for the nonself-consistent PBE+MBD model have been implemented independently by two groups and good results for optimized vdW complexes, peptide model structures, and organic crystals are reported.[202,203]

4.1.5. Dispersion corrections based on maximally localized Wannier functions. The vdW-WF method and all variants thereof[194,204−206] are semiclassical dispersion models that differ from the previous models in one aspect: the dispersion energy is not evaluated between atom pairs but instead between the centers of localized one-electron functions (i.e., localized occupied orbitals). In the method specification, "WF" denotes Wannier function, which is the solid state analogue of a localized MO.[207] However, by WF we generally abbreviate wave function and will only use the abbreviation WF for Wannier function within the common method abbreviation (e.g., vdW-WF) in this section. These one-electron functions are generated as maximally localized Wannier functions[208] by minimizing their summed spread:

$$\sum_i S_i^2 = \sum_i \left(\langle W_i|r^2|W_i\rangle - \langle W_i|\mathbf{r}|W_i\rangle^2\right) \tag{59}$$

Here, W_i is the ith Wannier function with spread S_i. In the vdW-WF approaches, the Wannier functions are approximated as spherically symmetric Slater-type functions (i.e., resembling an electron in a hydrogen atom),[204]

$$W_i(|\mathbf{r} - \mathbf{r}_i|) = \sqrt{\frac{{S_H}^3}{\pi {S_i}^3}}\ \exp\left(-\frac{\sqrt{3}}{S_i}|\mathbf{r} - \mathbf{r}_i|\right) \tag{60}$$

where $\mathbf{r}_i$ is the center of the orbital. Different flavors of the Wannier function based dispersion correction have been introduced, but in all of them the employed polarizabilities and dispersion coefficients are obtained by relating the spread S_i to the spread of an electron in the hydrogen atom, i.e., $S_H = \sqrt{3}$. Furthermore, they are restricted to the dipolar contributions. Two-body[204−207] as well as many-body inclusive[194] approaches were presented. The vdW-WF method partitions the density-dependent Andersson, Langreth, and Lundqvist (ALL) functional[209] (see section 4.2) to contributions between the centers $\mathbf{r}_i$ of the Wannier function and furthermore corrects for their density overlap (see refs 204 and 207 for details). In the revised version (vdW-WF2),[205] a modified expression for the dispersion energy has been used,

$$C_6^{ij} = \frac{3}{2}\sqrt{\gamma^3}\frac{\sqrt{n_i}v_i{S_i}^3\sqrt{n_j}v_j{S_j}^3}{\sqrt{n_iv_i{S_i}^3} + \sqrt{n_jv_j{S_j}^3}} \tag{61}$$

where n_i is the number of electrons in the orbital and v_i is the ratio of the *effective* and the *free* volume of the localized orbital. The *effective* volume is a reduced *free* volume where the amount of reduction depends on the overlap with other Wannier functions.[205] γ is an empirical proportionality factor relating the cube of the spread ${S_i}^3$ (which is proportional to the volume) of the Wannier function to its static polarizability (see eq 63). The pairwise dispersion energy is then evaluated according to eq 30, employing the Fermi-type damping function from eq 31. The vdW radii used in the damping function are again obtained from the relationship to the hydrogen atom,

$$R_{vdW,i} = R_{vdW,H}\frac{S_i}{S_H} \tag{62}$$

with $R_{vdW,H}$ = 1.2 Å. On the basis of the vdW-WF2, a many-body treatment employing quantum harmonic oscillators has been introduced recently.[194,206] The procedure resembles very much the one described in section 4.1.4. For this, the static polarizability of the Wannier function i is approximated by[194,206]

$$\alpha_i^0 = \zeta\frac{n_i}{\bar{\omega}_i^2} = \gamma{S_i}^3 \tag{63}$$

DOI: 10.1021/acs.chemrev.5b00533
Chem. Rev. XXXX, XXX, XXX−XXX

where $\bar{\omega}_i$ is the *effective* (or *average excitation*) frequency (c.f. eq 49) and ζ is another empirical parameter of the method. Once the spread is known, the static polarizability as well as the *effective* frequency are computed using the empirical parameters γ and ζ. In the most recent variant (vdW-QHO-WF-SCS-SR in ref 194), these are employed in eq 55 to obtain a screened static polarizability as well as a screened *effective* frequency. Similar to the MBD scheme, the many-body dispersion energy is computed according to eq 58, i.e., via the CFDM as the difference between coupled and uncoupled oscillators, but employing a different damping scheme in eq 57. Therefore, the vdW-QHO-WF-SCS-SR describes many-body effects (within the dipole approximation) between localized orbitals instead of atoms.

4.1.6. Exchange-dipole moment model. The exchange-dipole model (XDM) is a density-dependent, semiclassical dispersion correction.[22,83,84,210] The origin of its derivation, however, is not the long-range Coulomb correlation. Instead, Becke and Johnson noticed that an electron and its corresponding exchange hole (see eq 64) lead to nonvanishing multipole moments.[211] The exchange (or Fermi) hole arises from the Pauli exclusion principle and prevents two electrons of same spin σ to approach each other. It is given by

$$h_{X,\sigma}(\mathbf{r}_1, \mathbf{r}_2) = -\frac{1}{\rho_\sigma(\mathbf{r}_1)} \sum_{ij} \varphi_{i\sigma}(\mathbf{r}_2)\varphi_{j\sigma}(\mathbf{r}_2)\varphi_{i\sigma}(\mathbf{r}_1)\varphi_{j\sigma}(\mathbf{r}_1) \tag{64}$$

Here, σ labels either spin-up or spin-down electrons, and the summation is over all occupied orbitals i and j. The presence of an electron at $\mathbf{r}_2$ reduces the probability to find another electron at $\mathbf{r}_1$. Overall, the charge of the electron and its Fermi hole cancel exactly (zero charge). However, except for some special cases (like the uniform electron gas), the hole is not spherically symmetric around the electron, thus leading to a nonvanishing *exchange (hole) dipole moment* (exchange hole quadrupole and higher moments are defined analogously).

At a given point in space r_1, the exchange dipole moment is given by

$$\mu_{X,\sigma}(\mathbf{r}_1) = \left[\frac{1}{\rho_\sigma(\mathbf{r}_1)} \sum_{ij} \int \mathrm{d}\mathbf{r}_2\, \varphi_{i\sigma}(\mathbf{r}_2)\mathbf{r}_2\varphi_{j\sigma}(\mathbf{r}_2)\varphi_{i\sigma}(\mathbf{r}_1)\varphi_{j\sigma}(\mathbf{r}_1)\right] - \mathbf{r}_1 \tag{65}$$

The exchange dipole moment $\mu_{X,\sigma}(\mathbf{r}_1)$ generates an electric field that induces a response in another fragment B and vice versa. One can therefore imagine an instantaneous, mutual interaction between exchange and induced dipole moments in fragments A and B, similar to the Coulomb correlation picture (see section 4.1). The resulting dipole−dipole interaction between two fragments in XDM is proportional to the square of the respective exchange dipole moment. Furthermore, the molecules are fragmented into atoms, and the square of the atomic exchange dipole moment $\langle {\mu_{X,A}}^2 \rangle$ is

$$\langle {\mu_{X,A}}^2 \rangle = \sum_\sigma \int \mathrm{d}\mathbf{r}\, w_A(\mathbf{r})\rho_\sigma(\mathbf{r}){\mu_{X,\sigma}}^2(\mathbf{r}) \tag{66}$$

The Hirshfeld partitioning $w_A(\mathbf{r})$ is the same as in the TS approach (see eq 51). Apart from the initially proposed XDM method, which is based on the exact exchange hole (eq 64), a linearly scaling variant based on the *local* Becke−Roussel exchange hole[212] was presented in 2005.[22] The Becke−Roussel (BR) model is a local approximation to the exact exchange hole. This way, the squared exchange dipole moment ${\mu_{X,\sigma}}^2(\mathbf{r})$ (see eq 66) can be obtained locally, thus avoiding the time-consuming integration over all space as in the exact exchange model (eq 65).

$${\mu_{\mathrm{BRX},\sigma}}^2(\mathbf{r}) = \left(\frac{\mathrm{e}^{-x}}{8\pi\rho_\sigma(\mathbf{r})}\right)^{2/3} x^2 \tag{67}$$

The variable x is dependent on the density and on its curvature (i.e., $\nabla{\rho_\sigma}^2$) and is determined at each point $\mathbf{r}$. We refer the interested reader to ref 22 for a detailed description of the Becke−Roussel variant. Because of the improved computational efficiency and similar performance for dispersion coefficients,[22,213] the BR model is most widely used and can be considered the default choice. However, all upcoming expressions are valid in principle for both forms (exact and BR exchange) of XDM, and thus, we will drop the index BRX.

The dispersion coefficient for two atoms can be expressed by a modified version of the Slater−Kirkwood formula:[4,83,211,214]

$$C_6^{AB} = \frac{\alpha_A^0\alpha_B^0\langle {\mu_{X,A}}^2\rangle\langle {\mu_{X,B}}^2\rangle}{\langle {\mu_{X,A}}^2\rangle\alpha_B^0 + \langle {\mu_{X,B}}^2\rangle\alpha_A^0} \tag{68}$$

Again, the static polarizability α_A^0 of atom A within the molecular environment is used. It is obtained via eq 49 using the static polarizabilities $\alpha_{A,\mathrm{free}}^0$ of the free atoms from ref 215. Similarly, from the higher-order exchange multipole moments, the respective dispersion coefficients can be derived,[84,134,210,216]

$$C_8^{AB} = \frac{3}{2}\frac{\alpha_A^0\alpha_B^0[\langle {\mu_{X,A}}^2\rangle\langle {\Theta_{X,B}}^2\rangle + \langle {\Theta_{X,A}}^2\rangle\langle {\mu_{X,B}}^2\rangle]}{\langle {\mu_{X,A}}^2\rangle\alpha_B^0 + \langle {\mu_{X,B}}^2\rangle\alpha_A^0} \tag{69}$$

and

$$C_{10}^{AB} = 2\frac{\alpha_A^0\alpha_B^0[\langle {\mu_{X,A}}^2\rangle\langle {\Omega_{X,B}}^2\rangle + \langle {\Omega_{X,A}}^2\rangle\langle {\mu_{X,B}}^2\rangle]}{\langle {\mu_{X,A}}^2\rangle\alpha_B^0 + \langle {\mu_{X,B}}^2\rangle\alpha_A^0} + \frac{21}{5}\frac{\alpha_A^0\alpha_B^0\langle {\Theta_{X,A}}^2\rangle\langle {\Theta_{X,B}}^2\rangle}{\langle {\mu_{X,A}}^2\rangle\alpha_B^0 + \langle {\mu_{X,B}}^2\rangle\alpha_A^0} \tag{70}$$

Analogous to $\langle {\mu_{X,A}}^2\rangle$, the $\langle {\Theta_{X,A}}^2\rangle$ and $\langle {\Omega_{X,A}}^2\rangle$ are the squared exchange quadrupole and octupole moment of atom A, respectively. For a derivation of these expressions, see refs 84 and 210. The atom pairwise dispersion energy is then given as

$$E_{\mathrm{disp}}^{\mathrm{XDM}} = -\sum_{AB}\sum_{n=6,8,10} \frac{C_n^{AB}}{R^n} f_{\mathrm{damp}}^{(n)}(R) \tag{71}$$

where ${f_{\mathrm{damp}}}^{(n)}(R)$ is the Becke−Johnson damping function from eq 42 with radii $R_0 = 1/3(\sqrt{C_8^{AB}/C_6^{AB}} + \sqrt{C_{10}^{AB}/C_8^{AB}} + \sqrt[4]{C_{10}^{AB}/C_6^{AB}})$.[187]

In recent years, the XDM method has been extended to include the three-body Axilrod−Teller−Muto term (see eq 43). The dispersion coefficient C_9^{ABC} is calculated via

$$C_9^{ABC} = \langle {\mu_{X,A}}^2\rangle\langle {\mu_{X,B}}^2\rangle\langle {\mu_{X,C}}^2\rangle \times \frac{Q_A + Q_B + Q_C}{(Q_A + Q_B)(Q_A + Q_C)(Q_B + Q_C)} \tag{72}$$

with $Q_A = \langle {\mu_{X,A}}^2\rangle/\alpha_A^0$. Because the ATM contribution to the dispersion energy varies significantly with the applied damping scheme,[134] it is not used by default in XDM.

Because of the density dependence, a self-consistent XDM treatment is possible and has been presented by Kong et al.[217] However, the effect on the electron density due to a self-consistent treatment is negligibly small. Therefore, first and second energy derivatives may be computed to a good

DOI: 10.1021/acs.chemrev.5b00533
Chem. Rev. XXXX, XXX, XXX−XXX

approximation without a preceding XDM-inclusive SCF procedure. Because the dispersion coefficients in XDM are indirectly dependent on the nuclear positions, geometry optimizations are somewhat hampered and the dispersion coefficients are often assumed to be fixed in the gradient calculation.[218]

Overall, the XDM model takes into account the electronic structure in two ways. Like in TS, the static polarizabilities are dependent on the Hirshfeld partitioning. Furthermore, the perturbing dipoles (quadrupoles and octupoles) are evaluated from the occupied orbitals (exact) or locally from the density (BR). However, the origin of the perturbation is different from the long-range perturbation theory definition of the dispersion energy. The former involves fluctuations in the density leading to transition dipoles (eq 24, and higher multipoles) involving virtual orbitals (Coulomb correlation). In XDM, the dispersion energy is derived from the perturbation due to an electron and its exchange hole, thus involving only occupied orbitals (or density) in the integration. Initially, the XDM model has been developed as a purely heuristic approach[211] that successfully mimics the zero-point electron density fluctuations, which are responsible for dispersion forces. However, in three independent studies it was shown that the latter may in fact be approximated by interacting exchange multipole moments.[219−221] In XDM, virtual orbitals are implicitly included within the employed atomic polarizabilities (see eqs 68−70). Good results for the XDM approach are reported, among them the best results published so far for any corrected DFT approach on the S12L set.[201]

A related approach has been presented by Heßelmann in 2012.[222] Different from XDM, this so-called weighted exchange-hole (WXhole) model does not rely on empirical data for the static polarizabilities of the atoms. Instead, the dynamic polarizabilies are directly computed within the exchange dipole model, partitioned to the atoms employing Hirshfeld scheme (eq 51) and used in the numerical integration of the Casimir−Polder integral (eq 26), which makes the method computationally more expensive.

4.1.7. Density-dependent energy correction. Steinmann and Corminboeuf modified the atom pairwise XDM model first by changing the damping function[223] and secondly by replacing the BR exchange model with a GGA variant (the BR model is of meta-GGA type).[224] In the first modification, the BJ damping is replaced by the universal damping function of Tang and Toennies (TT) (see eq 13).[114] Different from other commonly used damping functions, it not only depends on the distance between the atoms A and B but also on b, which itself is a function of the interatomic separation R (for clarity, we prefer the short-hand notation of b over the lengthy $b(R)$ notation). In addition, the rather involved function b depends on the Hirshfeld volumes, a Hirshfeld-based covalent bond index[225] for the atom pair AB, and the nuclear and Hirshfeld charges of the atoms A and B. Subsequently, it has been modified in the course of the development of the density-dependent energy correction (dDsC) method, and therefore we refer to the original refs 223, 224, and 226 for details. The damping function contains two empirical parameters that are fitted for each functional.[227] Furthermore, Steinmann and Corminboeuf made use of the Hirshfeld-dominant scheme where the standard Hirshfeld weights at position $\mathbf{r}$ are replaced by Hirshfeld-dominant atomic weights $w_A^d(\mathbf{r})$ that can only have binary numbers. $w_A^d(\mathbf{r}) = 1$, if atom A out of all atoms has the largest Hirshfeld partition weight (see eq 51) at position $\mathbf{r}$; otherwise, $w_A^d(\mathbf{r}) = 0$.

The second modification concerns the exchange hole model.[224] Here, a PBE-based[148,149] (i.e., a GGA variant instead of the BR meta-GGA form in XDM) exchange hole is used,

$$\mu_{\mathrm{dDsCX},\sigma}{}^2(\mathbf{r}) = (2sr_s\ \mathrm{e}^{-s})^2 \tag{73}$$

where the reduced density gradient[224] is

$$s = |\nabla\rho(\mathbf{r})|/(2k_\mathrm{F}\,\rho(\mathbf{r})) \tag{74}$$

with the local Fermi wave vector,

$$k_\mathrm{F} = (3\pi^2\rho(\mathbf{r}))^{1/3} \tag{75}$$

and r_s is the Wigner−Seitz radius $r_s = \sqrt[3]{3/(4\pi\rho(\mathbf{r}))}$. Within the expression in eq 73, two parameters were adjusted and fixed according to reference data for rare gas dimers.[224]

In contrast to XDM, only the dipolar term (i.e., C_6^{AB}) is taken into account. The effect of the higher-order multipole terms C_8^{AB} and C_{10}^{AB} was included in the "dDsC10" scheme but was not found to be significant for the overall performance.[226] A self-consistent treatment for dDsC was presented,[228] and the effect of the dispersion interaction on the electron density was found to be negligible. Although the accuracy of dDsC is comparable to standard XDM, a central advantage of most semiclassical dispersion corrections is lost. In dDsC, the generally simple structure of most damping functions (directly dependent on R) is replaced by a very involved scheme that requires integration over the entire Cartesian space (for the Hirshfeld volumes and bond indices) and is both directly and indirectly dependent on R. Therefore, in addition to the density-dependent dispersion coefficients, the density-dependent damping function further hampers the formulation of efficient analytical gradients.[227] However, for dispersion effects in the excited state, it might be advantageous that the damping function automatically adjusts to the electronic state.

4.1.8. Local-response dispersion model. The local-response dispersion (LRD) model by Sato and Nakai[229,230] is an atom pairwise, density-dependent dispersion correction. Derived form second-order perturbation theory, the Casimir−Polder equation (see eq 26), however, is solved ad hoc in an approximate fashion involving only the density (i.e., occupied orbitals).

The dispersion energy in LRD is given as

$$E_\mathrm{disp}^{AB,\mathrm{LRD}} = -\sum_{AB}\sum_{n=6,8,10}\frac{C_n^{AB}}{R^n}f_\mathrm{damp}^{(n)}(R) \tag{76}$$

The dispersion coefficients are obtained for different interaction terms arising from the multipole expansion of the Coulomb operator,

$$C_n^{AB} = \sum_{l_1,l_1',l_2,l_2'} C^{AB}(l_1l_1',\, l_2l_2') \tag{77}$$

Here, l_1, l_1', l_2, and l_2' are angular momentum quantum numbers and the sum is over all terms fulfilling the condition $l_1 + l_1' + l_2 + l_2' + 2 = n$. Because of their negligible impact on the dispersion energy, the $l_1 \neq l_1'$ and $l_2 \neq l_2'$ combinations are not considered.[15] For a set of l_1 and l_2 that lead to a given n, the dispersion coefficient $C^{AB}(l_1,l_2)$ is evaluated as

DOI: 10.1021/acs.chemrev.5b00533
Chem. Rev. XXXX, XXX, XXX−XXX

$$C^{AB}(l_1, l_2) = \frac{1}{2\pi} \sum_{m_1,m_1',m_2,m_2'} S^{AB(l_1l_2)}_{m_1m_2} S^{AB(l_1l_2)}_{m_1'm_2'} \times \int_0^\infty \alpha^{A(l_1l_1)}_{m_1m_1'}(i\omega)\alpha^{B(l_2l_2)}_{m_2m_2'}(i\omega)\, d\omega \quad (78)$$

Here, $S^{AB(l_1l_2)}_{m_1m_2}$ is a geometric factor taking into account the distance between the two atoms A and B as well as the orientation (via m_1 and m_2) of the interacting mulitpoles.[15] $\alpha^{A(ll)}_{mm'}(i\omega)$ is the *local* atomic l-pole−l-pole polarizability at an imaginary frequency ω. The local expression for the polarizability is derived from the local-response function proposed by Dobson and Dinte,[231]

$$\alpha^{A(ll)}_{m_m'}(i\omega) = \int d\mathbf{r}\, {w_{A,\mathrm{Becke}}}^2(\mathbf{r}) \frac{\rho(\mathbf{r})}{{\omega_0}^2 + \omega^2} \nabla R_l^m(\mathbf{r} - \mathbf{R}_A) \times \nabla R_l^{m\prime}(\mathbf{r} - \mathbf{R}_A) \quad (79)$$

where ${w_{A,\mathrm{Becke}}}^2(\mathbf{r})$ are the Becke weights,[232] $\rho(\mathbf{r})$ is the electron density at position $\mathbf{r}$, and R_l^m represents a solid harmonic. For $\omega_0(\mathbf{r})$, the expression proposed by Vydrov and Van Voorhis is used,[233]

$$\omega_0(\mathbf{r}) = {k_\mathrm{F}}^2 \frac{(1 + \lambda s^2)^2}{3} \quad (80)$$

where k_F is the local Fermi wave vector, s is the reduced density gradient as given in eqs 75 and 74, respectively, and λ is an empirical parameter. The damping function in eq 76 is given by

$$f^{(n)}_{\mathrm{damp}}(R) = \exp\left[-\frac{n-4}{2}\left(\frac{\bar{R}_{AB}}{R}\right)^6\right] \quad (81)$$

Here, $\bar{R}_{AB} = \kappa[(\alpha^0_A)^{1/3} + (\alpha^0_B)^{1/3}] + R_0$.[229] κ and R_0 are global constants that were fitted to rare gas potential energy curves from high-level CCSD(T) calculations.[234] The static polarizabilities are obtained as $\alpha^0_A = 1/3\mathrm{Tr}[\alpha^{A(11)}(0)]$, i.e., employing eq 79 for the dipole−dipole case at zero frequency. This type of damping function was first proposed by Kamiya et al. for the C_6 term.[235]

From its theoretical derivation, the LRD is related to the density-dependent, nonlocal ALL[209] dispersion correction (see section 4.2) and mainly differs by its atom pairwise partitioning of the dispersion energy. Interatomic and intermolecular dispersion coefficients are accurate to ∼6%,[230] i.e., comparable to the dispersion coefficients in the TS model (5.5%)[86] and in the D3 model (4.7%).[11] So far, it has been only combined with variants of the BOP GGA functional.[161,236,237] An extension of the LRD approach to systems in electronically excited states (employing the excited-state density) has been presented as well.[15] For a recent and more detailed review of the LRD approach, see ref 15. Related to LRD, although rarely used, is the dispersion correction by Alves de Lima.[238]

4.2. Nonlocal density-based dispersion corrections

In this subsection we will discuss the essential developments of nonlocal (NL) density-dependent dispersion corrections with a special focus on recent efforts. All methods discussed here share the common feature that they only need the electron density as input to compute the dispersion energy and the corresponding integral kernel depends nonseparably on two electron coordinates (hence, the name "nonlocal", which refers to the DFT context where (semi)local functionals normally depend locally only on a single position in space).

As an instantaneous electron-correlation effect, vdW interactions should basically be included in the exchange-correlation energy $E_\mathrm{XC}[\rho]$[239] for which, however, various approximate forms are used in practice. VdW density functionals (vdW-DFs) constitute a first-principles DFT treatment of medium- and long-ranged interactions by means of a nonlocal exchange-correlation functional. The specific form of the latter defines the various methods that will be described in the following. For a more comprehensive discussion and historical perspective, particularly of the Rutgers−Chalmers vdW-DFs, the reader is referred to the recent review articles of Langreth et al.[240] and Berland et al.[241] Furthermore, the review article by DiLabio and Otero-de-la-Roza[218] also contains a section about nonlocal density-based dispersion corrections.

Semiclassical methods that rely on the electron density to partition dispersion coefficients (e.g., XDM, TS, MBD, and LRD)[22,86,87,229] are described in section 4.1, and exchange-correlation functionals that solely depend on a local density expansion are discussed in section 4.3.

4.2.1. van der Waals density functionals. Nonlocal vdW functionals model the contribution of the dispersion energy arising from electron density fluctuations in distant regions of a system by explicitly accounting for the interaction of those distant parts. The nonlocal correlation energy reads

$$E_\mathrm{c}^\mathrm{NL} = \frac{1}{2} \int d\mathbf{r}\, d\mathbf{r}'\, \rho(\mathbf{r})\Phi(\mathbf{r}, \mathbf{r}')\rho(\mathbf{r}') \quad (82)$$

where $\Phi(\mathbf{r}, \mathbf{r}')$ defines the correlation kernel. Basically, nonlocal functionals calculate the same attractive dispersion interaction as the C_6-based approaches but without the use of a local partitioning. Because the correlation energy (eq 82) is defined for the entire range of interaction distances and is added to the semilocal exchange correlation without specifying atoms or fragments, nonlocal functionals are often referred to as "seamless". In contrast to similar approaches such as, e.g., RPA, all nonlocal functionals do not depend explicitly on the orbitals (neither virtual nor occupied). They only depend on the density and its derivatives. Usually, nonlocal vdW functionals are constructed with little empiricism. Early studies with fundamental impact on the development of dispersion functionals are, for example, those of Zaremba and Kohn[242] and of Rapcewicz and Ashcroft (RA).[243] In the latter study it was pointed out that the coupling between fluctuations gives rise to an attractive interaction, which originates in the lowest-order fluctuation term of the interacting electron gas. Unlike DFT, which is linked to densities, this interaction is linked to density fluctuations either via dynamical properties or via explicit excitations.

In the separated (nonoverlapping) fragments limit, the second-order perturbation theory expression for the dispersion interaction is given by eq 29. The central quantity is the density−density response function χ or charge density susceptibility,[244] i.e., the linear response of the electron density with respect to a local perturbation in the external potential with frequency ω,

$$\delta\rho(\mathbf{r}, \omega) = \int d\mathbf{r}'\, \chi(\mathbf{r}, \mathbf{r}', i\omega)\delta V^\mathrm{ext}(\mathbf{r}', \omega) \quad (83)$$

The RA work showed that a plasmon picture can be applied to formulate a theory of vdW interactions in an electronic liquid, and hence the long-term experience with LDA and GGA, which can also be formulated in terms of plasmons, was useful for the further developments leading to vdW-DF. The density−density response function is related to the dynamic polarizability[13,244] by (cf. section 4.1 and eq 26 on pairwise dispersion corrections)

DOI: 10.1021/acs.chemrev.5b00533
Chem. Rev. XXXX, XXX, XXX−XXX

$$\alpha_{ij}(i\omega) = \int \mathrm{d}\mathbf{r}\, \mathrm{d}\mathbf{r}'\, \mathbf{r}_i\, \mathbf{r}'_j\, \chi(\mathbf{r}, \mathbf{r}', i\omega) \tag{84}$$

with i and j denoting the components of the polarizability tensor. The charge density susceptibility of the whole system can be used to reformulate the adiabatic connection formula, leading to a formally exact expression for the correlation energy,

$$E_c = -\frac{1}{2\pi}\int_0^1 \mathrm{d}\lambda \int \mathrm{d}\mathbf{r}\, \mathrm{d}\mathbf{r}' \frac{1}{|\mathbf{r}-\mathbf{r}'|} \times \int_0^\infty \mathrm{d}\omega\, [\chi_\lambda(\mathbf{r}, \mathbf{r}', i\omega) - \chi_0(\mathbf{r}, \mathbf{r}', i\omega)] \tag{85}$$

with λ representing the coupling strength variable and χ_0 denoting the response function for the noninteracting system. In the KS scheme, it has an analytical expression,

$$\chi_0(\mathbf{r}, \mathbf{r}', i\omega) = -4 \sum_i \sum_a \frac{\omega_{ai}}{{\omega_{ai}}^2 + \omega^2} \varphi_i(\mathbf{r})\varphi_a(\mathbf{r})\varphi_a(\mathbf{r}')\varphi_i(\mathbf{r}') \tag{86}$$

where a runs over virtual and i runs over occupied orbitals and ω_{ai} represents the orbital energy differences. It should be noted that the explicit calculation of the response function χ_λ for an interacting many-body system is quite cumbersome for extended systems.

All modern vdW-DF variants are based on the functionals derived in the seminal works of Dobson and Dinte (DD)[231] and Andersson, Langreth, and Lundqvist (ALL),[209] published independently in 1996. The DD/ALL functionals have similar expressions and can be considered as modifications of the RA functional that employ the density-response function of the homogeneous electron gas,

$$\chi(\omega) = \frac{1}{4\pi}\left[1 - \frac{1}{\varepsilon(\omega)}\right] = \frac{1}{4\pi}\frac{{\omega_p}^2}{{\omega_p}^2 - \omega^2} \tag{87}$$

with $\varepsilon(\omega) = 1 - {\omega_p}^2/\omega^2$ denoting the dielectric function and $\omega_p = \sqrt{4\pi\rho}$ representing the plasmon frequency of the uniform electron gas with density ρ. Applying the local approximation to the plasmon frequency $\omega_p(\mathbf{r}) = \sqrt{4\pi\rho(\mathbf{r})}$, the DD/ALL dispersion energy can be written as

$$E_{\mathrm{disp}}^{\mathrm{DD/ALL}} = -\frac{3}{32\pi^2}\int \mathrm{d}\mathbf{r}\, \mathrm{d}\mathbf{r}' \frac{1}{{r_{12}}^6} \frac{\omega_p(\mathbf{r})\omega_p(\mathbf{r}')}{\omega_p(\mathbf{r}) + \omega_p(\mathbf{r}')} \tag{88}$$

A prerequisite of this functional is the requirement of nonoverlapping interacting systems. The calculation of the dynamical polarizabilities and the dispersion interaction coefficients can be carried out in the same fashion.[209] Note the close connection between eq 88 and London's formula (eq 1 and eq 22) for the vdW interaction between two atoms A and B separated by the distance R if only one excitation frequency $\omega_{A/B}$ is considered for each atom.

However, the DD/ALL theory also has several disadvantages. Similar to RA, it contains a cutoff that specifies the spatial regions where the response to an electric field is set to zero, and the results can be very sensitive to the specific cutoff value. Nonetheless, results based on DD/ALL compare reasonably well with those of first-principles calculations of several atoms and molecules.[245] Moreover, the DD/ALL functional provides one of the foundations for the development of the more general vdW-DF, which was proposed nearly a decade later. Furthermore, it proves that a functional with a quadratic density dependence can be used to model London dispersion forces.[209]

More recently, Gräfenstein and Cremer[246] combined a GGA with an efficient evaluation of the ALL energy (and forces) in a partitioning scheme which they denoted quasi-self-consistent-field dispersion-corrected density-functional theory formalism (QSCF-DC-DFT). More precisely, the long-range-corrected Perdew−Burke−Ernzerhof exchange functional and the one-parameter progressive correlation functional of Hirao and co-workers were combined with the ALL long-range correlation functional. The time-demanding self-consistent incorporation of the ALL contribution in the DFT iterations necessary for the calculation of forces is avoided due to a posteriori calculation of the ALL term and its gradient using an effective separation of the global and intramonomer coordinates. They found good agreement with coupled-cluster calculations for, e.g., the benzene dimer.[246]

Langreth and co-workers subsequently proposed modifications of the ALL functional for various systems, including, e.g., a nonoverlapping formulation with a cutoff to account for overlaps,[247] a study of parallel infinite jellium surfaces,[248] and a functional for layered structures called vdW-DF0.[249] The latter treats screening by solving the Poisson equation, i.e., mapping the calculation of E_c^{NL} onto an electrodynamics problem.[248]

Dispersion interactions are often connected with asymptotic formulas, and in order to deal with the singular behavior occurring at small separations, saturation functions have been introduced. However, dispersion forces are also important for chemical bonds and reactions and, hence, are relevant in an extensive region of medium-range separations. While nonlocal correlation at short and medium range arises from various different plasmon modes and electron−hole pair excitations, the asymptotic behavior is described by long-wavelength excitations, i.e., the plasmon model for the small wavevector limit. Moreover, the known constraints for the homogeneous electron gas should be retained.[250] Hence, a generally applicable vdW-DF should be able to seamlessly connect between the description of the covalent bond regime and noncovalent binding separations.

vdW-DF1, proposed in 2004 by Dion et al.,[251,252] is the first truly general vdW functional. In vdW-DF1, the correlation energy is given as the sum of a local part, represented by LDA correlation, and a long-range nonlocal part according to eq 82:

$$E_c^{\mathrm{vdW\text{-}DF1}} = E_c^{sr} + E_c^{nl} \tag{89}$$

An important condition for a "seamless" functional is that the nonlocal part of the correlation energy vanishes for the uniform electron gas in order to avoid double counting. In the vdW-DF1 functional, approximations are introduced to the adiabatic connection formula (eq 85) based on a second-order expansion of $S = 1 - \varepsilon^{-1}$ (ε is the dielectric function) with a plasmon pole approximation to its plane wave representation. Using these approximations, the adiabatic connection formula is integrated in the coupling constant λ. The resulting kernel (employed in eq 82) can be reformulated as a function of two variables d and d' that only depend on the electron density ρ, the distance between $\mathbf{r}$ and $\mathbf{r}'$, and the gradient of ρ at those points. Their expressions read

$$d = |\mathbf{r} - \mathbf{r}'| q_0(\mathbf{r}) \tag{90}$$

$$d' = |\mathbf{r} - \mathbf{r}'| q_0(\mathbf{r}') \tag{91}$$

where

DOI: 10.1021/acs.chemrev.5b00533
Chem. Rev. XXXX, XXX, XXX−XXX

$$q_0(\mathbf{r}) = -\frac{4\pi}{3}(\varepsilon_c^{\mathrm{LDA}}(\mathbf{r}) + \varepsilon_x^{\mathrm{LDA}}(\mathbf{r})[1 + \lambda s^2(\mathbf{r})]) \quad (92)$$

includes the correlation energy densities, LDA exchange, and the reduced density gradient,

$$s = \frac{\nabla\rho}{2(3\pi^2)^{1/3}\rho^{4/3}} \quad (93)$$

as well as the parameter $\lambda = 0.8491/9$ controlling the relative weight of the gradient correction. The kernel $\Phi(d,d')$ has a numerically complicated expression, including a spatial double integral. However, the existence of the intermediate d variables facilitates the precomputation of a lookup table for Φ, and hence its values and derivatives can be efficiently interpolated in the actual SCF calculation.

A self-consistent plane wave implementation of vdW-DF1 has been reported by Thonhauser et al.[253] and for Gaussian basis sets by Vydrov et al.[254] In both cases, analytic energy gradients needed for geometry optimizations are available. The self-consistent treatment ensures that the change of the electron density due to dispersion effects is accounted for. The computational demands for calculating the nonlocal correlation energy become the bottleneck in the case of a semilocal exchange functional. However, it is not more costly than evaluating the nonlocal Fock exchange energy contribution in a hybrid or range-separated hybrid functional.[254,255] More efficient implementations for plane wave basis sets have been reported,[256] as well as an AO-based linear scaling implementation.[257]

The main field of application for the vdW-DF1 functional is systems with extensive electron−electron delocalization (efficient three-dimensional incorporation of long-range correlation effects for the homogeneous electron gas) such as, e.g., physisorption, metal surfaces, and interactions with graphene, where semiclassical models are not reliable. A review of typical applications has been published by Langreth et al.[240] In the original implementation, the revPBE functional was used.[258] Several other exchange functionals have been explored by other authors.[259] Opposed to its success for many solid-state applications, vdW-DF1 tends to underestimate hydrogen bond strengths and to overestimate molecular separations.[88,233]

Addressing the major problems in vdW-DF1, particularly for molecular interactions in the overlapping regime, Lee et al. proposed an improved functional denoted vdW-DF2.[88] The over-repulsive revPBE functional was replaced with the revised version of the PW86 functional (rPW86).[88,260] Additionally, the coefficient controlling the gradient correction to LDA in eq 92 was changed using the known behavior in the large electron number limit.[261] An improvement is evident in the calculation of lattice energies and geometries of molecular crystals,[262] but the largest improvement is achieved for small molecules. vdW-DF2 greatly improves the interaction energies for small, noncovalently bound organic complexes compared to vdW-DF1 (see also section 5.4). However, some problems with bulk matter and weakly chemisorbed systems remain. The newest development, vdW-DF-cx,[263] is driven by the aim of using a modified exchange, which should consistently describe all relevant density regions and, hence, will also be able to describe weak chemisorption accurately.[263] The vdW-DF family of functionals, specifically vdW-DF2, are in widespread use nowadays in the physics community. They are implemented in popular solid-state program packages like VASP,[264−266] Quantum ESPRESSO,[267] and SIESTA,[268] as well as in Q-Chem[269] for molecular calculations.

4.2.2. Vydrov and Van Voorhis functionals. Vydrov and Van Voorhis (VV) constructed a functional called vdW-DF-09[233] that includes reference-system optimization also for the nonlocal part but basically retains all essential constraints of vdW-DF. To improve on the poor performance of the original vdW-DF approach for noncovalently bound molecular complexes, VV proposed several modifications that led to the VV09[270−272] and VV10 functionals.[89] VV analyzed the problems in the vdW-DF and its inability to couple with either long-range corrected functionals or nonlocal Fock exchange. The VV family of functionals includes a small number of adjustable parameters (one and two, respectively) but violates a few conservation laws enforced in the original vdW functionals by Langreth and co-workers.[271,272] However, due to the additional flexibility, the results are significantly improved for molecular complexes. Specifically, VV09 includes an adjustable parameter that is fitted in order to reproduce atomic C_6 values. The latter are known to be in severe error for vdW-DF functionals (in particular for vdW-DF2 with errors of ∼60%).[273] Additionally, VV09 and VV10 are applicable to spin-polarized (open-shell) systems, and the integral kernel in eq 82 is analytical.

VV10 is the most accurate (for molecular systems) yet simplest functional[89] in the VV family. In the original VV10 scheme, the exchange functional can either be revised PW86 (rPW86)[88,260] or LC-ωPBE (with $\omega = 0.45$). The former is denoted simply VV10 (parameters $C = 0.0093$ and $b = 5.9$; see Table 1) and the latter is LC-VV10 ($C = 0.0089$ and $b = 6.3$). In both of them, the semilocal correlation functional is PBE correlation, and they depend on a spatially varying gap $\omega_g(\mathbf{r})$ in the plasmon-dispersion model. The nonlocal correlation energy in VV10 can be written as given in eq 82. The correlation kernel is introduced ad hoc according to the VV's experience,

Table 1. Optimized Values for the b Parameter (in a.u.) of Various DFT-NL Methods (def2-QZVP Basis Set) Taken from the Work of Aragó et al.[277] for the S66[276] NCI Benchmark Set; The C Parameter (in a.u.) Is Kept at Its Original Value of 0.0093

hybrid	b	(meta) GGA	b	double hybrid	b
revPBE0	4.3	TPSS	5.0	PBE0-DH	8.3
revPBE38	4.7	rPBE	4.0	TPSS0-DH	6.8
mPW1PW	5.3	revPBE	3.7	revPBE0-DH	5.7
PW1PW	7.7	PBE	6.4	B2PLYP	7.8
PBE0	6.9	BLYP	4.0		
PW6B95	9.0	rPW86PBE	5.9		
B3PW91	4.5				
B3P86	5.3				
B3LYP	4.8				
TPSS0	5.5				
TPSSh	5.2				

$$\Phi(\mathbf{r}, \mathbf{r}') = -\frac{3}{2gg'(g + g')} \quad (94)$$

with (g' and related primed quantities analogously)

$$g = g(\mathbf{r}, \mathbf{r}') = \omega_0(\mathbf{r})|\mathbf{r} - \mathbf{r}'|^2 + \kappa(\mathbf{r}) \quad (95)$$

The other quantities read

DOI: 10.1021/acs.chemrev.5b00533
Chem. Rev. XXXX, XXX, XXX−XXX

$$\omega_0(\mathbf{r}) = \sqrt{\omega_g^{\,2}(\mathbf{r}) + \frac{\omega_p^{\,2}(\mathbf{r})}{3}} \tag{96}$$

with ω_p being the local plasma frequency (see above) and the local band gap[273]

$$\omega_g^{\,2}(\mathbf{r}) = C\cdot\left|\frac{\nabla\rho(\mathbf{r})}{\rho(\mathbf{r})}\right|^4 \tag{97}$$

C is a fitted parameter and the other component of g reads

$$\kappa(\mathbf{r}) = b\frac{\nu_F^{\,2}(\mathbf{r})}{\omega(\mathbf{r})} = b\cdot\frac{3\pi}{2}\left[\frac{\rho}{9\pi}\right]^{1/6} \tag{98}$$

where $\nu_F = (3\pi^2\rho)^{1/3}$ is the local Fermi velocity and b is another adjustable parameter introduced in VV10 (in addition to the C parameter already present in VV09).

To ensure that the long-range correlation energy vanishes in the uniform electron gas limit, it is defined as the nonlocal part plus a constant multiplied by the number of electrons in the system,

$$\begin{aligned} E_c^{VV10} &= E_c^{NL} + \beta(b)N_{el} \\ &= \int d\mathbf{r}\,\rho(\mathbf{r})\left[\beta + \frac{1}{2}\int d\mathbf{r}'\,\rho(\mathbf{r}')\Phi(\mathbf{r},\mathbf{r}')\right] \end{aligned} \tag{99}$$

with

$$\beta(b) = \frac{1}{32}\left[\frac{3}{b^2}\right]^{3/4} \tag{100}$$

The VV10 functional is rather easy to implement and yields an improved error statistic for molecular NCI benchmark sets,[255,274] which can be attributed to the flexibility provided by its adjustable, functional-dependent parameters, b and C. The latter, which was originally fitted on the S22[275] test set for optimum C_6 coefficients, is usually not refitted because its influence is rather small and changing this parameter, which determines the long-range behavior, will lead to artificially large or small C_6 coefficients. Fitting the short-range attenuation parameter b, however, is important to meet the functional characteristics (i.e., inherent underbinding and overbinding tendencies, respectively) and to avoid spurious medium-range contributions, which can strongly decrease the accuracy. This can be related to the various damping functions (eqs 13, 31, 41, 42, and 81), which have been introduced for the semiclassical dispersion models in section 4.1. Hujo and Grimme[274] were the first to show that the VV10 dispersion correction with an adjusted b parameter can be successfully coupled to different standard functionals in a similar way as the "functional name-D3" combination (termed DFT-NL in analogy to DFT-D3 or for specific functionals as "functional name-NL").

Table 1 gives an overview of fitted b values (for the S66[276] test set) for various DFT-NL methods in use.[277] The short-range damping parameter can be used to judge the capabilities of the underlying semilocal density functional to describe London dispersion interactions. The rather repulsive GGAs like revPBE and BLYP have parameters around $b \approx 4$ (larger VV10 contribution at short range) while the more attractive GGAs like PBE, B95, and all double-hybrid functionals need a stronger damped VV10 contribution with $b \approx 8$.

The results for the S66 set are given in ref 255, and the results for the S22 set are compared to other dispersion corrections in section 5.4 of this Review. The results of Vydrov and Van Voorhis[255] for the S66 benchmark set revealed that vdW-DF2 tends to underbind molecular dimers on average, specifically those involving aromatic systems. In contrast, the semilocal VV10 overbinds hydrogen bonds, but this is cured when using the long-range corrected version, LC-VV10, which works specifically well for interactions between small molecules.[255,278]

However, results for layered systems indicate an inferior transferability across length scales of VV10 compared to vdW-DF.[279,280] This shortcoming may be due to the crude mechanism used to account for the saturation of vdW interactions at shorter separations because the constraint-based mechanisms inherent to vdW-DF are missing. Furthermore, VV10 would yield the wrong infinite separation limit for highly polarizable materials like, e.g., two interacting graphene sheets. On the other hand, the VV10 framework can easily be adapted to accurately describe different classes of systems. For example, Björkman reported a special-purpose functional for layered systems[281] (VV10sol). VV10 can also easily be coupled with hybrid and double-hybrid functionals, thus leading to a better asymptotic exchange behavior.[255,274] Hujo and Grimme[274] also tried to obtain a general formula for the parameter b for hybrid density functionals dependent on the amount of the nonlocal Fock-exchange admixture (HF-NL was fitted for this purpose as a side product), but no simple relation between the optimum value of b and the amount of Fock exchange included could be found. Hence, they suggested to optimize b for every density functional individually. For molecules involving weak hydrogen bonds, which are significantly influenced by dispersion interactions, the VV10 functional (and to a lesser degree also the vdW-DF2) showed good performance in a study performed by the same authors.[282] Since dispersion corrections also influence the description of thermochemistry where strong bonds are typically formed, it has to be tested whether the VV10 dispersion correction also improves the performance of density functionals for thermochemistry and kinetics. Hujo and Grimme investigated this point in detail using the unbiased and large GMTKN30[283] thermochemical database. They combined various GGA density functionals and global hybrids with the NL part of VV10 and fit the latter to the S22 set of NCI energies by adjusting only one parameter, i.e., the GGA part was not modified. Furthermore, they noted that the estimated accuracy for asymptotic molecular dispersion coefficients is slightly superior for D3 compared to VV10. The NL correction was applied nonself-consistently, i.e., a standard SCF run with the semilocal (hybrid) potential was performed first, and the E_c^{VV10} term based on the converged density was added. All VV10-type functionals performed well for the complete GMTKN30 database with an overall accuracy comparable to that of the respective DFT-D3 methods. Notably, the density-based dispersion correction produced smaller errors for some important chemical reaction energies while the accurate description of noncovalent interactions was still preserved. Possible electron-correlation double-counting effects were found to be of overall minor relevance. In agreement with the findings reported in ref 89, it is observed that the VV10 correction works best with rather repulsive functionals, i.e., those that give no significant binding for vdW complexes. Compared to the other tested VV10-type functionals, B3LYP-NL provides the best accuracy for basic properties, reaction energies, and the complete GMTKN30 database, while still yielding reasonably accurate results for noncovalent interactions.

Different from semiclassical corrections, vdW-DFs work well for metals for which partitioning of dispersion forces into atomic contributions is not well-defined. In a recent study[183]

DOI: 10.1021/acs.chemrev.5b00533
Chem. Rev. XXXX, XXX, XXX−XXX

investigating the thermochemistry of reactions involving large transition metal complexes in which long-range intramolecular London dispersion interactions contribute significantly to their stabilization, it was found that both modern dispersion-corrected density functionals, PW6B95[284]-D3(BJ) and B3LYP-NL, agree well with the experimental and theoretical DLPNO-CCSD(T)[23] reference reaction energies. Hence, the local dipole polarizability model in VV10 seems to reflect the change in the electronic environment in the reaction quite well, and the problem of computing dispersion effects for transition metal complexes seems to be less severe than often claimed. The very good agreement between conceptually quite different dispersion corrections (VV10 vs D3) is encouraging. For a comprehensive discussion on the performance of dispersion-corrected DFT methods for organometallic complexes, the reader is referred to the recent review article by Sperger et al.,[285] and for a general view on the role of noncovalent interactions in transition metal coordination, see the article by Petrović et al.[286]

A self-consistent implementation of VV09 and VV10[287] including analytic gradients for geometry optimizations is available in the Q-Chem program package.[269] Single-point energy calculations with VV10 (and other DFT-NL variants; see Table 1) on molecules can be also performed with the ORCA quantum chemistry program,[288] while the version implemented in TURBOMOLE[289] can also compute analytical gradients.

4.3. Effective one-electron potentials and further aspects

Although the London dispersion interaction arises due to correlated electron movement and is intrinsically a two-particle interaction, it can be empirically described to some extent via effective one-electron potentials. As we have seen in the previous sections, it is indeed possible to describe London dispersion by just knowing local properties such as the local dynamic polarizability. However, the methods reviewed in this section try to describe dispersion interactions even without nonlocal density information or considering dynamical (frequency-dependent) properties. Basically, two different one-electron approaches are commonly used: atom-centered external potentials (which are normally applied to efficiently model core electrons) and semilocal density functionals, which are capable of describing dispersion interactions at least in the overlapping region.

4.3.1. External potentials. The idea of dispersion-corrected atom-centered potentials (DCACPs) can be explained by early works of Feynman.[290] The London dispersion force between two separated atoms is interpreted as arising from distorted charge distributions with higher concentrations between the nuclei compared to the free atoms. This distortion from the central symmetry induces a dipole moment in each atom, which leads to an effective attraction of the positively charged nuclei. In this case, the nuclei are attracted by the distorted charge distribution of their own electrons.[291] This distorted charge distribution due to dispersion has been demonstrated recently for two interacting Drude oscillators.[292] Although it does not describe the physical origin of dispersion interactions, the Feynman picture can be used to explain the effective attractive force and why it may be modeled through modified external potentials. This picture does not involve the "cause" of dispersion effects, which are rooted in instantaneous electron correlations and not in static dipoles.

Röthlisberger, von Lilienfeld, and co-workers describe London dispersion by adding atom-centered potentials to the external potential otherwise generated solely by the nuclei.[293,294] Early applications include weakly bonded complexes of aliphatic and aromatic carbon compounds, biomolecules, hydrogen-bonded systems, and adsorption on graphite surfaces.[295−298] Similar approaches were proposed by Sun et al. combining local atomic potentials with GGA density functionals in a converged plane wave basis set.[299] DiLabio and co-workers designed dispersion-correcting potentials for global and range-separated hybrid functionals, which are evaluated in a fixed Gaussian orbital basis set of small and medium size.[300−302] DCACPs specifically designed for a certain DFA/basis set combination are typically called "DCPs" in the literature. Recently, a DCP variant in combination with the D3 dispersion correction has been published.[303] The D3 covers the long-range part, while the DCP improves the semilocal density functional description in the medium-range and bonded region.

For the mathematical form of the potentials, projected Gaussian functions corresponding to different angular momenta are typically used,

$$r^2 V_{\mathrm{ext}}^{\mathrm{DCACP}}(r) = \sum_l \left[\sum_{k=1}^{m_l} r^{n_{lk}} C_{lk} \exp(-\alpha_{lk} r^2) \right] P_l \tag{101}$$

where r is the distance from the nuclei, P_l is the projection corresponding to the angular momentum l, and the coefficients C and exponents α have to be optimized on certain training sets for the considered elements. These forms are not uncommon and are normally used, for example, to replace core electrons of heavy elements to effectively describe their relativistic behavior[304,305] and correct for self-interaction errors in GGA density functionals[306,307] or underestimated band gaps, respectively.[308] They are available in all major quantum chemistry codes and have a high degree of flexibility. This flexibility can be used to adjust the external potential on large reference databases. The "first-generation" DCACPs have been calibrated against MP2 reference data,[309,310] and later versions are optimized on basis set converged CCSD(T) reference energies. A summary of the parametrized elements is given in Table 2. The original DCACP potentials are parametrized with the Goedecker or Troullier−Martins pseudopotentials for different GGA density functionals (PBE, BLYP, and BP86) and are available for organic as well as rare gas elements. The DCP potentials are typically designed with the B3LYP hybrid functional for the elements H, C, N, and

Table 2. Summary of Available Dispersion-Corrected Atom-Centered Potentials

	DCACP		DCP	
element	Goedecker[a]	Troullier−Martins[a]	CP corrected[b]	non-CP corrected[b]
H	yes	yes	yes	yes
B	yes	yes	yes	yes
C	yes	yes	yes	yes
N	yes	yes	yes	yes
O	yes	yes	yes	yes
S	yes	yes	no	no
He	yes	yes	no	no
Ne	yes	yes	no	no
Ar	yes	yes	no	no
Kr	yes	yes	no	no

[a]Elements H, C, B, O, He, Ar, and Kr from ref 309. S from ref 310 tested for the PBE, BLYP, and BP density functionals. [b]Parametrization for H, C, N, and O done on B3LYP/6-31+G(2p,2d) level either with or without a counterpoise (CP) correction (other functionals and basis sets have been tested as well).[35,300,301]

DOI: 10.1021/acs.chemrev.5b00533
Chem. Rev. XXXX, XXX, XXX−XXX

O. This limited list (originating from the parametrization problem) directly translates to a restricted applicability, which is not the case for most of the other modern dispersion corrections considered in this Review.

In contrast to the C_6-based, post-SCF energy corrections, the DCPs influence the SCF by the additional external potential. Due to the nonspherical symmetry of the potential for $l > 0$, electron densities in different chemical environments behave differently. For instance, the DCPs are able to distinguish sp^2 and sp^3 carbons (type-A effects), which is a prerequisite for an accurate London dispersion correction. Although the current forms of DCPs do not reproduce the correct $1/R^6$ London limit correctly, it is in principle possible to improve this behavior by inclusion of a more complete set of (high l) potential functions. However, this also increases the numerical and parametrization complexity. While the three-center ECP-type integrals are typically evaluated much faster than the four-center integrals needed for the Coulomb energy, small exponents combined with a high angular momentum function can hamper the SCF convergence significantly. To which extent higher-order effects (many-body interactions and higher multipoles) can be fitted into the DCP parameters is currently not clear. Although a direct inclusion of the correct physical interactions is often superior to an "overfitting" prone determination of a too large parameter set, this has to be specifically tested on benchmark systems. The recent composite method of DiLabio and co-workers (B3LYP-DCP/6-31++G(2p,2d)) shows excellent performance on small NCI benchmark sets like S22 and S66.[35]

4.3.2. Semilocal functionals. Fundamentally different one-electron approaches are the various semilocal density functionals that incorporate London dispersion forces in the medium distance range by construction of the functional form. In all semilocal functionals the correlation kernel is expressed in a finite expansion of the local density, which decays exponentially.[311,312] Thus, long-range vdW interaction with the $-1/R^6$ behavior cannot be described. However, in a noncovalently bonded complex around the equilibrium distance, both fragments have a significant WF/density overlap; thus, it is possible to extract information about the attractive dispersion interaction from the accumulated density and its distortion.

Early density functional developments have already been tested for their capabilities to describe binding energies and geometries of nonbonded systems like rare gas dimers or π-stacked benzene dimers (see section 3). Standard global hybrid functionals like B3LYP[53,54] perform rather badly.[276,313] Progress was made with the X3LYP functional for rare gas dimers and strongly hydrogen-bonded systems, but the benzene dimer could not be described well.[314−316] A combination of Hartree−Fock exchange and Wilson−Levy correlation was used for studying weakly bonded systems with reasonably accurate results.[317]

A step forward in functional development was achieved by using Taylor expansions in the exchange-correlation functionals and incorporating higher orders in the gradient derivative. These functionals typically depend on the local spin density ρ_σ, its dimensionless derivative $s_\sigma = \frac{|\nabla \rho_\sigma|}{\rho_\sigma^{4/3}}$, and the local kinetic energy density $\tau_\sigma = \sum_i |\nabla \varphi_{i\sigma}|^2$. The Tao−Perdew−Staroverov−Scuseria (TPSS) meta-GGA functional (and its hybrid variant TPSSh)[318,319] can describe rare gas dimers around their equilibrium distances reasonably well (although not accurately) but fail for larger vdW complexes and, of course, cannot reproduce the correct long-range behavior.[319,320] A specifically refitted Perdew−Wang functional in a hybrid model (mPW1PW) was also able to describe some rare gas dimers with satisfying accuracy.[321] Becke optimized the exchange-correlation functional by a systematic Taylor expansion and fitted the dozens of parameters toward thermochemical reference data,[151] leading to the widely used B97 form. Although it was not without criticism, Handy and co-workers investigated the capabilities of these flexible forms[322,323] further without considering explicit dispersion corrections but obtained only limited improvement for some noncovalently bound systems.

The usage of a flexible functional form with extensive parameter fitting on huge reference data sets was brought to perfection by Truhlar and co-workers in the Minnesota functional family. Their general strategy with a detailed benchmarking (in comparison with other approaches) is outlined in ref 324. A sketch of the successive developments is summarized in Figure 11, sorted chronologically and according

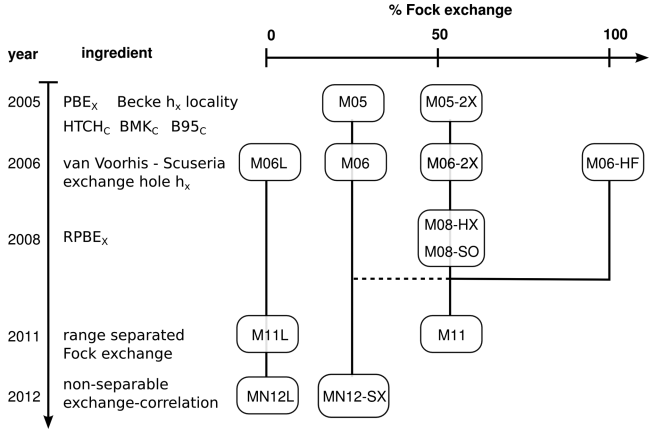

Figure 11. Development of the Minnesota functional family.

to the amount of Fock exchange included. The design strategy of all Minnesota functionals is similar. First, a parametrized expansion of the exchange-correlation terms is introduced. Then, the parameters are fitted on a broad set of reference systems, generating various parameter sets for different target properties. Typically, a meta-GGA for organometallic systems, a large Fock-exchange (up to 100%) variant for excitation energies, and a general purpose functional with a medium amount of Fock exchange is generated. Finally, the accuracy of the density functional is tested on benchmark sets that differ from the training set used for the parameter determination.

In the first development (M05[325] and M05-2X[325−327]), the exchange takes the following form

$$E_x^{\mathrm{M05}} = \sum_\sigma \int \mathrm{d}\mathbf{r}\, \epsilon_{x\sigma}^{\mathrm{PBE}} \left(\sum_{i=0}^{m} a_i \omega_\sigma^i \right) \tag{102}$$

The basis is the PBE[148,149] exchange-energy expression multiplied by a series expansion using the Becke measure of the exchange-hole locality[328] $\omega = \frac{\tau^{\mathrm{unif}}/\tau - 1}{\tau^{\mathrm{unif}}/\tau + 1}$ to the order $m = 11$. Some coefficients a_i are fixed by certain constraints (e.g., $a_0 = 1$ to recover the uniform electron gas limit), while the rest are treated as free parameters. The M05 correlation is based on ingredients from the HCTH,[323] BMK,[329] and B95[330] functionals with 10 free parameters. In the next generation (M06-L,[331] M06,[332] M06-2X,[332] and M06-HF[333]), an additional contribution from the Van Voorhis and Scuseria functional is used[334]

DOI: 10.1021/acs.chemrev.5b00533
Chem. Rev. XXXX, XXX, XXX−XXX

$$E_x^{\mathrm{M06}} = \sum_\sigma \int \mathrm{d}\mathbf{r} \left[\epsilon_{x\sigma}^{\mathrm{PBE}} \left(\sum_{i=0}^{m} a_i \omega_\sigma^i \right) + \epsilon_{x\sigma}^{\mathrm{LDA}} h_x(s_\sigma, \tau_\sigma) \right] \tag{103}$$

depending on the density gradient s_σ and the kinetic energy density τ_σ. At the same time, the correlation energy is expanded with ingredients from the same work of Van Voorhis and Scuseria,[334] leading to a total of 32 parameters that have to be fitted. In further developments, M08,[335] M11,[336,337] and MN12[338−340] mixing of RPBE exchange,[341] range separation of the Fock exchange, and a combined (nonseparable) exchange-correlation series are successively introduced. Hundreds of reference points are employed for the parameter training containing atomization energies, ionization potentials, electron affinities, proton affinities, barrier heights, noncovalent interactions, transition metal ligand energies, alkyl bond dissociations, isomeric reactions, excitation energies, bond lengths, and vibrational frequencies. In the latest forms,[338] both exchange and correlation are expressed in a general Taylor expansion generated by different powers of functions depending on the density ρ, its dimensionless gradient s, and kinetic energy density τ without physical constraints on the parameters c_{ijk}:

$$E_x^{\mathrm{MN12}} = \sum_\sigma \int \mathrm{d}\mathbf{r} \left[\epsilon_{x\sigma}^{\mathrm{LDA}} \sum_{i=0}^{3} \sum_{j=0}^{3-i} \sum_{k=0}^{5-i-j} c_{ijk}^x f_1(\rho_\sigma)^i f_2(s_\sigma)^j f_3(\tau_\sigma)^k \right] \tag{104}$$

The authors argue that the exchange functional does not need to obey the spin-scaling relations and in this way additionally accounts for correlation effects.

The Minnesota functionals have been shown to perform excellently for thermochemistry and kinetics on large databases.[283,324,342] The success of the Minnesota functionals to model noncovalent interactions is related to its gradient derivatives. Specifically, the kinetic energy term is semilocally dependent on the Kohn−Sham orbitals (rather than the density).[343,344] In this sense, all meta-GGAs are semilocal in the orbitals, which is not necessarily translated into a locality in the density. The Minnesota functionals use this orbital-dependent nonlocality to empirically fit London dispersion interactions into the density functional by choosing proper training sets for the parameter fit. However, the accuracy for noncovalent interactions is only of medium quality. While the M06L and M06-2X functionals perform best for NCIs among their functional family, the atom pairwise approaches are superior without higher computational costs (see next section). This is partially due to the lack of the long-range $-C_6/R^6$ contribution, and it has been shown that inclusion of an additional dispersion correction (e.g., D3(0)) can improve this deficiency[183,313] (some examples are also shown below). Another problem for practical applications is the strong grid dependence of most Minnesota functionals and the slower convergence with respect to the one-particle basis set expansion.[345] This is especially pronounced in geometries far from equilibrium as shown in several studies.[255,346] A recent one on rare gas dimers demonstrated that nearly all Minnesota functionals give unphysical dissociation curves with none or multiple potential minima.[347]

A related meta-GGA functional was recently constructed by Perdew and co-workers.[348] The strongly constrained and appropriately normed (SCAN) functional also relies on expansions of the exchange-correlation functional:

$$E_x^{\mathrm{SCAN}} = \sum_\sigma \int \mathrm{d}\mathbf{r}\, \epsilon_{x,\sigma}^{\mathrm{unif}} F_x(s_\sigma, \alpha_\sigma) \tag{105}$$

The exchange enhancement factor F_x is much more flexible compared to the original PBE version and is based on the density gradient s_σ and a dimensionless kinetic energy density $\alpha_\sigma = \frac{\tau_\sigma - \tau_\sigma^W}{\tau_\sigma^{\mathrm{unif}}}$, which is related to the Weizsäcker kinetic energy and scaled by the uniform electron gas limit. The latter variable distinguishes between different bonding situations, for instance, a covalent single bond ($\alpha_\sigma = 0$), a metallic bond ($\alpha_\sigma \approx 1$), and a weak vdW bond ($\alpha_\sigma \gg 1$). Contrary to the approach of Truhlar and co-workers, in the SCAN functional most parameters are determined by fulfilling exact constraints, and only seven remaining parameters are fitted empirically to reference energies. Although a limited set of free parameters is exploited, the SCAN functional seems to perform similarly to M06L for the S22 set and also captures some portion of medium-range dispersion interactions. Again, this should be significantly improvable by adding a long-range dispersion correction. Because it is a problematic issue in the related Minnesota functional family, the grid and basis set dependence of the SCAN functional has yet to be tested.

4.3.3. Dispersion-mimicking and dispersion-compensating effects. Some approximations in quantum chemical approaches can lead to attractive interatomic forces that artificially mimic dispersion effects. However, all those mentioned below share the unpleasant property that they are due to some kind of inconsistency in the electronic structure description or the way the calculations are typically conducted and hence do not have the correct asymptotic distance dependence. Solvation and entropy effects counteract the dispersion energy, thus leading to a subtle balance between these omnipresent physical forces, particularly relevant for reactions in solution.[198,349]

Basis set superposition error. The most abundant among the dispersion mimics is the attractive force arising from the basis set superposition error (BSSE) between overlapping molecular fragments. It is omnipresent in all MF approaches, which are based on atom-centered basis set expansions. The BSSE mimic of dispersion effects is most strongly pronounced for small Gaussian double-ζ basis set expansions such as in the widely used B3LYP/6-31G* approach, where this issue was analyzed in detail.[350] Although the error cancellation between the neglect of dispersion correction and the BSSE may work in some cases, it is not systematic (different dependence on the fragment separation) and can lead to significant errors in interaction energies, thermochemistry, and bond distances.[351] Given that simple schemes exist to systematically correct for both BSSE and dispersion at negligible cost, relying on this type of error cancellation is generally not justified and should be avoided.[352]

Range-separated exchange. Artificial attractive forces may furthermore arise from the use of range-separated hybrid (RSH) functionals. This effect was first noticed by Hirao and co-workers[235] and later confirmed in other studies.[353,354] Hirao and co-workers showed that a RSH of the BOP functional in combination with a dispersion correction performed better for van der Waals complexes compared to the respective GGA. In the context of isodesmic reactions, Johnson et al.[355] state that "GGAs effectively overestimate the effect of repulsion between the 1,3-carbons in *n*-alkanes. [...] The inclusion of dispersion, long-range exact exchange, or MP2 correlation, each act to reduce this bias, restoring the good agreement with reference

DOI: 10.1021/acs.chemrev.5b00533
Chem. Rev. XXXX, XXX, XXX−XXX

data." Apparently, the range separation of the exchange potential leads to an inconsistent description of the Pauli exchange-repulsion energy (cf. E_{EXR} in eq 9). In any global hybrid functional (including the two extrema $a_x = 0$ and $a_x = 1$; see eq 5), the E_{EXR} will have a destabilizing effect on the supramolecular complex *AB*. In typical RSH functionals, an attractive force between two fragments can arise due to the smaller (less-repulsive) E_{EXR} contribution from DFA exchange at short range compared to the larger (more-repulsive) Fock exchange at long range. This leads to minima in the NCI distance regime without applying any dispersion correction.[235,353] The magnitude of this attractive interaction consequently depends on the extent and shape of range separation as well as the underlying DFA. It should be noted that, depending on the density functional, this effect may be reversed and the RSH variant may become more repulsive.[235] In cases where the range separation leads to an attractive force, one should be aware that it is not related to the origin of dispersion forces (correlation effect), and consequently, neither the asymptotic behavior nor the interaction strength is described correctly.

Nevertheless, together with various dispersion-correcting schemes, the flexibility of RSH functionals to tune the attractive behavior in the medium-range has been exploited to obtain an improved transition between the long-range (London dispersion) and short-range correlation regimes.[147,235,356,357] An extensive study has recently been conducted resulting in the ωB97X-V functional (i.e., a RSH with VV10 correction).[357] A review on RSH functionals has been published recently.[358]

Subsystem DFT. Subsystem density functional theory (also termed DFT-in-DFT embedding) has been developed as an alternative to conventional DFT for large systems.[359] Early works on weakly bonded vdW systems with an approximate kinetic energy functional for the subsystem coupling showed an improved description compared to the plain KS-DFT treatment. In this context, the PW91 functional has shown improved van der Waals bonding distances and energies when applied in the framework of Kohn−Sham DFT with constrained electron density.[360,361] However, similar to the two cases mentioned above, the additional attraction arises from an unphysical and unbalanced treatment of the intrasubsystem interaction compared to the intersubsystem interaction. A recent study analyzed this behavior in detail.[362] It was shown that subsystem DFT fortuitously reproduces the interaction energy at the equilibrium distance reasonably close to the reference, while the true minimum occurs at too short distances and is energetically strongly overbound. Furthermore, the shape of the potential energy surfaces strongly depends on the underlying DFA and the choice of the kinetic energy approximation. Intrinsically more-repulsive functionals can be corrected via additional dispersion terms.[362] Because of the overly attractive behavior, this is not possible with reasonable accuracy for PW91. In our view, the ideal subsystem DFT treatment should not aim at reproducing reference energies of weakly bound complexes but rather should stay as close as possible to the full KS result. In this way, one will be able to describe larger systems and use the methodologies presented here to correct for missing London dispersion interactions in a physically sound manner.

Compensating effects. There are physical effects that, at least partially, compensate the omnipresent, attractive intermolecular dispersion interactions in nearly all cases, and the two most important are mentioned here: solvation and entropy.[198,349] As an example we will take a typical supramolecular (intermolecular) association reaction "host + guest → complex". The pincer system **3a** from the S12L benchmark set[198] will be taken as an example to show the various contributions that counteract the dispersion energy. As in most of these chemical problems, equilibrium situations are considered, and hence the Gibbs free energy ΔG has to be computed (at 298 K under standard conditions). Table 3 shows the data that are added up in a dispersion-corrected DFT treatment including the continuum model derived solvation free energy ΔG_{solv} as computed by COSMO-RS[363] for CH_2Cl_2 (for details, see ref 198).

Table 3. Contributions to Interaction (Free) Energies (kcal/mol) for the Association of a Pincer Molecule with an Unsaturated π-System To Form a Supramolecular Complex (See Figure 12 for a Sketch of the Structure); The Term $E \rightarrow G_{TRV}$ Denotes the Gas-Phase Correction from Energy to Free Energy (Solvent: CH_2Cl_2)

contribution	energy
$\Delta E_{DFT(TPSS)}$	5.5 (unbound)
$\Delta E_{D3^{atm}}$	−29.5
$\Delta E_{DFT\text{-}D3^{atm}}$	−24.0
$\Delta(E \rightarrow G)_{TRV}$	17.6
ΔG^{gas}	−6.4
$\Delta(G_{gas} \rightarrow G_{solv})$	5.4
$\sum = \Delta G^{calc}$	**−1.0**
ΔG^{exptl}	**−2.3**

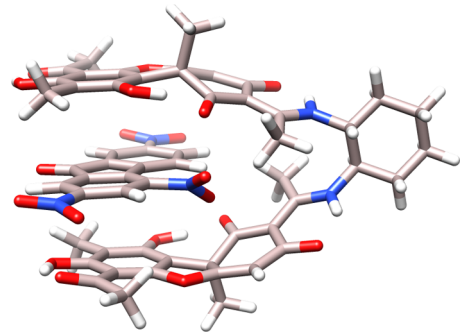

Figure 12. Molecular structure of the pincer complex with 4-chloro-7-nitro-benzofurazane (126 atoms, system **3a** from the S12L benchmark set).

According to these data, the strong gas-phase interaction is totally dominated by the dispersion energy. The resulting dispersion-corrected interaction energy of −24 kcal/mol is quenched dominantly by entropy (one complex is formed out of two molecules) and a solvation penalty of ∼5 kcal/mol (the complex has a smaller solvent-accessible surface for vdW interactions with the solvent than the separated fragments). The values given above are typical for complexes of this size (100−200 atoms) and common organic solvents.[95] They show that the counteracting attractive and repulsive effects are sizable and of the same order of magnitude. Hence, an overall accurate treatment for the resulting small free association energy of only a few kcal/mol requires accurate calculations for all individual contributions. Although such a basically nonempirical ansatz is computationally nontrivial, specifically for the solvation term, eventually not only a reasonable final value is computed but also further chemical insight can be gained by the analysis of the separate contributions.

DOI: 10.1021/acs.chemrev.5b00533
Chem. Rev. XXXX, XXX, XXX−XXX

4.3.4. Dispersion in periodic systems. Our general description of the various interactions in the previous paragraphs was mostly based on a molecular chemistry picture. However, modern materials and interfaces are usually modeled as crystals with periodic boundary conditions. For electrostatic interactions, the periodic picture introduces problems of diverging energy contributions, which can be efficiently handled by modern variants of the Ewald summation.[364,365] As demonstrated above, the leading term in the London dispersion interaction decays with $1/R^6$, and thus a three-dimensionally integrated dispersion contribution decays with $1/R^3$ (cf. Figure 13). For the D2 and TS schemes, Ewald summations have been implemented in some program packages (e.g., VASP[265]). Alternatively, the dispersion energy can be evaluated in real space as a sum with certain cutoff radii,

$$E_{\mathrm{disp}}^{(6)} = -\lim_{k\to\infty} \sum_{A,B} \sum_{\mathbf{T}\in\mathcal{P}_k} \frac{C_6^{AB}}{|\mathbf{R}+\mathbf{T}|^6} \tag{106}$$

where $\mathbf{T}$ runs over all translationally invariant vectors (multiples of unit cell vectors) within the cutoff sphere $\mathcal{P}_k$. Because of the fast convergence, a real-space cutoff of ∼50 Å is generally sufficient. The higher-order terms (both in the multipole and in the many-body sense) decay even faster, and smaller real-space cutoffs are then applicable. Especially for molecular crystals or larger interfaces with only a few symmetry elements and large unit cells, the reciprocal space scheme is no longer efficient and the real space summation is usually preferred.

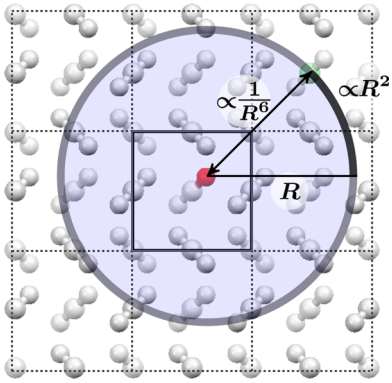

Figure 13. Exemplifying the real space summation of dispersion interactions on the (001) projection of the CO_2 crystal. Because the leading interaction decays with $1/R^6$ and the surface of additional contributions increases with the square of the distance R^2, the integrated interaction converges rapidly with $1/R^3$.

However, for semiempirical methods or classical force fields, the summation of dispersion interactions can be a substantial part of the computational costs. For these situations and for highly symmetric crystals, it might be advantageous to sum up parts of the interaction in reciprocal space. Using established integral identities,[366] the dispersion energy can be computed as

$$E_{\mathrm{disp}}^{(6)} = -\sum_{A,B} \sum_{\mathbf{T}\in\mathcal{P}_k} \frac{C_6^{AB} g_6(\beta|\mathbf{R}+\mathbf{T}|)}{|\mathbf{R}+\mathbf{T}|^6} - \frac{\pi^{3/2}\beta^3}{V} \sum_m f_6\left(\frac{\pi|m|}{\beta}\right) \sum_{A,B} C_6^{AB} \exp(-2\pi i m R) + \frac{\beta^6}{18} \sum_A C_6^{AA} \tag{107}$$

where the interaction is separated via the parameter β into a short-range regime evaluated in real space (first sum) and a long-range regime evaluated in reciprocal space (second sum). The last term removes the self-interaction terms arising for $R = 0$. The reciprocal (Fourier) part is normalized by the unit cell volume V, and the "switching functions" can be expressed via the complementary error function,

$$f_6(x) = \frac{1}{3}[(1-2x^2)\exp(-x^2) + 2x^3\sqrt{\pi}\,\mathrm{erfc}(x)] \tag{108}$$

$$g_6(x) = \left(1 + x^2 + \frac{1}{2}x^4\right)\exp(-x^2) \tag{109}$$

Modern implementations of the (particle mesh) Ewald summation have a favorable $O(N\log(N))$ scaling with system size N compared to the $O(N^2)$ scaling for real space summation.[365,367]

Nearly all of the methods introduced above have been implemented into standard quantum chemistry methods, which can handle periodic boundary conditions with different basis set schemes. Specifically, these are (projector-augmented) plane-wave basis sets (VASP[265] and QuantumEspresso[267]), local Gaussian basis sets (CRYSTAL,[368] Gaussian,[369] TURBOMOLE,[289] and Siesta[268]), Slater-type basis sets (ADF BANDS[370]), and numerical basis sets (FHI-AIMS[371]), and also combinations of Gaussian and plane-wave basis sets are in use (CP2K[372]).

4.3.5. Dispersion-corrected semiempirical MO methods. Semiempirical molecular orbital (SE-MO) methods are low-cost mean-field approaches that are approximations to either the HF or the KS-DFT problem (for recent articles reviewing SE-MO methods, see refs 373−375). Similarly, dispersion interactions are not captured by SE-MO approaches, and thus, they require dispersion corrections as well. Typically, SE-MO methods employ minimal basis sets and approximations, e.g., neglect of diatomic differential overlap (NDDO), in the evaluation of the costly two-electron integrals. For the latter, empirical element-specific parameters are introduced that have to be fitted to experimental or theoretical benchmarks. These approximations lead to a significant reduction of the computational cost by up to 4 orders of magnitude compared to the DFT or HF MF methods. In Figure 14, we highlight the different approximations leading to the significant speed-up.

However, the simplifications lead to a worsened description of the electron density compared to regular MF approaches with large basis sets. For both reasons, combining SE-MO methods with any kind of density-dependent dispersion correction is not recommended. On the one hand, the quality of such dispersion corrections could suffer from the approximate description of the electron density by SE-MO approaches, and on the other hand, the numerical integration typically necessary for density-dependent dispersion corrections would become the rate-limiting step and slow down the overall computation.

DOI: 10.1021/acs.chemrev.5b00533
Chem. Rev. XXXX, XXX, XXX−XXX

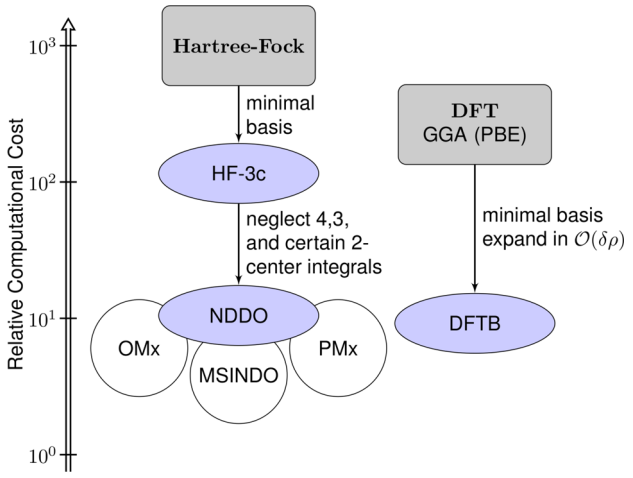

Figure 14. Classification of low-cost, minimal basis set based quantum chemical methods according to their specific approximations.

Consequently, purely geometry-dependent semiclassical approaches (like D2[81] or D3[85]) are the most natural choice. Both correction schemes (including others[82] that resemble D2) were combined with fast SE-MO methods in the past. The first step in this direction was taken by Elstner and co-workers in their seminal paper on dispersion-corrected density functional tight-binding (DFTB).[119] Different HF-based SE-MO approaches have been combined with the D2 dispersion correction[81] (or the related scheme by Jurečka et al.[82]).[152−156,376−378] More recently, HF-based SE-MO methods[176,177,179,379] as well as DFTB[178] were combined with the more sophisticated D3 approach.[85] As expected, the proper inclusion of dispersion generally improves the performance of SE-MO methods for noncovalent interactions. However, the PM7[378] method is mentioned here as a counterexample of proper inclusion of dispersion. Here, the dispersion energy is damped down and even truncated at long range. While the performance of this method is satisfactory for small systems (due to the fitting procedure on similar benchmark sets), it breaks down completely for larger complexes.[95,179] Therefore, proper treatment (i.e., correct in the long-range limit) of dispersion is mandatory.

The accuracy of dispersion-corrected SE-MO methods is highly dependent on the employed SE-MO approach. In principle, the dispersion can be treated very accurately, and some methods can reach average errors in binding energies that are only a factor of 2 worse when compared with dispersion-corrected GGA functionals.[179] However, the employed integral simplifications and the neglect of all many-center contributions in most SE-MO methods often result in underestimated and faster-decaying Pauli exchange-repulsion terms (cf. eq 9). Because the balance between Pauli exchange repulsion and dispersion is important for a good description of NCIs (cf. Figure 6), the intermolecular distances are often underestimated.[178,179]

A better description in this range can be achieved with the minimal basis Hartree−Fock method including three corrections (HF-3c).[130] Here, the two-electron integrals are evaluated exactly, thus improving the description of the Pauli exchange repulsion. The errors in the covalent and noncovalent bonds due to the underlying minimal basis HF are corrected by atom pairwise corrections (including D3 dispersion). This method is typically faster than DFT in larger basis sets (e.g., triple-ζ) but more costly compared to the NDDO-based SE-MO methods.[179]

4.4. Methodological perspective

Having introduced various methods to describe London dispersion interactions, it seems important to put their practical relevance into context. In Figure 15, the number of citations for

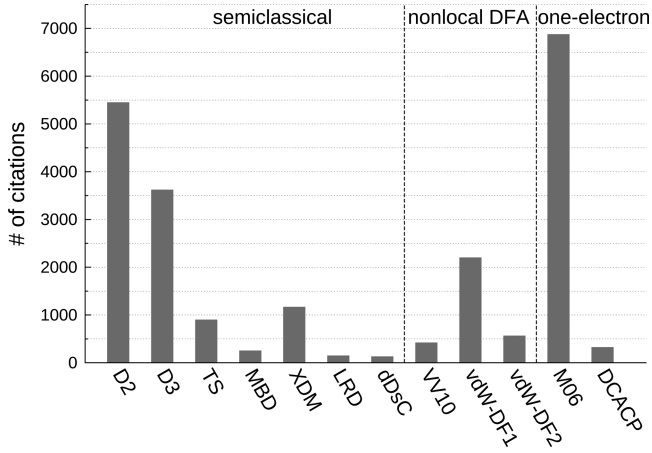

Figure 15. Number of citations found for the key papers of different dispersion corrections as obtained from the Web of Science.[6] Whenever the definition of a single seminal paper is not suitable, the summed number of citations for several key articles is presented. The considered articles are D2,[81] D3,[85,129] TS,[86] MBD,[87,136,196] XDM,[22,83,84,210,211,216] LRD,[229,230] dDsC,[224,226] VV10,[89,270,274] vdW-DF1,[251,252,259] vdW-DF2,[88] M06,[331,332] and DCACP.[293]

different dispersion corrections is depicted (only methods with more than 100 citations in total are considered). The number of citations is not intended as a measure of quality but rather serves as an indicator for the popularity of a method in the scientific community.

The semiclassical D2[81] and D3[85] approaches are the most widely applied correction schemes, surpassed only by the medium-range dispersion-inclusive Minnesota density functionals from 2006.[331,332] The reason why these three approaches are most popular is likely due to, apart from their generally good performance, the straightforward way in which they can be applied. While the M06 class of functionals works in the same way as any other MF approach, the density-independent D2 and D3 approaches are easily implemented and are available in combination with a large class of standard density functionals. Furthermore, D2/D3 is efficient for geometry optimizations and, in addition, provides more or less automatic insight into the origin and spatial distribution of the dispersion energy. Some key properties of the approaches presented above are listed in Table 4. Note that no comparative accuracy judgment is made at this point (see next section). However, a wrong asymptotic limit or missing higher-order terms can already indicate inconsistencies from a purely theoretical point of view.

We try to judge the numerical complexity of the different methods by comparison with a corresponding plain semilocal functional treatment (e.g., PBE). In this regard, the nonlocal density functionals of the vdW-DF family produce the largest computational overhead, leading to significantly larger computation times.[209,231] However, recent efforts in efficient implementations make their usage in periodic systems affordable,[256] and a linear scaling implementation was also reported by Gulans et al.[257] By modeling the local response function through a very simple kernel, a significant speed-up could be achieved in the VV10 variant.[89] If used nonself-

DOI: 10.1021/acs.chemrev.5b00533
Chem. Rev. XXXX, XXX, XXX−XXX

Table 4. Overview of the Capabilities and Theoretical Properties of the Previously Introduced London Dispersion Correction Schemes

model	numerical complexity[a]	ρ based	limit[b]	multipoles[c]	many-body[d]	elements[e]
nonlocal density based						
vdW-DF	high	yes	yes	yes	no	all
VV10	medium	yes	yes	yes	no	all
C_6 based						
D2	low	no	yes	no	no	54
D3	low	no[f]	yes	yes[g]	yes[h]	94
TS	low	yes	yes	no	no	80
MBD	medium	yes	yes	no	yes[i]	80
XDM	medium	yes	yes	yes[j]	yes[k]	103
one-electron potentials						
DCP	medium	yes	no	?	no	few[l]
Minnesota	medium	yes	no	?	no	all

[a]Numerical complexity compared to underlying DFT calculation. [b]Long-range limit $-C_6/R^6$. [c]Higher multipoles ($l > 1$), i.e., induced quadrupoles, octupoles, etc. [d]Higher many-body terms ($n > 2$, i.e., three-body, four-body, etc.). [e]Parameters for all elements with $Z \leq xx$. Methods without element-specific parameters are applicable to all elements (indicated by "all"). [f]Information on chemical environment from fractional coordination number. [g]Dipole−quadupole contribution. [h]Three-body ATM term. [i]Full many-body summation of coupled dipoles. [j]Dipole−quadupole, quadupole−quadrupole, and dipole−octupole contributions. [k]Three-body ATM term is available but not used in typical applications [l]Potentials need specific parametrization (typically H, B, C, N, and O).[35,300,301]

consistently, VV10 calculations are only a few percent slower than uncorrected treatments. The C_6-based D2, D3, and TS methods cause practically no additional computation time compared to HF and semilocal DFT methods.[81,85,86,380] An efficient analytical derivative of the three-body interaction for the D3 scheme was implemented recently.[381] The diagonalization of the dipole-coupling matrix in the MBD scheme is slightly more expensive, especially if nuclear gradients are considered. The computational cost of the exchange-hole integration to generate the XDM dispersion coefficients is substantial, and the XDM method is probably the most costly C_6-based dispersion correction (only surpassed by the related dDsC approach).[22,213] Particularly for nuclear gradients, approximations to avoid self-consistent treatments of XDM were presented.[217,227] The one-electron-based potentials are intrinsically inexpensive but can slow down the SCF convergence with respect to the number of SCF cycles.[345,346]

Because the nonlocal and the Minnesota-type density functionals evaluate the dispersion energy solely from the electron density, no element-specific parameters are introduced and these methods are applicable to all elements in the periodic table. All semiclassical methods, however, rely on element-specific atomic data. In D3, the element-pair-specific parameters are the precomputed dispersion coefficients,[85] TS (and MBD) uses element-specific, precomputed static polarizabilities and homoatomic dispersion coefficients,[86] and XDM employs empirical static polarizabilities.[210] While the limited availability of element-specific parameters was the natural limitation of early dispersion approaches (see section 3) and D2 was in fact one of the first methods available for a large number of elements, the modern dispersion-correction schemes cover major parts of the periodic table and have basically no practical limitation. All the semiclassical approaches rely on certain tabulated parameters and hence include a certain amount of empiricism. While D3 uses precalculated C_6 coefficients for each element in different coordination numbers (on average three reference points per element), TS and MBD use precalculated C_6 coefficients and static polarizabilities of the free atom for each element (two values per element) and XDM uses experimental static polarizabilities of the free atom for each element (one parameter per element). Additionally, all the semiclassical methods use predefined cutoff radii in the short-range damping function together with (one or two) global parameters to adjust the damping to a certain mean-field method. Note that the precalculated C_6 coefficients in the D3 scheme are nonempirically computed by time-dependent DFT (TDDFT) but with an empirically adjusted hybrid density functional (PBE38). DCP approaches require specific parametrization for certain elements in combination with a given basis set and density functional. Consequently, their applicability is typically restricted to only a few elements.

Nearly all of the presented methods are in some way, directly or indirectly, based on the electron density. Only the D2 and D3 schemes depend solely on the molecular geometry. The direct dependence on the density has the advantage of seamlessly modeling all atoms in a system in their current electronic structure (e.g., oxidation state), which is not possible in purely geometry-dependent approaches. The quality of the density depends on the underlying mean-field approach and may deteriorate if intrinsic errors of the latter become apparent (e.g., charge-delocalization error in semilocal density functionals).[382] Because of the use of a minimal basis set and the integral approximations, this is in particular the case for semiempirical methods. In such cases, the D3 scheme can be ideally coupled with semiempirical Hamiltonians without deteriorating the results.[176,179,379] Very promising results are obtained in combination with a tight-binding Hamiltonian,[178] and zero differential overlap methods have also been successfully combined with D2[152−156] and D3.[377,379,383] Due to the semiclassical character, D3 can be used without modification in a classical force field.[180]

The nonlocal density functionals and all C_6-based schemes describe the long-range interactions correctly by construction. Only the one-electron based potentials cannot recover the correct $-C_6/R^6$ limit. The importance of higher multipoles in the perturbing field and the inclusion of higher many-body interactions in dispersion corrections is under a very active debate. There seems to be evidence that the required order in the multipole expansion depends crucially on the underlying exchange-correlation functional.[201] The Minnesota functional

DOI: 10.1021/acs.chemrev.5b00533
Chem. Rev. XXXX, XXX, XXX−XXX

family and the double-hybrid functionals[384] in particular seem to cover the medium-range correlation regime to a large degree, and because the dispersion correction should be very long range in character, these only require corrections for the leading order dipole term. This is substantially different in intrinsically more repulsive functionals like BLYP or revPBE. It has been reported that some dispersion corrections perform better in combination with these more repulsive functionals.[139,260] There is also some consensus that many-body dispersion contributions are important for large and condensed systems. However, their magnitude seems to depend on the specific dispersion model. In the D3 and XDM models,[134,172] the three-body contribution typically amounts to <5% of the total dispersion energy, which seems to agree with the analysis of WF expansions.[385,386] On the contrary, in the MBD scheme the many-body contribution is substantially larger, partially due to the higher-order many-body series, but probably also due to the conceptually different model (coupled, anisotropic QHOs) employed.

In Figure 16, we sketch the different dispersion coefficients C_k as arising from different many-body orders and increasing number of terms in the multipole expansion. The contributions covered by the D3, MBD, and XDM methods are highlighted.

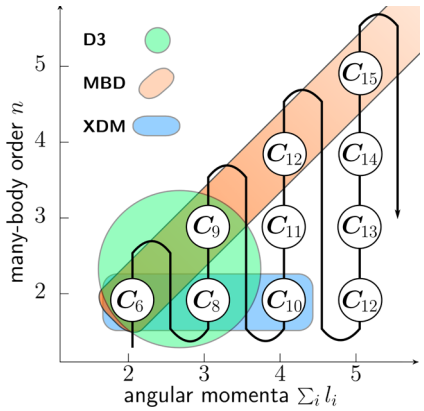

Figure 16. Dispersion coefficients as arising in the asymptotic limit from different many-body orders and increasing number of terms in the multipole expansion. The contributions covered by the D3, MBD, and XDM methods are highlighted.

number of terms in the multipole expansion. This reflects the physical origin from the perturbative treatment described in section 4.1. Note that spherically symmetric atoms are assumed, no $l = 0$ contribution exists because of the vanishing transition monopole moments, and a many-body order n smaller than the sum of all angular momenta $\sum_i l_i$ is required (lower triangle). The distance dependence is given by

$$E \propto -\frac{C_k}{R^k} \tag{110}$$

$$k = 2\sum_{i=1}^{n} l_i + n \tag{111}$$

i.e., following the C_k connecting line leads to a faster decay of the interaction with R. Because MF methods (e.g., the semilocal DFAs) represent an expansion in powers of the local density, the interaction depends on the density overlap. This overlap decays exponentially with the distance R, and the molecular or atomic ionization potentials determine the corresponding exponent. Therefore, it is reasonable to cover the remaining long-range correlations up to a certain power in R via the dispersion correction. In this sense, the D3 method covers consistently all terms up to $1/R^9$, while in XDM (in its typically applied form) the C_9 contribution is missing. MBD covers all many-body orders, but all higher multipoles (C_8, C_{10}, ...) are neglected. In contrast to all other methodologies, MBD also includes a model for dispersion-screening effects (type-B nonadditive effects as described by Dobson).[80] The older D2 and TS methods only cover the leading order C_6 term, which corresponds to a consistent distance dependence following the discussion given above. The Minnesota functionals and DCP methods do not have the correct physical origin of dispersion interactions, and hence an identification of the many-body and multipole order is not appropriate. The vdW-DF methods yield only two-body contributions; otherwise, the trace (spacial integration) has to be constructed over multiple centers. While the underlying model depends on the dipolar polarizability and approximations to the local response, the true charge density is integrated, thus representing the multipoles to all orders.

While the dispersion treatment by one-electron potentials is purely empirical, the nonlocal density and the C_6-based dispersion schemes model the correct physical interaction. In the latter schemes, an empirically adjusted damping function has to interpolate between the long-range and the short-range regime, similar to all atom pairwise schemes. A similar damping is also used to couple VV10 to various different density functionals. Although the vdW-DF functional form is typically kept fixed, the respective semilocal exchange correlation functional is empirically adjusted in the later versions to ideally fit to the long-range regime.

A typical approximation used in many dispersion correction schemes is the spherical averaging of the dynamic polarizabilities, i.e., the pairwise dispersion energy solely depends on the interatomic distance (compare with eqs 21 and 22). While this is exact for free atoms, a nonsymmetric environment can perturb the atom and remove this symmetry. In first order, this asymmetric dynamic polarizability leads to a C_7 pairwise dispersion coefficient, which was estimated by Geerlings and co-workers for the atom pairwise schemes to contribute ~5−20% of the total dispersion energy.[387] This could be reproduced in the D3 framework by generating the C_7 from the C_6 coefficients by a local asymmetry measure.[388] The s_7 and s_8 coefficients in eq 40 were optimized on the standard S66 NCI reference database, yielding on average a contribution of ~7% from the asymmetry term. However, the total dispersion energy is only very slightly modified, and hence no significant improvement of the resulting binding energies is gained. Apparently, this small contribution can be absorbed in the C_8 contribution. Note that only a uniform C_7/R^7 dependence is tested and the true anisotropy has a directional dependence. Incidentally, it is mentioned that an R^7 dispersion energy term has recently been added to the EFP method.[389,390] The MBD dispersion scheme includes the atomic asymmetry to some extent via the dipolar coupling within the nonsymmetric molecular environment, which is typically not considered in all the other presented methods.[87] Note that the discussed anisotropy of the atoms in pairwise dispersion schemes is not related to the overall dispersion anisotropy of a molecule, which is approximately included by all methods (see ref 11 for a more detailed discussion including numerical examples).

In the original paper of Casimir and Polder, the response of the electric field was considered with a finite propagation of the Coulomb interaction at the speed of light.[60] If retardation (i.e., the electrons "move" while the photon "travels" between them) is taken into account, a C_7/R^7 distance dependence is recovered.

DOI: 10.1021/acs.chemrev.5b00533
Chem. Rev. XXXX, XXX, XXX−XXX

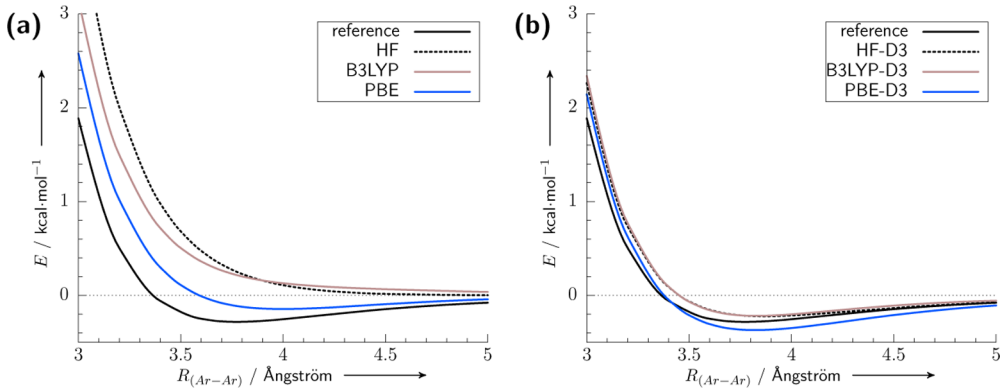

Figure 17. Computed (aug-cc-pV5Z AO basis) potential energy curves for two interacting Ar atoms with and without dispersion correction in comparison to an accurate reference.

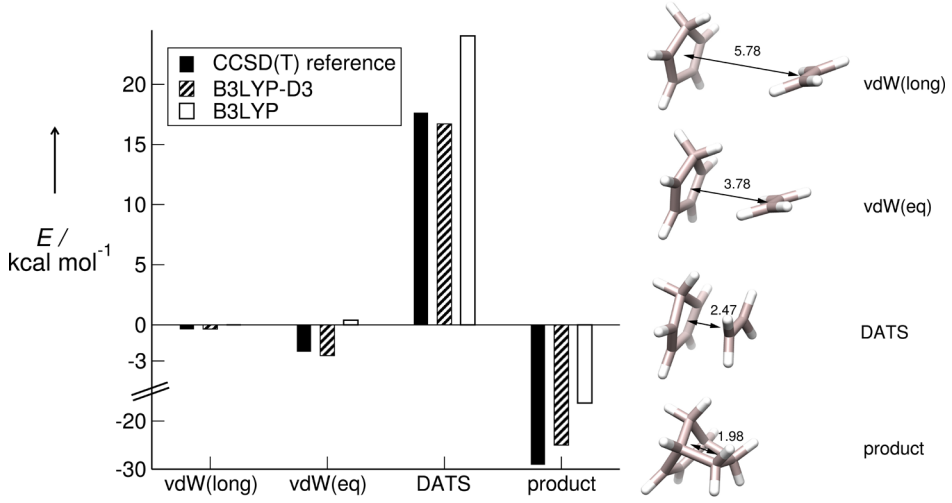

Figure 18. Four selected points on the potential energy surface for the reaction of ethene with cyclopentadiene to yield norbornene (TPSS-D3/def2-TZVP geometries). Uncorrected B3LYP/def2-QZVP and B3LYP-D3/def2-QZVP are compared to CCSD(T)/est CBS reference data. For the long-distance vdW regime, the equilibrium center-of-mass distance (indicated by an arrow and values given in Å) in the reactant complex is increased by 2 Å.

In the methods presented here, all interactions occur instantaneously and no retardation effects are included. However, at typical chemical distances, this should be a valid approximation because the retardation is only significant if the fragment separation R is much larger than the wavelength of the transmitting electromagnetic radiation.

A severe approximation may be the local partitioning of the polarizability $\alpha(i\omega)$, which assumes a localized polarization response, and is the basis of most methods discussed (except for the Minnesota-type functionals). If this partitioning cannot be applied as in delocalized systems (e.g., in bulk metals), type-C nonadditivity effects play a major role and one should not expect good results from dispersion-corrected MF methods. Note that not only do the C_6-based schemes rely on the local character of the dynamic polarizability but also the vdW density functionals are derived from a local approximation to the charge density susceptibility.

5. TYPICAL APPLICATIONS AND BENCHMARKS

5.1. Exemplifying the distance regimes of the dispersion energy

Dispersion is omnipresent in electronic systems (like gravitation in systems with mass) and is always attractive (energy lowering). Its natural, also omnipresent, antagonist is exchange repulsion (EXR) due to the Pauli exclusion principle, and in nonpolar systems, these two terms dominate the medium- and long-distance regimes. However, their distance dependence is very different (R^{-6} vs exponential in R), and hence different chemical systems or the paths along a reaction coordinate are influenced differently by the two terms. The situation is complicated by the fact that the various MF methods (in particular the "zoo" of DFAs) account for EXR and dispersion effects rather differently. As already mentioned in section 2, the inherent short-/medium-range "repulsiveness" of a MF method is an important classification criterion. In this section, these connections are initially discussed with the help of specific chemical examples, the argon dimer potential (Figure 17), the reaction of ethene with cyclopentadiene to yield norbornene (Figure 18), the potential energy curves for the formation of the $\pi-\pi$ stacked coronene dimer (Figure 19), and the association of two bimolecular frustrated Lewis pairs (FLPs, Figure 20). In the first chemical reaction example, a vdW bound complex is transformed into a covalently bonded species, i.e., intermolecular dispersion changes to intramolecular dispersion (correlation) energy, while in the case of the coronene dimer the whole distance range of the vdW interaction in a large complex is considered. The long-range regime, which is of particular importance for the (nonconducting) condensed phase, can be described practically

DOI: 10.1021/acs.chemrev.5b00533
Chem. Rev. XXXX, XXX, XXX−XXX

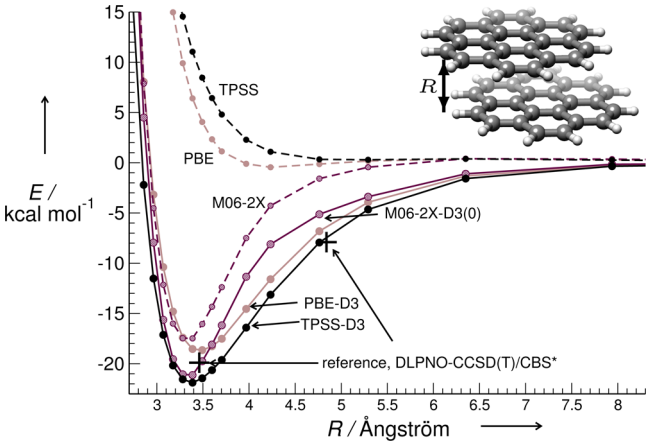

Figure 19. Potential energy curves for the $\pi-\pi$ stacked coronene dimer with dispersion-corrected and uncorrected density functionals in comparison to DLPNO-CCSD(T)/CBS*[395] reference points for the equilibrium and one elongated structure ($1.4 \times R_e$). The example is taken from the L7 benchmark set.[44]

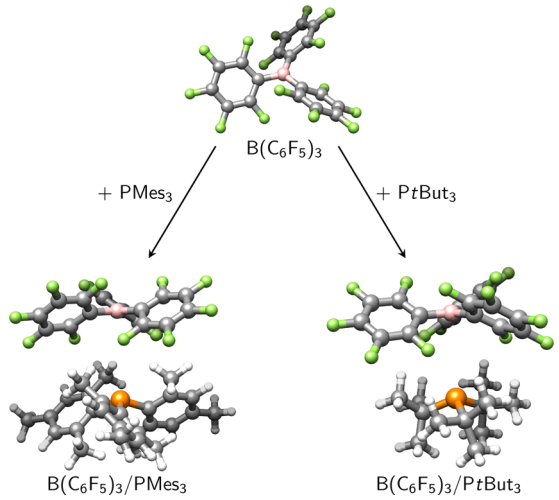

Figure 20. Structures of the molecules involved in the association reaction of $B(C_6F_5)_3$ with either $PMes_3$ or $PtBut_3$ (color codes: white = hydrogen, pink = boron, gray = carbon, green = fluorine, orange = phosphorus).

exactly with pairwise interactions (see section 4.1). Note that, although the chosen systems and tested density functionals are typical representatives, one should be careful not to overgeneralize these data. In particular, polar systems can be dominated by electrostatic, induction, or charge-transfer interactions. For consistency and because it is a well-tested method, D3 is used as a representative and asymptotically correct dispersion correction. Nevertheless, it should be noted that other asymptotically correct and well-performing schemes (see Tables 4 and 9, respectively) could have been used for this purpose.

We introduced the argon dimer in section 2 as a prototypical example, where most MF methods fail to describe the potential energy surface (PES) even qualitatively correctly. Here, we show the PES for HF, the B3LYP hybrid functional, and the PBE GGA functional again and compare the results with the corresponding dispersion-corrected ones (parts a and b of Figure 17, respectively). We apply the D3 dispersion correction in the latest Becke–Johnson damping scheme as described in section 4.1. All three D3-corrected MF methods yield PES in good quantitative agreement with the reference. The C_6^{Ar-Ar} coefficient is the same in all cases, but even though the plain MF PES differ significantly, the differences between the MF-D3 PES are tiny. This is a rather general observation that the often large differences between various density functional approximations are "washed out" by dispersion corrections. The Becke–Johnson damping function seems to be capable of smoothly interpolating between the D3 and the MF contributions; particularly, the HF-D3 and B3LYP-D3 potentials are nearly identical. The dispersion-corrected version of the intrinsically more attractive PBE functional overstabilizes the argon dimer around the equilibrium structure. This highlights the empirical observation that the semiclassical dispersion corrections can be ideally combined with inherently more repulsive density functionals'[139,260] which seems to avoid correlation double-counting effects.

In the example of a typical Diels–Alder reaction, uncorrected B3LYP is compared with its D3(BJ)-corrected variant B3LYP-D3 and to accurate CCSD(T)/est CBS reference data. Four points along the reaction coordinate are shown: the equilibrium vdW complex structure with a typical center-of-mass distance between the fragments of ~3.8 Å, the same complex geometry but at an elongated distance of 5.8 Å as an example of the asymptotic regime, the Diels–Alder transition state (DATS) at ~2.5 Å where the new CC bonds are almost formed, and finally the product state where typical covalent distances < 2 Å occur. As will be discussed below in more detail for a vdW equilibrium structure benchmark set (S22), dispersion-uncorrected over-repulsive functionals like B3LYP yield unbound vdW complexes around equilibrium distances. This is seen in Figure 18 from the positive interaction energy (unfilled bar) while B3LYP-D3 agrees well with the reference value of about −2.3 kcal/mol. This furthermore holds for the vdW (long) structure with a still significant interaction of about −0.3 kcal/mol while B3LYP is essentially unbound (noninteracting). In this asymptotic region the electron density overlap is tiny due to its exponential decay, and hence, practically no interaction remains for a nonpolar system with a dispersion-devoid MF method. Interestingly, the over-repulsive behavior of B3LYP is also sizable in the much tighter bound DATS and product states. The reaction barrier is overestimated with uncorrected B3LYP by ~6 kcal/mol, and even the reaction exothermicity is underestimated by 5 kcal/mol. These failures are almost perfectly cured by the D3 scheme indicating that (a) this method relatively accurately accounts also for medium-range correlation effects and (b) these effects are practically absent in plain B3LYP but important for an accurate description of standard thermochemistry. Similar observations were made in the mid-2000s for even simpler hydrocarbon isomerization reactions.[391−394] As will be shown below in other examples, the above-described poor property of B3LYP is typical for many density functional approximations except those from the Minnesota family that capture correlation/dispersion effects at least for medium distances.[28,332]

Figure 19 shows results for the coronene dimer with uncorrected PBE,[148] TPSS,[318] and M06-2X[332] density functionals in comparison to their D3-corrected counterparts and two DLPNO-CCSD(T)/CBS*[395] (i.e., DLPNO-CCSD(T) with tight cutoff values and a newly developed approximate CBS extrapolation scheme denoted CBS*) reference data points.

The graph clearly shows that plain PBE and TPSS yield physically incorrect unbound vdW states and that the D3-corrected versions perform well in the equilibrium as well as asymptotic regions (the same holds true for, e.g., B3LYP). The

DOI: 10.1021/acs.chemrev.5b00533
Chem. Rev. XXXX, XXX, XXX−XXX

residual deviations from the reference for the equilibrium interaction energy are 1−2 kcal/mol (5−10%), which represents the typical small deviation for those kind of semilocal functionals. Note that the estimated error of the reference DLPNO-CCSD(T)/CBS* values is about ±0.5 kcal/mol, mainly due to the remaining basis set incompleteness error, is quite significant in this comparison. The M06-2X functional performs considerably better than the standard functionals near the equilibrium structure and underbinds by only 2.5 kcal/mol even without further (long-range) dispersion corrections. This example shows that the empirical adjustment of the large number of parameters in the M06-2X functional (>30) to equilibrium data of small vdW complexes seems to capture the correct physics. In this part of the potential, the electron densities overlap significantly and are sufficiently strongly deformed relative to those of the fragments. However, the situation is different already at slightly larger interfragment distances where M06-2X starts to underbind systematically. Particularly, this holds true for the asymptotic regime, which is already reached at a distance of ∼5 Å where the M06-2X interaction has almost vanished. Although this can be partially cured by adding the D3(0) correction, it is evident from the DLPNO-CCSD(T) data that the combination of D3(BJ) with purely repulsive functionals works better. This conclusion is quite general and is related to the fact that electron-correlation double-counting effects in the medium-range dispersion regime are difficult to avoid with equilibrium-binding functionals of, for example, the M06 type. This effect is also the reason why only the zero-damping variant D3(0) could be coupled reasonably well with M06-2X.[129] Recent experience has shown that functionals with intermediate repulsiveness and a coadjustment of the semilocal functional part with the dispersion correction are most effective to get accurately and robustly working MF methods[351] (see also refs 139 and 357 for related functional developments).

In a very recent study,[396] the association of two bimolecular FLPs was investigated. In this example the mostly noncovalently bound complex between the Lewis acid $B(C_6F_5)_3$ and the Lewis base ($PMes_3$ or $PtBut_3$) is chemically relevant because a specific preorganization and molecular flexibility are required to activate small molecules like H_2[397] (see Figure 20). A selection of the computed association energies (using the def2-QZVP[398,399] AO basis set) from ref 396 is presented in Table 5. According to reference calculations at the DLPNO-CCSD(T)/CBS* level,[395] the association energies of both FLPs are very similar. If dispersion-exclusive methods like plain B3LYP or HF are used, positive association energies (unbound complexes) are obtained. The magnitude of these positive energies reflects the repulsive character of the respective MF approach. Adding dispersion corrections leads to very good agreement (close to or even within chemical accuracy) with the reference values. The HF-D3 approach performs remarkably well in this particular case, because the association is a purely noncovalent process accompanied by only little changes within the covalent frameworks. The same excellent agreement is observed for B3LYP-D3. This shows again that, through the damping function parameters, the D3(BJ) correction[85,129] can be reasonably applied with different MF approaches. The B3LYP-NL scheme typically performs well also; however, in this particular case it performs slightly worse than B3LYP-D3.

Table 5. Association Energies (kcal/mol) of $B(C_6F_5)_3/PMes_3$ and $B(C_6F_5)_3/PtBut_3$; If Not Noted Otherwise, the Values Are Taken from Ref 396 and Were Obtained with the def2-QZVP Basis Set

method	$B(C_6F_5)_3/PMes_3$	$B(C_6F_5)_3/PtBut_3$
B3LYP	5.5	2.8
B3LYP-D3	−10.5	−11.2
B3LYP-NL	−11.7	−12.7
M06-2X[a]	−5.3	−8.4
M06-2X-D3(0)[a]	−9.0	−11.4
HF	7.7	4.2
HF-D3	−10.2	−11.3
reference[a,b]	−10.3	−10.8

[a]This work. [b]From DLPNO-CCSD(T)/CBS* calculation.[395]

Comparison of the two systems reveals that the contribution of dispersion is smaller in $B(C_6F_5)_3/PtBut_3$ than in $B(C_6F_5)_3/PMes_3$, as plain B3LYP and HF already yield smaller association energies for the former. In the larger $PMes_3$ unit, a significant contribution of the association energy results from long-range dispersion interactions (>5 Å).[396] This is indicated by the performance of the M06-2X functional. Covering dispersion at medium range only, it yields almost the correct association energy for $B(C_6F_5)_3/PtBut_3$ (error of ∼2 kcal/mol), while its deviation from the reference is much larger for $B(C_6F_5)_3/PMes_3$ (∼5 kcal/mol). Including long-range dispersion by means of the D3(0) scheme significantly improves the results (see Table 5). In the discussion of the potential energy curve for the coronene dimer, the importance of the asymptotically correct treatment of dispersion interactions has been emphasized (see above). Here, we have given an additional example that the proper inclusion of dispersion interactions (also at long range) is necessary to accurately describe the thermochemistry even of moderately sized molecules. For the additional consideration of solvation effects and their partial compensation of dispersion corrections, see ref 396 (cf. also section 4.3.3).

5.2. Peptide conformation potential

Our next example is the unfolding of the Ace-Ala-Gly-Ala-NMe tetrapeptide from a folded, right-handed α-helix structure to the unfolded β-strand. As starting structures for the folded and unfolded conformation, we used the α_R- and β_a-geometries, respectively, from ref 400. They were then optimized using the recently proposed composite approach PBEh-3c[351] as implemented in the TURBOMOLE suite of programs (version 7.0).[289] Five intermediate structures were generated and optimized with constrained Ace-NMe distance. Single-point calculations were performed on these geometries (B3LYP[53,54,58,161,162]/def2-QZVP[398,399]) and two dispersion-correction schemes were applied: the semiclassical D3(BJ)[85,129] scheme (see Figure 9) and the density-dependent, nonlocal VV10 correction (NL)[89,274] nonself-consistently in a post-SCF manner. The relative energies with respect to the folded conformer are plotted in Figure 21 as a function of the separation between the terminal carbon atoms and compared to high-level reference data at the DLPNO-CCSD(T)/CBS* level (estimated error: ± 0.5 kcal/mol).[395] Further comparisons are made with the B3LYP-DCP/6-31+G(2p,2d)[35] composite scheme (shortly denoted as DCP in Figure 21) as well as the Minnesota hybrid functional M06-2X.[332]

According to our calculations, the folded α-helix conformer is more stable than the unfolded β-strand structure (differences from the relative stability reported in refs 400 and 401 may arise from the constrained dihedral angles used therein). Apparently, dispersion stabilizes the compact, folded structure. Without correction, the B3LYP functional leads to an incorrect relative

DOI: 10.1021/acs.chemrev.5b00533
Chem. Rev. XXXX, XXX, XXX−XXX

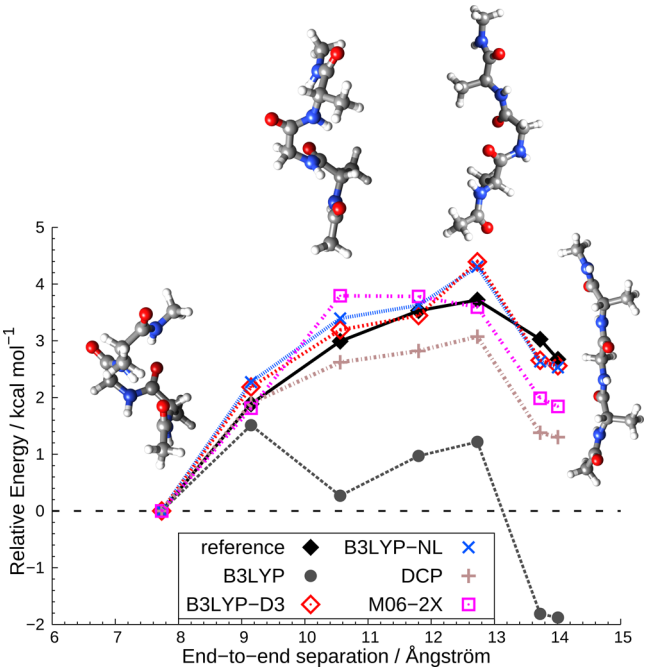

Figure 21. Potential energy curve for unfolding of the tetrapeptide Ace-Ala-Gly-Ala-NMe. For the B3LYP, B3LYP-D3, B3LYP-NL, and M06-2X calculations, the def2-QZVP basis set was used. DCP represents B3LYP-DCP/6-31+G(2p,2d).[35] The reference energies are obtained at the DLPNO-CCSD(T)/CBS*[395] level. The geometries of points **1** (folded), **3**, **5**, and **7** (unfolded) are depicted as well.

stability of the folded compared to the unfolded conformer. The plain B3LYP functional includes Pauli exchange repulsion, which is also stronger in the folded than in the unfolded conformation, thus destabilizing the former. The stabilizing effect due to hydrogen bonds, which are present in the folded conformer and mostly captured by B3LYP, is not sufficient for an accurate description of the relative stability. Including dispersion in a semiclassical way (B3LYP-D3) or using the nonlocal VV10 correction (B3LYP-NL) stabilizes the folded conformer, resulting in excellent agreement with the reference data (discrepancy less than 0.15 kcal/mol). Furthermore, it is observed that, for plain B3LYP, the PES is very bumpy, which is not the case for the reference method (DLPNO-CCSD(T)/CBS*). B3LYP-D3 and B3LYP-NL show excellent mutual agreement, yielding a comparably smooth PES close to the reference. Only one geometry (point **5**) is somewhat understabilized for both schemes, and thus, it seems to be caused by a functional specific artifact (B3LYP-DCP/6-31+G(2p,2d) shows a similar kink here). Overall the long-range dispersion correction, the density functional (at short range), and even the interplay at medium range (strongly dependent on the damping function) work remarkably well in both schemes. Comparison with the plain B3LYP data reveals that additive dispersion corrections (following eq 10) and their attachment to the functional provide the necessary physics to describe such an unfolding process in a quantitatively correct manner.

The B3LYP-DCP/6-31+G(2p,2d) and M06-2X follow conceptually different approaches (see section 4.3). Both are capable of predicting qualitatively the correct relative stability for the folded and unfolded conformers (points **1** and **7** in Figure 21). However, in both approaches the relative energy of the unfolded conformer is too low, particularly in the DCP scheme. This is likely due to the lack of long-range dispersion part (see Table 4), which seems to contribute more strongly to the

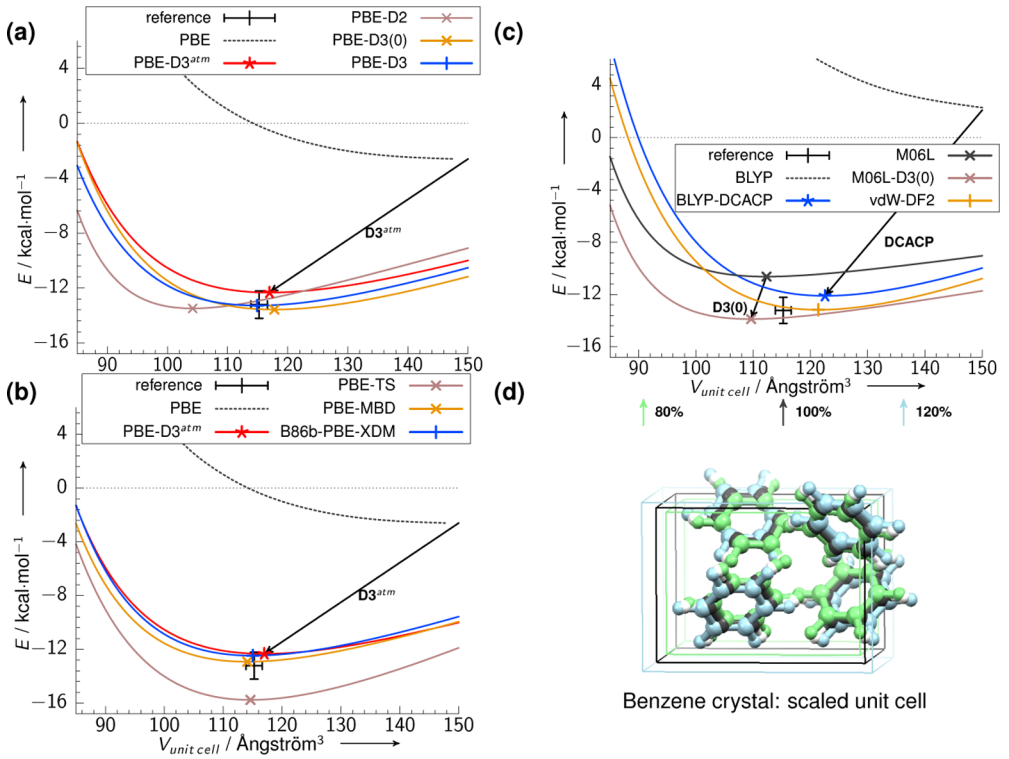

Figure 22. Lattice energy of the benzene crystal based on constrained volume optimizations (TPSS-D3 level) with single-point evaluations of various dispersion-corrected MF methods. For each method, the cross shows the position of the energy minimum and the arrow indicates the effect of the added dispersion correction. The reference lattice energy refers to a recent CCSD(T) estimate.[419]

DOI: 10.1021/acs.chemrev.5b00533
Chem. Rev. XXXX, XXX, XXX−XXX

stabilization of the folded conformer. The comparably similar structure **2** is described extremely well by both approaches. For B3LYP-DCP/6-31+G(2p,2d) all subsequent geometries are systematically calculated to be too stable. M06-2X draws a different picture. While the unfolded and similar structures (**7** and **6**, respectively) are too stable, the intermediate structures **3** and **4** are computed to be too high in energy.

In conclusion, for a correct description of this unfolding process (and this may hold for polypeptides in general), a proper description of dispersion at long range is mandatory. Good agreement with the reference is obtained for both the B3LYP-D3 and the B3LYP-NL approaches, which produce almost identical results. M06-2X performs well, too, with a slight underestimation of the unfolded conformer likely due to the missing long-range dispersion. B3LYP-DCP/6-31+G(2p,2d) yields qualitatively correct relative energies but quantitatively underestimates the long-range dispersion contribution.

5.3. Benzene crystal

To shed light on the long-range behavior of dispersion-corrected MF methods and, in particular, their influence in more dense (condensed) systems, the analysis of a nonpolar, and therefore dispersion energy-dominated, organic crystal is presented. A sufficiently fast and, at the same time, reasonably accurate electronic structure method would be beneficial for the growing field of organic crystal structure prediction.[402−404] Crystalline benzene is one of the simplest organic molecular crystals with aromatic π-stacking. It has various energetically close polymorphs[405,406] and serves as the prototypical example to test and judge electronic structure methods based on wave function expansions,[407−411] dispersion-corrected DFT,[173,174,262,381,412−414] and even SE-MO methods.[178,179,415]

In Figure 22, we show a potential energy surface (PES) of the benzene crystal. It corresponds to constrained volume optimizations around the equilibrium geometry calculated at the TPSS-D3 level. For the various dispersion-corrected MF methods, single-point energies in a converged projector-augmented wave (PAW)[416,417] basis set are evaluated on this PES as calculated with the VASP program.[264−266] The experimental sublimation enthalpy and geometry have been back-corrected for zero-point and thermal effects as described in refs 174, 351, and 418 with the corresponding error estimates. The estimated experimental lattice energy is replaced here by a recent CCSD(T) based estimate[419] as theoretical reference value.

In parts a and b, semiclassical C_6-based and in part c one-electron-based and nonlocal dispersion schemes are shown. The geometric changes of the crystal are depicted in part d. From Figure 22d, one can see that the noncovalent stacking distance is mainly influenced by the volume constraint PES scan, while the covalent bond distances do not change significantly, as expected for a vdW crystal. The plain density functionals PBE[148] and BLYP[161,162] cannot describe the binding in a qualitatively correct manner. While PBE shows a very shallow minimum, the BLYP PES is purely repulsive. The binding energy is reasonably good with PBE-D2, but the unit cell volume is significantly underestimated. This probably originates from inaccurate C_6 coefficients in the old D2 method. The carbon C_6 coefficients are actually closer to the carbon C_6 within ethyne (compare with Figure 8) and are too high by ∼20% for the benzene crystal. The PBE-D3 potentials are substantially better and agree very well with the reference. For the benzene crystal, both damping variants seem to be appropriate and yield similar results. The three-body contribution in the ATM approximation has only a small effect and decreases the binding by ∼7%. The PES calculated with PBE-TS has a significantly underestimated minimum (too attractive interaction). However, the minimum geometry is reproduced well at the PBE-TS level. All well-established semiclassical dispersion corrections, namely, D3,[85] MBD,[87] and XDM,[22,210,211,216] are very close to each other and agree with the reference within its estimated uncertainty (cf. Figure 22a; the errors are smaller than 1 kcal/mol and 1.3%, respectively, for the lattice energy and the unit cell volume).

Both the empirical one-electron potentials (M06L[331,332] and DFT-DCACP[293]) and the nonlocal vdW density functional (vdW-DF2[251]) provide less-accurate potentials. M06L is too repulsive, which can be partially cured with the D3(0) scheme. However, the geometry is too dense and the overall improvement is only minor. BLYP-DCACP and vdW-DF2 yield a reasonable lattice energy close to the reference, but the equilibrium volume is significantly larger as shown in Figure 22b. These results highlight again the importance of a consistent treatment of dispersion interactions in all distance regimes. In condensed systems, the long-range part is especially significant and must not be neglected.

An important point in these comparisons has to be emphasized as a number of studies compare calculated lattice energies or equilibrium geometries directly with the measured observables.[203,412,420] Especially for organic crystals of small molecules, the impact of zero-point vibrational (ZPV) and thermal contributions to both the sublimation enthalpy and the minimum geometry (on the free energy surface) can be substantial.[418,421,422] For instance, the computed hydrogen cyanide mass density of 1.06 g/cm^3 and lattice energy of 10.3 kcal/mol (at TPSS-D3/est CBS level) may be misinterpreted as a failure of the dispersion-corrected density functional. However, the errors of 9% and 21% for the mass density and sublimation enthalpy, respectively, diminish to values of only 1% and 5% when ZPV and thermal effects are properly accounted for.[423]

5.4. Standard benchmark sets for noncovalent interactions

Up to this point, we described individual examples specifically selected for showing representative trends and behaviors. To support the above conclusions, we summarize the performance of different methodologies for well-established benchmark sets. We focus on interaction energy benchmarks for purely noncovalently bound systems, because for these standard test sets sufficient data exist for most methods in the literature. Recently, some effort has been devoted to the investigation of dispersion effects on geometric properties including covalent bonds, rotational constants of medium-sized molecules, noncovalent bond distances, and crystal mass densities.[24,324,351,424,425]

Concerning the energy benchmarks, two different strategies for the compilation of reference data exist. For sufficiently small systems (S22[275,426,427] and S66[276]), high-level wave function based reference calculations are feasible and typically the CCSD(T) level extrapolated to the CBS limit is applied. For larger systems (S12L,[198] S30L,[95] X23,[174,262] and ICE10[418]), which are the true target of MF methods, one has to rely on experimental data, which requires proper back-correction of, e.g., thermal, vibrational zero-point, and solvation effects.[198] For systems of medium size, e.g., for parts of the S12L set, (local) correlated wave function and quantum Monte Carlo methods are nowadays feasible.[175] The use of theoretical references is

DOI: 10.1021/acs.chemrev.5b00533
Chem. Rev. XXXX, XXX, XXX−XXX

preferred because no experimental errors occur and geometric, thermal, and various condensed-phase effects are absent.

To provide comprehensible benchmark data, we first summarize the test sets and give the corresponding reference values used in the later comparison. We show results for three typical, standard interaction energy benchmark sets. The first is the very well-known and widely used S22 set of Hobza and co-workers,[275] comprising small- to medium-sized, mostly organic complexes in their equilibrium structure summarized in Table 6.

Table 6. Reference Energies of the S22 Test Set for Noncovalent Interactions As Introduced by Hobza and Co-workers[275] with Refined CCSD(T)/CBS(est) Reference Values (ΔE) by Sherrill and Co-workers[427]

no.[a]	name	symmetry[b]	$\Delta E \pm 1\%$[c]
1	ammonia dimer	C_{2h}	−3.13
2	water dimer	C_s	−4.99
3	formic acid dimer	C_{2h}	−18.75
4	formamide dimer	C_{2h}	−16.06
5	uracil dimer	C_{2h}	−20.64
6	2-pyridoxine·2-aminopyridine	C_1	−16.93
7	adenine·thymine	C_1	−16.66
8	methane dimer	D_{3d}	−0.53
9	ethene dimer	D_{2d}	−1.47
10	benzene·methane	C_3	−1.45
11	benzene dimer	C_{2h}	−2.65
12	pyracine dimer	C_s	−4.26
13	uracil dimer	C_2	−9.81
14	indole·benzene	C_1	−4.52
15	adenine·thymine (stack)	C_1	−11.73
16	ethene·ethine	C_{2v}	−1.50
17	benzene·water	C_s	−3.28
18	benzene·ammonia	C_s	−2.31
19	benzene·cyanide	C_s	−4.54
20	benzene dimer	C_{2v}	−2.72
21	indole·benzene (T-shape)	C_1	−5.63
22	phenol dimer	C_1	−7.10

[a]Running number according to ref 275. [b]Symmetry of complex. [c]Binding energy in kcal/mol as given in ref 427 with estimated error.

This set covers hydrogen-bonded as well as typical vdW complexes, and it has become the defacto standard in the field of theoretical noncovalent interaction calculations. Note that the S22 reference values have been revised twice,[426,427] and we use the latest published values here.

However, because S22 does not include large systems with >50 atoms, it is not appropriate for testing the performance of methods in the asymptotic, large interatomic distance regime (although systems apart from the S22 equilibrium distances were already analyzed in its original publication).[275] Furthermore, charged as well as multiple interacting fragments giving rise to various many-body effects are absent in S22. Such systems are contained in the S12L benchmark set of supramolecular complexes,[198] which is used here to demonstrate the performance of methods in realistic applications. The S12L reference is based on back-corrected experimental (free) energies.[95] The reliability of these estimated gas-phase interaction energies has been confirmed independently by diffusion Monte Carlo[175] and DFT-SAPT calculations.[428] Moreover, they compare well with DLPNO-CCSD(T)/CBS*[395] values (to be published elsewhere).

The third set (X23) of (mostly) organic molecular crystals[174,262] can be considered as a periodic extension of the S22 where the asymptotic parts of the noncovalent interaction, specifically the dispersion component, may dominate. The benchmark set X23 was compiled by Otero-de-la-Roza and Johnson[262] and further refined by Reilly and Tkatchenko.[174] Experimental sublimation enthalpies are corrected for zero-point and thermal effects yielding electronic lattice energies that allow convenient benchmarking. The latter study also estimates the impact of anharmonic contributions on the sublimation energy, and we use these values for benchmarking.[174]

For all three test sets, the same consistent strategy of comparing the data from the MF methods with reference interaction energies was applied: (i) single-point interaction energies for the given reference structures were computed or taken from the literature, (ii) single-particle basis sets were tried to converge to the basis set limit to rule out incompleteness effects as much as possible, and (iii) composite methods or separate dispersion corrections were applied in the standard form as defined in the original publications. Because many dispersion-correction schemes can be coupled with various MF methods, there exists a plethora of variants that could be tested. To provide a reasonable but still comprehensible picture, we decided to

Table 7. Reference Energies of the S12L Test Set for Supramolecular Host−Guest Complexes As Introduced by Grimme[198] with Refined Back-Corrected Experimental Reference Values from Ref 95

no.[a]	no.[b]	name	charge	solvent[c]	temperature[d]	ΔG[e]	$\Delta E \pm 5\%$[f]
1	2a	TCNA@tweezer	0	$CHCl_3$	298	−4.2	−29.0
2	2b	DCB@tweezer	0	$CHCl_3$	298	−1.4	−20.8
3	3a	3c@pincer	0	CH_2Cl_2	298	−2.3	−23.5
4	3b	3d@pincer	0	CH_2Cl_2	298	−1.3	−20.3
9	4a	C_{60}@catcher	0	toluene	293	−5.3	−28.4
10	4b	C_{70}@catcher	0	toluene	293	−5.1	−29.8
17	5a	GLH@mcycle	0	$CHCl_3$	298	−8.3	−33.4
18	5b	BQ@mcycle	0	$CHCl_3$	298	−3.3	−23.3
27	6a	$BuNBH_4$@CB6	+1	formic acid/H_2O	298	−6.9	−82.2
28	6b	$PrNH_4$@CB6	+1	formic acid/H_2O	298	−5.7	−80.1
	7a	FECP@CB7	+2	H_2O	298	−21.1	−132.7[g]
21	7b	ADOH@CB7	0	H_2O	298	−14.1	−24.2

[a]Running number according to ref 95. [b]Running number according to ref 198. [c]Solvent of experimental measurement. [d]Temperature of ΔG measurement in K. [e]Experimental ΔG in kcal/mol. [f]Back-corrected ΔE in kcal/mol with estimated error. [g]Reference value identical to procedure in ref 95.

DOI: 10.1021/acs.chemrev.5b00533
Chem. Rev. XXXX, XXX, XXX−XXX

Table 8. Reference Energies of the X23 Test Set for Molecular Crystals As Introduced by Otero-de-la-Roza and Johnson[262] and Refined by Reilly and Tkatchenko;[174] We Use the Back-Corrected References from Ref 174 with Individual Replacements As Indicated Below

no.[a]	no.[b]	name	space group	Z (unit)[c]	temperature[d]	ΔH[e]	$\Delta E \pm 5\%$[f]
1	1	cyclohexanedione	$P2_1$	2	233	19.39	21.18
2	2	acetic acid	$Pna2_1$	4	40	16.24	17.40
3	3	adamantane	$P\bar{4}2_1c$	2	188	13.97	16.59
4	4	ammonia	$P2_13$	4	160	7.12	8.89
5	5	anthracene	$P2_1a$	2	94	23.46	26.94
6	6	benzene	Pbca	4	218	10.78	13.22[g]
7	7	CO_2	$Pa\bar{3}$	4	150	5.88	6.50
8	8	cyanamide	Pbca	8	108	18.05	19.05
9	9	cytosine	$P2_12_12_1$	4	298	37.05[h]	38.57[i]
10	10	ethylcarbanate	$P2\bar{1}$	2	168	18.81	20.63
11	11	formamide	$P2_1/n$	4	90	17.15	18.93
12		hexamine	$I\bar{4}3m$	1	100	18.12	20.60
13	12	imidazole	$P2_1/c$	4	123	19.45	20.75
14	13	naphthalene	$P2_1/a$	2	10	17.03	19.53
15	14	oxalic acid α	Pcba	4	298	22.39	23.01
16	15	oxalic acid α	$P2_1/c$	2	298	22.38	22.97
17	16	pyrazine	Pmnn	2	184	13.45	14.65
18	17	pyrazole	$P2_1cn$	8	108	17.29	18.57
19		succinic acid	$P2_1/c$	2	100	29.42	31.14
20	18	triazine	$R\bar{3}c$	6	298	13.30	14.75
21	19	trioxane	R3c	6	103	13.44	15.87
22	20	uracil	$P2_1/a$	4	298	30.87	32.43
23	21	urea	$P\bar{4}2_1/m$	2	298	22.42	24.50

[a]Running number according to ref 174. [b]Running number according to ref 262. [c]Number of molecules in the primitive unit cell. [d]Temperature of X-ray measurement in K. [e]Experimental ΔH at T_0 = 298 K in kcal/mol. [f]Back-corrected zero-point exclusive ΔE at T_0 = 0 K in kcal/mol with estimated error. [g]Value replaced by CCSD(T) estimate from ref 419. [h]Value replaced by current NIST entry registry number 71-30-7.[429] [i]Value adjusted to match updated ΔH.

Table 9. Mean Deviations (MDs), Mean Absolute Deviations (MADs), and Maximum Absolute Deviations (MAXs) in kcal/mol as Well as Mean Absolute Relative Deviations (MARD%) in % of Interaction Energies Calculated with Selected Dispersion-Corrected MF Methods for the Benchmark Sets S22,[275] S12L,[198] and X23;[174,262] Missing Data Are Indicated with Hyphens

	S22[a]				S12L[b]				X23[p]			
	MD	MAD	MAX	MARD%	MD	MAD	MAX	MARD%	MD	MAD	MAX	MARD%
PBE	−2.5[c]	2.6	10.1	55.5	−26.5[d]	26.5	46.1	82.0	−11.6[e]	11.6	28.4	59.5
semiclassical methods + PBE												
PBE-D2	0.5[c,r]	0.6	1.6	13.1	1.2[d]	1.5	3.6	5.2	1.5[e]	1.8	6.4	9.5
PBE-D3[o]	0.1[c,r]	0.5	1.7	9.9	−2.3[d]	2.3	9.1	5.9	−0.5[f]	1.2	3.8	6.4
PBE-TS	0.3[r]	0.3	1.0	10.8	6.5[d,r]	6.5	15.1	20.9	2.3[g]	2.4	8.5	12.6
PBE-MBD	0.0[r]	0.5	1.9	9.4	−0.4[h,r]	1.0	3.2	3.4	1.2[g]	1.5	3.5	7.9
PBE-XDM	−0.3[r]	0.5[o]	2.7	9.2	−0.9[I]	1.5	3.2	5.1	−0.9[r,e]	1.1	3.9	5.9
semiclassical methods + hybrid												
PBE0-MBD	0.1[r]	0.6	1.8	8.6	1.3[h,r]	1.7	4.2	4.7	0.3[g]	0.9	2.2	5.6
PBE0-XDM	−0.1[r]	0.5	2.1	7.1	1.0[I]	1.5	3.8	5.3	–	–	–	–
PBE0-D3[o]	0.1[c,r]	0.5	1.9	8.7	–	–	–	–	−0.4[j]	1.1	3.1	6.2
PW6B95-D3[o]	−0.2[c,r]	0.3	1.2	5.8	0.0[k]	1.6	3.3	4.8	–	–	–	–
nonlocal density based												
PBE-NL	0.2[r]	0.5	1.8	8.3	2.9[d]	3.1	7.3	10.2	–	–	–	–
vdW-DF2	−0.4[m]	0.5	2.8	6.4	–	–	–	–	1.3[r,e]	1.5	3.5	8.5
effective one-electron potentials												
B3LYP-DCP	−0.2[n]	0.3	0.8	5.4	–	–	–	–	5.1[r,l]	5.1	9.6	26.4
M06L	−0.8[c]	0.8	1.7	18.1	−1.2[d]	2.2	5.6	7.7	−1.9[q,r]	2.3	5.5	11.3
M06-2X	−0.2[c]	0.4	1.5	7.4	−2.3[d]	2.5	7.5	7.4	–	–	–	–

[a]Reference data from Table 6. [b]Reference data from Table 7. [c]Data from ref 283. [d]Data from ref 172. [e]Data from ref 262; oxalic acid α and β replaced by ref 412. [f]Data from ref 173. [g]Data from ref 174. [h]Data from ref 175. [I]Data from ref 201. [j]Data from ref 381. [k]Data from ref 198. [l]Data from ref 352; the number of systems was reduced to 16. [m]Data from ref 88. [n]Data from ref 430. [o]Including the three-body dispersion energy (ATM). [p]Reference data from Table 8. [q]Energies computed on PBE-D3 structures. [r]This work; individual data for XDM and TS/MBD related methods kindly provided by A. Otero-de-la-Roza, E. Johnson, and A. Tkatchenko.

DOI: 10.1021/acs.chemrev.5b00533
Chem. Rev. XXXX, XXX, XXX−XXX

concentrate on the widely used and well-known PBE functional as the underlying MF scheme for the semiclassical as well as the VV10 dispersion corrections. For comparison, we also show results for four hybrid functional variants (PBE0-MBD, PBE0-XDM, PBE0-D3, and PW6B95-D3), two Minnesota functionals (M06L and M06-2X), and B3LYP-DCP.

Note that, because of the larger molecular sizes in S12L (up to ∼160 atoms), the average (gas-phase) interaction energy is much larger than that for S22 (44 kcal/mol vs 7.3 kcal/mol; the average interaction energy per molecule in the unit cell for the X23 set is 20.2 kcal/mol). Therefore, in addition to the absolute error measures mean deviation (MD), mean absolute deviation (MAD), and maximum absolute deviation (MAX), we also provide the mean absolute relative deviation (MARD%) from the reference values in Table 9. We use the individual interaction energies as given in the indicated references of Table 9 and recompute the statistical measures according to the reference values from Tables 6, 7, and 8. Missing data were either recomputed in this work or indicated as a footnote.

Because extensive experience exists for the very basic S22 set, we will discuss these data first. Note that most of the methods considered here were empirically developed or explicitly fitted to S22 or similar systems, and hence a good performance for the S22 is a more or less necessary but not fully sufficient condition for general applicability. For this benchmark set, MAD values < 0.5 kcal/mol can be considered as satisfactory while values of 0.2−0.3 kcal/mol (i.e., approaching the accuracy of the reference data) indicate excellent performance. As can be seen from the data in the first row of Table 9, dispersion-uncorrected PBE performs rather poorly with an MAD of 2.6 kcal/mol and an MARD% of >50% for S22. The MD value is negative and has about the same absolute value as the MAD, which indicates that almost all interaction energies are underestimated (underbound complexes). Note that PBE belongs to the class of functionals with intermediate repulsiveness, and even worse results (i.e., more strongly underbound complexes) are obtained for uncorrected BLYP, B3LYP, or TPSS (MAD values are 4.8, 3.8, and 3.5 kcal/mol, respectively[11]). All semiclassical schemes provide good corrections leading to MAD and MARD% values of about 0.5 kcal/mol and 10%, respectively. The nonlocal methods PBE-NL and vdW-DF2 perform similarly, and this also holds for D3-corrected standard functionals (MAD values of 0.29−0.46 kcal/mol; see, e.g., ref 11). The tendency of vdW-DF1 to overestimate dispersion interactions at equilibrium distances diminishes in the revised version, vdW-DF2.[233] For comparison, the MAD of vdW-DF1 on the S22 set is 1.44 kcal/mol with revPBE,[287] 1.03 kcal/mol with revised PW86,[287] and 0.23 kcal/mol with a specifically adapted version of the B88 functional denoted opt-B88,[259] and rPW86-VV09 yields an MAD of 1.20 kcal/mol[287] with LDA correlation contributing significantly to the binding. In the class of hybrids, PW6B95-D3 yields excellent results, while among the one-electron potential-based methods, B3LYP-DCP stands out. From this analysis and additional results for the related S66 set[313] (including many other functionals), one can conclude that various, rather differently constructed dispersion corrections to MF methods provide similarly accurate results for small- and medium-sized noncovalent complexes. The dependence of the underlying functional is roughly the same (or even larger) as that of the various dispersion-correction schemes. The typical error is 5−10% of the interaction energy. To put this into perspective, we mention the MAD on the S22 set obtained for the computationally cheapest post-HF WFT method, MP2, which is 0.78 kcal/mol[431] (at the estimated CBS), i.e., worse than for dispersion-corrected MF methods.

The situation for the S12L set of large supramolecular complexes is similar to the S22, but the spread of the performance of the methods is generally larger. As noted above, the MAD values are much larger (e.g., 25.8 kcal/mol for plain PBE) while relative deviations are similar to those in the S22 (e.g., 5−10% for well-performing methods that have MAD values of 2−3 kcal/mol for this set). A notable outlier is PBE-TS with an MARD% of 21.9%, but this is cured at the MBD level. Its poor performance has been attributed to the strong contribution of many-body dispersion in supramolecular complexes (or more dense materials in general).[175] However, recently it was shown that, within the PBE-XDM model, higher multipole terms (C_8 and C_{10}) seem to be more important compared to high-order many-body contributions.[201] It was furthermore concluded that PBE clearly represents the best MF method for this set of complexes in combination with XDM, which is different from conclusions for S22/S66 where many MF methods perform similarly. The observation that the asymptotic part of the dispersion treatment is more relevant for the larger S12L complexes than for the S22 is not very obvious from inspection of the data. While the MARD% of PBE increases from 55.5% to 81.7% in S12L, the MD for the London dispersion-devoid M06L functional is similar for S22 and S12L, and for M06-2X the corresponding increase of the MD from −0.2 to −1.7 kcal/mol is only moderate.

The results for the X23 solid-state, lattice-energy benchmark set are in between those of S22 and S12L and lead to similar conclusions. The atom pairwise schemes (except PBE-TS) perform very well with almost no systematic deviations, small MAD values of 1−2 kcal/mol, and MARD% of 6−8%. PBE0-MBD is within the chemical accuracy of 1 kcal/mol on the X23 set. While PBE0-D3 has a similar (slightly higher) error, the currently best method is the dispersion-corrected screened hybrid HSE06-D3(ATM) with MAD of 0.8 kcal/mol (corresponding to MARD of 4.6%). This highlights again that, in addition to the dispersion-correction scheme, the underlying semilocal density functional is of importance. We want to stress at this point that the interpretation of benchmark data has to be done carefully as averaged trends are discussed. For instance, the CO_2 crystal seems to be a special case, where all considered semiclassical models compute an underestimated lattice energy. However, a benchmark set of 10 ice polymorphs (ICE10: from low- to high-density polymorphs)[418] confirms some general trends where PBE-TS and PBE-D3 overestimate the lattice energy. This can be partially attributed to the PBE functional, but other combinations (BLYP-D3 and PBE0-D3) show similar trends.

The empirically proven consistency of the theoretical description of the interactions between small molecules, e.g., in dimers and in complex interaction networks like the condensed phase, is a very important result. To what extent the lowest achieved MAD in this work for the X23 set of ∼1 kcal/mol for absolute lattice energies transfers to a corresponding accuracy for relative energy differences of crystal polymorphs has to be studied in more detail. A few studies analyzed the polymorphism of glycine or aspirin,[432−435] but this analysis has to be done more rigorously for an extended set of data. This is especially important for the in silico crystal structure prediction.[402−404] In the 2015 crystal structure prediction blind test, a variety of dispersion-corrected density functionals have been applied, and especially

DOI: 10.1021/acs.chemrev.5b00533
Chem. Rev. XXXX, XXX, XXX−XXX

the newest developments lead to a significant improvement of calculated polymorph landscapes.[436]

Furthermore, for the pairs of corrections D2 vs D3 as well as TS vs MBD, one notices a significantly improved accuracy for the theoretically better founded method (i.e., D3 and MBD), which is encouraging. Both hybrid functional approaches (PBE0-D3 and PBE0-MBD) lead to further improvement in accuracy (probably due to better EXR/es/ind noncovalent interaction contributions), while vdW-DF2 is on the same level as the PBE/semiclassical methods. M06L and B3LYP-DCP perform significantly worse by all statistical measures. Particularly, this holds for B3LYP-DCP, which yields quite good results for the small-molecule set S22. Tentatively, this inconsistency can be attributed to the very empirical character of the dispersion correction, which is less transferable to different systems compared to asymptotically correct methods.

6. SUMMARY AND OUTLOOK

In the almost 40 years since their first use, corrections for the London (long-range) dispersion energy in mean-field methods like Hartree−Fock or approximate Kohn−Sham DFT have come of age and are now routinely applied in chemistry and physics. Concomitantly to their theoretical and numerical development, we notice an increasing awareness and general acceptance of London dispersion interactions as an important and fruitful general chemical concept. In particular, this involves the new idea of intramolecular dispersion effects and their impact in thermochemistry and for structural problems. The basic reason why it took so long to establish, for example, the widely used DFT-D methods is that the dispersion energy, as a mostly additive quantity, shows up chemically only for relatively large systems (>20−30 atoms). Molecules of this size were simply inaccessible in the early days of quantum chemistry, while nowadays DFT calculations are routinely done on 100−200 atoms and in periodic boundaries even for the condensed phase.

In this work, the theoretical foundations of the corrections as well as various approaches have been reviewed. A comprehensive picture of the accuracy of the most widely used methods in applications to typical chemical problems has also been presented. The most prominent correction schemes can be classified into three groups: (i) nonlocal, density-based functionals, (ii) semiclassical C_6 based, and (iii) one-electron effective potentials. The properties and pros and cons of these methods were discussed. There seems to be consensus that asymptotic correctness (right $-1/R^{-6}$ decay behavior with interfragment distance) is a key property for large systems and hence that many methods in group (i) and (ii) yield equally high accuracy for various noncovalent interaction motifs. Furthermore, methods from group (iii) (e.g., highly parametrized density functionals) can be combined with group (i)/(ii) schemes to obtain systematically high accuracy for long- as well as short-range correlation effects.

These modern dispersion-corrected mean-field (DCMF) methods are meanwhile widely applied in the chemical and physical community to describe various standard properties like energies or structures. However, there are less well investigated issues like phonon dispersion, elastic and dielectric constants, or excited states that depend on long-range dispersion interactions as well, and this seems to be a promising field that still needs further exploration. A related, but still not completely solved problem that was only briefly discussed in this Review is solvation. Dispersion effects are omnipresent and also occur for any molecule when it is solvated as in most chemical applications. Molecular dispersion effects are then partly quenched, i.e., intramolecular contributions are replaced by intermolecular ones with the solvent. An accurate account of these effects requires sophisticated solvation models with the same high accuracy as DCMF, which is difficult to obtain at present.

Despite the versatility and general reliability of modern DCMF, intense research efforts are devoted to advance even further the current frontiers of (i) generality/robustness, (ii) many-body effects, and (iii) accuracy. The situation regarding the last point is relatively clear: often the accuracy of the approximated long-range dispersion energy (typical relative error of 5%) is on an absolute scale higher than that of the underlying mean-field method (i.e., a typical semilocal(hybrid) functional like B3LYP). Hence, further development of accurate short-range exchange-correlation functionals seems warranted before turning back to the dispersion problem. This, however, mostly holds for saturated, electronically localized large gap systems where dispersion is inherently a local phenomenon with small many-body contributions. The latter become more significant in metals or for quasi-metallic situations, and here the errors are larger (but sometimes still acceptable). The question remains open whether the separation of dynamical and static electron correlation is still valid in this case or if DCMF theory is applicable at all. Higher many-body contributions in the nonlocal density functionals via an Axilrod−Teller−Muto-type triple spatial integral is another potential development area in this context.

The competitors to DCMF methods are, of course, correlated wave function based approaches like the coupled-cluster "gold standard" CCSD(T), its various local approximations (wave function truncations), and quantum Monte Carlo methods. While these methods are fundamentally more accurate and general, they are still hampered in practice by the slow convergence with the basis set size, related large basis set superposition errors, the huge computational effort involved, and their (technical) inability to efficiently provide the very important nuclear gradients. What is said here about CCSD(T) and related WFTs also partially applies to a number of modern DFT-based methods that are able to directly capture dispersion interactions seamlessly and that have not been described in this review: RPA,[29] ab initio DFT,[437] SAPT using DFT monomer descriptions,[31] double-hybrid functionals,[384] or range-separated functionals with a long-range correlation contribution from wave function methods.[438] All these methods are often less empirical than dispersion-corrected DFT methods. They may also be generally more applicable and resolve other shortcomings of standard DFT like the self-interaction error or static correlation problems. However, the fact that the correlation functional of these methods depends also on virtual orbitals results in an increased computational cost that severely limits their applicability. Hence, it is clear that, in the foreseeable future, DCMFs will continue to hold their ground, particularly for structure optimization or molecular dynamics treatments. In any case, the most promising way seems to be a combination of DCMF structures with accurate WFT methods in single-point energy mode or WFT-generated reference data to check the DCMF results. Regarding this "third" combined DCMF/WFT way, the future for an accurate electronic structure theory for large or condensed systems is bright.

DOI: 10.1021/acs.chemrev.5b00533
Chem. Rev. XXXX, XXX, XXX−XXX

AUTHOR INFORMATION

Corresponding Author

*E-mail: grimme@thch.uni-bonn.de.

Notes

The authors declare no competing financial interest.

Biographies

Stefan Grimme studied Chemistry and finished his Ph.D. in 1991 in Physical Chemistry on a topic in laser spectroscopy. He did his habilitation in Theoretical Chemistry in the group of Sigrid Peyerimhoff. In 2000 he got the C4 chair for Theoretical Organic Chemistry at the University of Münster. In 2011 he accepted an offer as the head of the newly founded Mulliken Center for Theoretical Chemistry at the University of Bonn. He has published more than 400 research articles in various areas of quantum chemistry. He is the recipient of the 2013 Schroedinger medal of the World Organization of Theoretically Oriented Chemists (WATOC) and the 2015 Gottfried-Wilhelm-Leibniz prize of the DFG. His main research interests are the development and application of quantum chemical methods for large molecules, density functional theory, noncovalent interactions, and their impact in chemistry.

Andreas Hansen studied chemistry and physics at the TU Chemnitz and the University of Bonn with a special focus on theory. In 2007, he received his diploma degree in chemistry for a thesis about open-shell ab initio single reference methods. Afterwards, he joined the MPI for chemical energy conversion at Mülheim a. d. Ruhr, continued his research on efficient correlated wave function methods, and finished his Ph.D. under the supervision of Frank Neese in 2012. Since then he has been working at the Mulliken Center of Theoretical Chemistry (University of Bonn) as a lecturer and administrative officer in the group of Stefan Grimme. His research interests are the development and benchmarking of wave function and density functional theory methods for large and challenging systems.

Jan Gerit Brandenburg received his physics diploma in 2012 from the Institute for Theoretical Physics at Heidelberg University. In 2015 he finished his Ph.D. in theoretical chemistry summa cum laude in the group of Stefan Grimme at University of Bonn, where he stayed half a year as postdoctoral researcher. He is awarded a Feodor-Lynen fellowship of the Humboldt foundation for a joint project with Angelos Michaelides and Sarah L. Price at University College London beginning April 2016. His research concentrates on the development and application of fast electronic structure methods, with particular focus on organic crystals and their polymorph prediction.

Christoph Bannwarth received his Master's degree in chemistry from the RWTH Aachen University in 2012. For his Master's thesis, he joined the group of Robert W. Woody at the Colorado State University (Fort Collins, U.S.A.). He is currently a third-year Ph.D. student in the group of Stefan Grimme at the University of Bonn. His research deals with the development and application of efficient electronic structure methods in particular with simplified treatments for excited states and related properties.

ACKNOWLEDGMENTS

We are grateful to the Deutsche Forschungsgemeinschaft within the SPP 1807 "Control of London dispersion interactions in molecular chemistry" for financial support and to J.-P. Djukic, C. A. Bauer, J. Antony, A. Dunlap-Smith, L. Goerigk, M. Korth, R. Sure, and J. Kubelka for proofreading of the manuscript. Furthermore, we greatly acknowledge S. D. Peyerimhoff for her continuous support. We thank E. R. Johnson, A. Otero-de-la-Roza, A. Tkatchenko, and J. Hoja for helpful discussions and kindly providing reference values concerning the MBD and XDM methods, respectively.

REFERENCES

(1) Eisenschitz, R.; London, F. Über das Verhältnis der van der Waalsschen Kräfte zu den homöopolaren Bindungskräften. *Eur. Phys. J. A* **1930**, *60*, 491−527.
(2) London, F. Zur Theorie und Systematik der Molekularkräfte. *Eur. Phys. J. A* **1930**, *63*, 245−279.
(3) London, F. The general theory of molecular forces. *Trans. Faraday Soc.* **1937**, *33*, 8b−26.
(4) Stone, A. J. *The Theory of Intermolecular Forces*; Oxford University Press: Oxford, U.K., 1997.
(5) Kaplan, I. G. *Intermolecular Interactions*; J. Wiley & Sons: Chichester, U.K., 2006.
(6) According to the Web of Science, http://www.webofknowledge.com (accessed December 2, 2015).
(7) Gross, E. K. U.; Dobson, J. F.; Petersilka, M. Density functional theory of time-dependent phenomena. *Top. Curr. Chem.* **1996**, *181*, 81−172.
(8) Grimme, S.; Antony, J.; Schwabe, T.; Mück-Lichtenfeld, C. Density functional theory with dispersion corrections for supramolecular structures, aggregates, and complexes of (bio)organic molecules. *Org. Biomol. Chem.* **2007**, *5*, 741−758.
(9) Johnson, E. R.; Mackie, I. D.; DiLabio, G. A. Dispersion interactions in density-functional theory. *J. Phys. Org. Chem.* **2009**, *22*, 1127−1135.
(10) Burns, L. A.; Vazquez-Mayagoitia, A.; Sumpter, B. G.; Sherrill, C. D. A Comparison of Dispersion Corrections (DFT-D), Exchange-Hole Dipole Moment (XDM) Theory, and Specialized Functionals. *J. Chem. Phys.* **2011**, *134*, 084107.
(11) Grimme, S. Density functional theory with London dispersion corrections. *WIREs Comput. Mol. Sci.* **2011**, *1*, 211−228.
(12) Klimes, J.; Michaelides, A. Perspective: Advances and challenges in treating van der Waals dispersion forces in density functional theory. *J. Chem. Phys.* **2012**, *137*, 120901.
(13) Dobson, J. F.; Gould, T. Calculation of dispersion energies. *J. Phys.: Condens. Matter* **2012**, *24*, 073201.
(14) Grimme, S. In *The Chemical Bond: Chemical Bonding Accross the Periodic Table*; Frenking, G., Shaik, S., Eds.; Wiley-VCH: Weinheim, Germany, 2014; pp 477−499.
(15) Ikabata, Y.; Nakai, H. Local Response Dispersion Method: A Density-Dependent Dispersion Correction for Density Functional Theory. *Int. J. Quantum Chem.* **2015**, *115*, 309−324.
(16) Tkatchenko, A. Current Understanding of Van der Waals Effects in Realistic Materials. *Adv. Funct. Mater.* **2015**, *25*, 2054−2061.
(17) Hellmann, H. *Einführung in die Quantenchemie*; Franz Deuticke: Leipzig und Wien, 1937.
(18) Akimov, A. V.; Prezhdo, O. V. Large-Scale Computations in Chemistry: A Bird's Eye View of a Vibrant Field. *Chem. Rev.* **2015**, *115*, 5797−5890.
(19) Grimme, S.; Huenerbein, R.; Ehrlich, S. On the Importance of the Dispersion Energy for the Thermodynamic Stability of Molecules. *ChemPhysChem* **2011**, *12*, 1258−1261.
(20) Wagner, J. P.; Schreiner, P. R. London Dispersion in Molecular Chemistry-Reconsidering Steric Effects. *Angew. Chem., Int. Ed.* **2015**, *54*, 12274−12296.
(21) Koide, A. A new expansion for dispersion forces and its application. *J. Phys. B: At. Mol. Phys.* **1976**, *9*, 3173.
(22) Becke, A. D.; Johnson, E. R. A density-functional model of the dispersion interaction. *J. Chem. Phys.* **2005**, *123*, 154101.
(23) Riplinger, C.; Sandhoefer, B.; Hansen, A.; Neese, F. Natural triple excitations in local coupled cluster calculations with pair natural orbitals. *J. Chem. Phys.* **2013**, *139*, 134101.
(24) Grimme, S.; Steinmetz, M. Effects of London Dispersion Correction in Density Functional Theory on the Structures of Organic

DOI: 10.1021/acs.chemrev.5b00533
Chem. Rev. XXXX, XXX, XXX−XXX

Molecules in the Gas Phase. *Phys. Chem. Chem. Phys.* **2013**, *15*, 16031−16042.
(25) Ruzsinszky, A.; Perdew, J. P. Twelve outstanding problems in ground-state density functional theory: A bouquet of puzzles. *Comput. Theor. Chem.* **2011**, *963*, 2−6.
(26) Cohen, A. J.; Mori-Sanchez, P.; Yang, W. Challenges for Density Functional Theory. *Chem. Rev.* **2012**, *112*, 289−320.
(27) Becke, A. D. Perspective: Fifty years of density-functional theory in chemical physics. *J. Chem. Phys.* **2014**, *140*, 18A301.
(28) Peverati, R.; Truhlar, D. G. Quest for a universal density functional: the accuracy of density functionals across a broad spectrum of databases in chemistry and physics. *Philos. Trans. R. Soc., A* **2014**, *372*, 20120476.
(29) Eshuis, H.; Bates, J. E.; Furche, F. Electron correlation methods based on the random phase approximation. *Theor. Chem. Acc.* **2012**, *131*, 1084.
(30) Szalewicz, K. Symmetry-adapted perturbation theory of intermolecular forces. *WIREs Comput. Mol. Sci.* **2012**, *2*, 254−272.
(31) Jansen, G. Symmetry-adapted perturbation theory based on density functional theory for noncovalent interactions. *WIREs Comput. Mol. Sci.* **2014**, *4*, 127−144.
(32) Rajchel, L.; Żuchowski, P. S.; Szcześniak, M. M.; Chałasiński, G. Density Functional Theory Approach to Noncovalent Interactions via Monomer Polarization and Pauli Blockade. *Phys. Rev. Lett.* **2010**, *104*, 163001.
(33) Helgaker, T.; Jørgensen, P.; Olsen, J. *Molecular Electronic-Structure Theory*; J. Wiley: New York, 2000.
(34) Kruse, H.; Grimme, S. A geometrical correction for the inter- and intra-molecular basis set superposition error in Hartree-Fock and density functional theory calculations for large systems. *J. Chem. Phys.* **2012**, *136*, 154101.
(35) DiLabio, G. A.; Johnson, E. R.; Otero-de-la Roza, A. Performance of conventional and dispersion-corrected density-functional theory methods for hydrogen bonding interaction energies. *Phys. Chem. Chem. Phys.* **2013**, *15*, 12821−12828.
(36) Maurer, S. A.; Lambrecht, D. S.; Kussmann, J.; Ochsenfeld, C. Efficient distance-including integral screening in linear-scaling Møller-Plesset perturbation theory. *J. Chem. Phys.* **2013**, *138*, 014101.
(37) Schütz, M.; Masur, O.; Usvyat, D. Efficient and accurate treatment of weak pairs in local CCSD(T) calculations. II. Beyond the ring approximation. *J. Chem. Phys.* **2014**, *140*, 244107.
(38) Eriksen, J. J.; Baudin, P.; Ettenhuber, P.; Kristensen, K.; Kjærgaard, T.; Jørgensen, P. Linear-Scaling Coupled Cluster with Perturbative Triple Excitations: The Divide-Expand-Consolidate CCSD(T) Model. *J. Chem. Theory Comput.* **2015**, *11*, 2984−2993.
(39) Kállay, M. Linear-scaling implementation of the direct random-phase approximation. *J. Chem. Phys.* **2015**, *142*, 204105.
(40) Møller, C.; Plesset, M. S. Note on an Approximation Treatment for Many-Electron Systems. *Phys. Rev.* **1934**, *46*, 618−622.
(41) Jung, Y.; Lochan, R. C.; Dutoi, A. D.; Head-Gordon, M. Scaled opposite-spin second order Møller−Plesset correlation energy: An economical electronic structure method. *J. Chem. Phys.* **2004**, *121*, 9793−9802.
(42) Cybulski, S. M.; Lytle, M. L. The origin of deficiency of the supermolecule second-order Møller-Plesset approach for evaluating interaction energies. *J. Chem. Phys.* **2007**, *127*, 141102.
(43) Riley, K. E.; Platts, J. A.; Řezáč, J.; Hobza, P.; Hill, J. G. Assessment of the Performance of MP2 and MP2 Variants for the Treatment of Noncovalent Interactions. *J. Phys. Chem. A* **2012**, *116*, 4159−4169.
(44) Sedlak, R.; Janowski, T.; Pitoňák, M.; Řezáč, J.; Pulay, P.; Hobza, P. Accuracy of Quantum Chemical Methods for Large Noncovalent Complexes. *J. Chem. Theory Comput.* **2013**, *9*, 3364−3374.
(45) Pitoňák, M.; Heßelmann, A. Accurate Intermolecular Interaction Energies from a Combination of MP2 and TDDFT Response Theory. *J. Chem. Theory Comput.* **2010**, *6*, 168−178.
(46) Huang, Y.; Goldey, M.; Head-Gordon, M.; Beran, G. J. O. Achieving High-Accuracy Intermolecular Interactions by Combining Coulomb-Attenuated Second-Order Møller-Plesset Perturbation Theory with Coupled Kohn-Sham Dispersion. *J. Chem. Theory Comput.* **2014**, *10*, 2054−2063.
(47) Grimme, S. Improved second-order Møller−Plesset perturbation theory by separate scaling of parallel- and antiparallel-spin pair correlation energies. *J. Chem. Phys.* **2003**, *118*, 9095−9102.
(48) Marchetti, O.; Werner, H.-J. Accurate Calculations of Intermolecular Interaction Energies Using Explicitly Correlated Coupled Cluster Wave Functions and a Dispersion-Weighted MP2Method. *J. Phys. Chem. A* **2009**, *113*, 11580−11585.
(49) Tkatchenko, A.; DiStasio, R. A.; Head-Gordon, M.; Scheffler, M. Dispersion-corrected Møller−Plesset second-order perturbation theory. *J. Chem. Phys.* **2009**, *131*, 094106.
(50) Goldey, M. B.; Belzunces, B.; Head-Gordon, M. Attenuated MP2 with a long-range dispersion correction for treating non-bonded interactions. *J. Chem. Theory Comput.* **2015**, *11*, 4159−4168.
(51) Hättig, C.; Klopper, W.; Köhn, A.; Tew, D. P. Explicitly Correlated Electrons in Molecules. *Chem. Rev.* **2012**, *112*, 4−74.
(52) Hohenstein, E. G.; Sherrill, C. D. Wavefunction methods for noncovalent interactions. *WIREs Comput. Mol. Sci.* **2012**, *2*, 304−326.
(53) Becke, A. D. Density-functional thermochemistry. III. The role of exact exchange. *J. Chem. Phys.* **1993**, *98*, 5648−5652.
(54) Stephens, P. J.; Devlin, F. J.; Chabalowski, C. F.; Frisch, M. J. Ab Initio Calculation of Vibrational Absorption and Circular Dichroism Spectra Using Density Functional Force Fields. *J. Phys. Chem.* **1994**, *98*, 11623−11627.
(55) Henderson, T. M.; Janesko, B. G.; Scuseria, G. E. Range Separation and Local Hybridization in Density Functional Theory. *J. Phys. Chem. A* **2008**, *112*, 12530−12542.
(56) Arbuznikov, A. V.; Kaupp, M. Advances in local hybrid exchange-correlation functionals: from thermochemistry to magnetic-resonance parameters and hyperpolarizabilities. *Int. J. Quantum Chem.* **2011**, *111*, 2625−2638.
(57) Iikura, H.; Tsuneda, T.; Yanai, T.; Hirao, K. A long-range correction scheme for generalized-gradient-approximation exchange functionals. *J. Chem. Phys.* **2001**, *115*, 3540−3544.
(58) Becke, A. D. A new mixing of Hartree-Fock and local density-functional theories. *J. Chem. Phys.* **1993**, *98*, 1372−1377.
(59) Csonka, G. I.; Perdew, J. P.; Ruzsinszky, A. Global Hybrid Functionals: A Look at the Engine under the Hood. *J. Chem. Theory Comput.* **2010**, *6*, 3688−3703.
(60) Casimir, H. B. G.; Polder, D. The Influence of Retardation on the London-van der Waals Forces. *Phys. Rev.* **1948**, *73*, 360−372.
(61) Davidson, E. R.; Feller, D. Basis set selection for molecular calculations. *Chem. Rev.* **1986**, *86*, 681−696.
(62) Hirschfelder, J. O. Almost degenerate perturbation theory. *Chem. Phys. Lett.* **1978**, *54*, 1−3.
(63) Claverie, P. Theory of intermolecular forces. I. On the inadequacy of the usual Rayleigh-Schrödinger perturbation method for the treatment of intermolecular forces. *Int. J. Quantum Chem.* **1971**, *5*, 273−296.
(64) Morgan, J. D.; Simon, B. Behavior of molecular potential energy curves for large nuclear separations. *Int. J. Quantum Chem.* **1980**, *17*, 1143−1166.
(65) Adams, W. H. Perturbation theory of intermolecular interactions: What is the problem, are there solutions? *Int. J. Quantum Chem.* **1990**, *38*, 531−547.
(66) Kutzelnigg, W. Does the polarization approximation converge for large R to a primitive or a symmetry-adapted wavefunction? *Chem. Phys. Lett.* **1992**, *195*, 77−84.
(67) Adams, W. H. True or false? Order is not uniquely defined in symmetry adapted perturbation theory. *J. Mol. Struct.: THEOCHEM* **2002**, *591*, 59−65.
(68) Williams, H. L.; Chabalowski, C. F. Using Kohn-Sham Orbitals in Symmetry-Adapted Perturbation Theory to Investigate Intermolecular Interactions. *J. Phys. Chem. A* **2001**, *105*, 646−659.
(69) Heßelmann, A.; Jansen, G. First-order intermolecular interaction energies from Kohn-Sham orbitals. *Chem. Phys. Lett.* **2002**, *357*, 464−470.

DOI: 10.1021/acs.chemrev.5b00533
Chem. Rev. XXXX, XXX, XXX−XXX

(70) Heßelmann, A.; Jansen, G. Intermolecular induction and exchange-induction energies from coupled-perturbed Kohn-Sham density functional theory. *Chem. Phys. Lett.* **2002**, *362*, 319−325.
(71) Heßelmann, A.; Jansen, G. Intermolecular dispersion energies from time-dependent density functional theory. *Chem. Phys. Lett.* **2003**, *367*, 778−784.
(72) Misquitta, A. J.; Szalewicz, K. Intermolecular forces from asymptotically corrected density functional description of monomers. *Chem. Phys. Lett.* **2002**, *357*, 301−306.
(73) Misquitta, A. J.; Jeziorski, B.; Szalewicz, K. Dispersion Energy from Density-Functional Theory Description of Monomers. *Phys. Rev. Lett.* **2003**, *91*, 033201.
(74) Misquitta, A. J.; Szalewicz, K. Symmetry-adapted perturbation-theory calculations of intermolecular forces employing density-functional description of monomers. *J. Chem. Phys.* **2005**, *122*, 214109.
(75) Jeziorska, M.; Jeziorski, B.; Čížek, J. Direct calculation of the Hartree-Fock interaction energy via exchange-perturbation expansion. The He··· He interaction. *Int. J. Quantum Chem.* **1987**, *32*, 149−164.
(76) Jeziorski, B.; Moszynski, R.; Szalewicz, K. Perturbation Theory Approach to Intermolecular Potential Energy Surfaces of van der Waals Complexes. *Chem. Rev.* **1994**, *94*, 1887−1930.
(77) Peach, M. J. G.; Williamson, M. J.; Tozer, D. J. Influence of Triplet Instabilities in TDDFT. *J. Chem. Theory Comput.* **2011**, *7*, 3578−3585.
(78) Řezáč, J.; Huang, J.; Hobza, P.; Beran, G. J. O. Benchmark Calculations of Three-Body Intermolecular Interactions and the Performance of Low-Cost Electronic Structure Methods. *J. Chem. Theory Comput.* **2015**, *11*, 3065−3079.
(79) Gordon, M. S.; Slipchenko, L.; Li, H.; Jensen, J. H. The Effective Fragment Potential: A General Method for Predicting Intermolecular Interactions. *Annu. Rep. Comput. Chem.* **2007**, *3*, 177−193.
(80) Dobson, J. F. Beyond Pairwise Additivity in London Dispersion Interactions. *Int. J. Quantum Chem.* **2014**, *114*, 1157−1161.
(81) Grimme, S. Semiempirical GGA-type density functional constructed with a long-range dispersion correction. *J. Comput. Chem.* **2006**, *27*, 1787−1799.
(82) Jurečka, P.; Černý, j.; Hobza, P.; Salahub, D. R. Density functional theory augmented with an empirical dispersion term. Interaction energies and geometries of 80 noncovalent complexes compared with ab initio quantum mechanics calculations. *J. Comput. Chem.* **2007**, *28*, 555−569.
(83) Johnson, E. R.; Becke, A. D. A post-Hartree-Fock model of intermolecular interactions. *J. Chem. Phys.* **2005**, *123*, 024101.
(84) Johnson, E. R.; Becke, A. D. A post-Hartree-Fock model of intermolecular interactions: Inclusion of higher-order corrections. *J. Chem. Phys.* **2006**, *124*, 174104.
(85) Grimme, S.; Antony, J.; Ehrlich, S.; Krieg, H. A consistent and accurate ab initio parametrization of density functional dispersion correction (DFT-D) for the 94 elements H-Pu. *J. Chem. Phys.* **2010**, *132*, 154104.
(86) Tkatchenko, A.; Scheffler, M. Accurate Molecular Van Der Waals Interactions from Ground-State Electron Density and Free-Atom Reference Data. *Phys. Rev. Lett.* **2009**, *102*, 073005.
(87) Tkatchenko, A.; DiStasio, R. A.; Car, R.; Scheffler, M. Accurate and Efficient Method for Many-Body van der Waals Interactions. *Phys. Rev. Lett.* **2012**, *108*, 236402.
(88) Lee, K.; Murray, É D.; Kong, L.; Lundqvist, B. I.; Langreth, D. C. Higher-accuracy van der Waals density functional. *Phys. Rev. B: Condens. Matter Mater. Phys.* **2010**, *82*, 081101.
(89) Vydrov, O. A.; Van Voorhis, T. Nonlocal van der Waals density functional: the simpler the better. *J. Chem. Phys.* **2010**, *133*, 244103.
(90) Tkatchenko, A.; von Lilienfeld, O. A. Popular Kohn-Sham density functionals strongly overestimate many-body interactions in van der Waals systems. *Phys. Rev. B: Condens. Matter Mater. Phys.* **2008**, *78*, 045116.
(91) von Lilienfeld, O. A.; Tkatchenko, A. Two- and three-body interatomic dispersion energy contributions to binding in molecules and solids. *J. Chem. Phys.* **2010**, *132*, 234109.
(92) Dobson, J. F.; White, A.; Rubio, A. Asymptotics of the Dispersion Interaction: Analytic Benchmarks for van der Waals Energy Functionals. *Phys. Rev. Lett.* **2006**, *96*, 073201.
(93) Due to nonadditivity effects, the C_6 dispersion coefficient of the C_{60} dimer turns out to be too small (i.e., less attractive) by 10−20% if computed by atom pairwise schemes.[137,138] However, compared to experimentally derived data, the atom pairwise D3 scheme still yields the correct bonding distance (within 0.1 Å) and energy (within 0.5 kcal/mol).[94] Counterintuitively, the association energy of C_{60} containing vdW complexes are overestimated (by up to 25%) with atom pairwise D3, which improves if the Axilrod−Teller−Muto term is included (overestimation by ∼10%).[95]
(94) The potential curve for C_{60} has been conducted at the TPSS-D3(BJ) and BLYP-D3(BJ) in the group of S. Grimme.
(95) Sure, R.; Grimme, S. Comprehensive Benchmark of Association (Free) Energies of Realistic Host-Guest Complexes. *J. Chem. Theory Comput.* **2015**, *11*, 3785−3801.
(96) Gobre, V. V.; Tkatchenko, A. Scaling laws for van der Waals interactions in nanostructured materials. *Nat. Commun.* **2013**, *4*, 2341.
(97) Tao, J.; Perdew, J. P. Communication: Non-additivity of van der Waals interactions between nanostructures. *J. Chem. Phys.* **2014**, *141*, 141101.
(98) Kristyán, S.; Pulay, P. Can (semi)local density functional theory account for the London dispersion forces? *Chem. Phys. Lett.* **1994**, *229*, 175−180.
(99) Pérez-Jordá, J. M.; Becke, A. D. A density-functional study of van der Waals forces: rare gas diatomics. *Chem. Phys. Lett.* **1995**, *233*, 134−137.
(100) Hobza, P.; Šponer, J.; Reschel, T. Density functional theory and molecular clusters. *J. Comput. Chem.* **1995**, *16*, 1315−1325.
(101) Lacks, D. J.; Gordon, R. G. Pair interactions of rare-gas atoms as a test of exchange-energy-density functionals in regions of large density gradients. *Phys. Rev. A: At., Mol., Opt. Phys.* **1993**, *47*, 4681−4690.
(102) Meijer, E. J.; Sprik, M. A density-functional study of the intermolecular interactions of benzene. *J. Chem. Phys.* **1996**, *105*, 8684−8689.
(103) Ziegler, T. Approximate density functional theory as a practical tool in molecular energetics and dynamics. *Chem. Rev.* **1991**, *91*, 651−667.
(104) van Mourik, T.; Gdanitz, R. J. A critical note on density functional theory studies on rare-gas dimers. *J. Chem. Phys.* **2002**, *116*, 9620−9623.
(105) Dalrymple, D. L.; Reinheimer, J. D.; Barnes, D.; Baker, R. London force interactions in the reactions of benzyl chlorides. *J. Org. Chem.* **1964**, *29*, 2647−2652.
(106) Ghotra, J. S.; Hursthouse, M. B.; Welch, A. J. Three-co-ordinate scandium(III) and europium(III); crystal and molecular structures of their trishexamethyldisilylamides. *J. Chem. Soc., Chem. Commun.* **1973**, 669−670.
(107) Cohen, J. S.; Pack, R. T. Modified statistical method for intermolecular potentials. Combining rules for higher van der Waals coefficients. *J. Chem. Phys.* **1974**, *61*, 2372−2382.
(108) Gordon, R. G.; Kim, Y. S. Theory for the Forces between Closed-Shell Atoms and Molecules. *J. Chem. Phys.* **1972**, *56*, 3122−3133.
(109) Rae, A. I. M. A theory for the interactions between closed shell systems. *Chem. Phys. Lett.* **1973**, *18*, 574−577.
(110) Gianturco, F. A.; Paesani, F.; Laranjeira, M. F.; Vassilenko, V.; Cunha, M. A.; Shashkov, A. G.; Zolotoukhina, A. F. Computed and measured thermal diffusion factor for CO-He mixtures: a test of recent interaction potentials. *Mol. Phys.* **1997**, *92*, 957−972.
(111) Gianturco, F. A.; Paesani, F.; Laranjeira, M. F.; Vassilenko, V.; Cunha, M. A.; Shashkov, A. G.; Zolotoukhina, A. F. Computed and measured transport coefficients for CO-He mixtures: testing a density functional approach. *Mol. Phys.* **1998**, *94*, 605−622.
(112) Gianturco, F. A.; Paesani, F.; Laranjeira, M. F.; Vassilenko, V.; Cunha, M. A. Intermolecular forces from density functional theory. III. A multiproperty analysis for the Ar(^{1}S)-CO($^1\Sigma$) interaction. *J. Chem. Phys.* **1999**, *110*, 7832−7845.

DOI: 10.1021/acs.chemrev.5b00533
Chem. Rev. XXXX, XXX, XXX−XXX

(113) Gianturco, F. A.; Paesani, F. The rovibrational structure of the Ar−CO complex from a model interaction potential. *J. Chem. Phys.* **2001**, *115*, 249−256.
(114) Tang, K. T.; Toennies, J. P. An improved simple model for the van der Waals potential based on universal damping functions for the dispersion coefficients. *J. Chem. Phys.* **1984**, *80*, 3726−3741.
(115) Seponer, J.; Leszczynski, J.; Hobza, P. Base stacking in cytosine dimer. A comparison of correlated ab initio calculations with three empirical potential models and density functional theory calculations. *J. Comput. Chem.* **1996**, *17*, 841−850.
(116) Hobza, P.; Šponer, J. Structure, Energetics, and Dynamics of the Nucleic Acid Base Pairs: Nonempirical *Ab Initio* Calculations. *Chem. Rev.* **1999**, *99*, 3247−3276.
(117) Müller-Dethlefs, K.; Hobza, P. Noncovalent Interactions: A Challenge for Experiment and Theory. *Chem. Rev.* **2000**, *100*, 143−167.
(118) Wu, X.; Vargas, M. C.; Nayak, S.; Lotrich, V.; Scoles, G. Towards extending the applicability of density functional theory to weakly bound systems. *J. Chem. Phys.* **2001**, *115*, 8748−8757.
(119) Elstner, M.; Hobza, P.; Frauenheim, T.; Suhai, S.; Kaxiras, E. Hydrogen bonding and stacking interactions of nucleic acid base pairs: a density-functional-theory based treatment. *J. Chem. Phys.* **2001**, *114*, 5149−5155.
(120) Wu, Q.; Yang, W. Empirical correction to density functional theory for van der Waals interactions. *J. Chem. Phys.* **2002**, *116*, 515−524.
(121) Zimmerli, U.; Parrinello, M.; Koumoutsakos, P. Dispersion corrections to density functionals for water aromatic interactions. *J. Chem. Phys.* **2004**, *120*, 2693−2699.
(122) Elstner, M.; Porezag, D.; Jungnickel, G.; Elsner, J.; Haugk, M.; Frauenheim, T.; Suhai, S.; Seifert, G. Self-consistent-charge density-functional tight-binding method for simulations of complex materials properties. *Phys. Rev. B: Condens. Matter Mater. Phys.* **1998**, *58*, 7260−7268.
(123) Hepburn, J.; Scoles, G.; Penco, R. A simple but reliable method for the prediction of intermolecular potentials. *Chem. Phys. Lett.* **1975**, *36*, 451−456.
(124) Ahlrichs, R.; Penco, R.; Scoles, G. Intermolecular forces in simple systems. *Chem. Phys.* **1977**, *19*, 119−130.
(125) Conway, A.; Murrell, J. N. The exchange energy between neon atoms. *Mol. Phys.* **1974**, *27*, 873−878.
(126) Pawliszyn, J.; Szczesniak, M. M.; Scheiner, S. Interactions between aromatic systems: dimers of benzene and s-tetrazine. *J. Phys. Chem.* **1984**, *88*, 1726−1730.
(127) Čársky, P.; Selzle, H. L.; Schlag, E. W. Ab initio calculations on the structure of the benzene dimer. *Chem. Phys.* **1988**, *125*, 165−170.
(128) Gonzalez, C.; Allison, T. C.; Lim, E. C. Hartree-Fock Dispersion Probe of the Equilibrium Structures of Small Microclusters of Benzene and Naphthalene: Comparison with Second-Order Møeller-Plesset Geometries. *J. Phys. Chem. A* **2001**, *105*, 10583−10587.
(129) Grimme, S.; Ehrlich, S.; Goerigk, L. Effect of the Damping Function in Dispersion Corrected Density Functional Theory. *J. Comput. Chem.* **2011**, *32*, 1456−1465.
(130) Sure, R.; Grimme, S. Corrected small basis set Hartree-Fock method for large systems. *J. Comput. Chem.* **2013**, *34*, 1672−1685.
(131) Conrad, J. A.; Gordon, M. S. Modeling Systems with $\pi-\pi$ Interactions Using the Hartree-Fock Method with an Empirical Dispersion Correction. *J. Phys. Chem. A* **2015**, *119*, 5377−5385.
(132) Guidez, E. B.; Gordon, M. S. Dispersion Correction Derived from First Principles for Density Functional Theory and Hartree-Fock Theory. *J. Phys. Chem. A* **2015**, *119*, 2161−2168.
(133) Clementi, E.; Corongiu, C. Van der Waals Interaction Energies of Helium, Neon, and Argon with Naphthalene. *J. Phys. Chem. A* **2001**, *105*, 10379−10383.
(134) Otero-de-la-Roza, A.; Johnson, E. R. Many-body dispersion interactions from the exchange-hole dipole moment model. *J. Chem. Phys.* **2013**, *138*, 054103.
(135) Mavroyannis, C.; Stephen, M. Dispersion forces. *Mol. Phys.* **1962**, *5*, 629−638.
(136) Tkatchenko, A.; Ambrosetti, A.; DiStasio, R. A. Interatomic methods for the dispersion energy derived from the adiabatic connection fluctuation-dissipation theorem. *J. Chem. Phys.* **2013**, *138*, 074106.
(137) Ruzsinszky, A.; Perdew, J. P.; Tao, J.; Csonka, G. I.; Pitarke, J. M. Van der Waals Coefficients for Nanostructures: Fullerenes Defy Conventional Wisdom. *Phys. Rev. Lett.* **2012**, *109*, 233203.
(138) Kauczor, J.; Norman, P.; Saidi, W. A. Non-additivity of polarizabilities and van der Waals C6 coefficients of fullerenes. *J. Chem. Phys.* **2013**, *138*, 114107.
(139) Pernal, K.; Podeszwa, R.; Patkowski, K.; Szalewicz, K. Dispersionless Density Functional Theory. *Phys. Rev. Lett.* **2009**, *103*, 263201.
(140) Stanton, J. F. Calculation of C_6 dispersion constants with couyled-cluster theory. *Phys. Rev. A: At., Mol., Opt. Phys.* **1994**, *49*, 1698−1703.
(141) van Gisbergen, S. J. A.; Snijders, J. G.; Baerends, E. J. A Density Functional Theory Study of Frequency-Dependent Polarizabilities and van der Waals Dispersion Coefficients for Polyatomic Molecules. *J. Chem. Phys.* **1995**, *103*, 9347−9354.
(142) Osinga, V. P.; van Gisbergen, S. J. A.; Snijders, J. G.; Baerends, E. J. Density Functional Results for Isotropic and Anisotropic Multipole Polarizabilities and C_6, C_7 and C_8 van der Waals Dispersion Coefficients for Molecules. *J. Chem. Phys.* **1997**, *106*, 5091−5101.
(143) Cybulski, S. M.; Haley, T. P. New approximations for calculating dispersion coefficients. *J. Chem. Phys.* **2004**, *121*, 7711−7716.
(144) Tao, J.; Perdew, J. P.; Ruzsinszky, A. Accurate van der Waals coefficients from density functional theory. *Proc. Natl. Acad. Sci. U. S. A.* **2012**, *109*, 18−21.
(145) Toulouse, J.; Rebolini, E.; Gould, T.; Dobson, J. F.; Seal, P.; Angyán, J. G. Assessment of range-separated time-dependent density-functional theory for calculating C6 dispersion coefficients. *J. Chem. Phys.* **2013**, *138*, 194106.
(146) Grimme, S. Accurate Description of van der Waals Complexes by Density Functional Theory Including Empirical Corrections. *J. Comput. Chem.* **2004**, *25*, 1463−1473.
(147) Chai, J.-D.; Head-Gordon, M. Long-range corrected hybrid density functionals with damped atom-atom dispersion corrections. *Phys. Chem. Chem. Phys.* **2008**, *10*, 6615−6620.
(148) Perdew, J. P.; Burke, K.; Ernzerhof, M. Generalized Gradient Approximation Made Simple. *Phys. Rev. Lett.* **1996**, *77*, 3865−3868.
(149) Perdew, J. P.; Burke, K.; Ernzerhof, M. Generalized Gradient Approximation Made Simple [Phys. Rev. Lett. 77, 3865 (1996)]. *Phys. Rev. Lett.* **1997**, *78*, 1396−1396.
(150) Adamo, C.; Barone, V. Toward reliable density functional methods without adjustable parameters: The PBE0 model. *J. Chem. Phys.* **1999**, *110*, 6158−6170.
(151) Becke, A. D. Density-functional thermochemistry. V. Systematic optimization of exchange-correlation functionals. *J. Chem. Phys.* **1997**, *107*, 8554−8560.
(152) Collignon, B.; Hoang, P.; Picaud, S.; Liotard, D.; Rayez, M.; Rayez, J. A semi-empirical potential model for calculating interactions between large aromatic molecules and graphite surfaces. *J. Mol. Struct.: THEOCHEM* **2006**, *772*, 1−12.
(153) McNamara, J. P.; Hillier, I. H. Semi-empirical molecular orbital methods including dispersion corrections for the accurate prediction of the full range of intermolecular interactions in biomolecules. *Phys. Chem. Chem. Phys.* **2007**, *9*, 2362−2370.
(154) Morgado, C. A.; McNamara, J. P.; Hillier, I. H.; Burton, N. A.; Vincent, M. A. Density functional and semiempirical molecular orbital methods including dispersion corrections for the accurate description of noncovalent interactions involving sulfur-containing molecules. *J. Chem. Theory Comput.* **2007**, *3*, 1656−1664.
(155) Tuttle, T.; Thiel, W. OM x-D: semiempirical methods with orthogonalization and dispersion corrections. Implementation and biochemical application. *Phys. Chem. Chem. Phys.* **2008**, *10*, 2159−2166.
(156) Řezáč, J.; Fanfrlík, J.; Salahub, D.; Hobza, P. Semiempirical Quantum Chemical PM6 Method Augmented by Dispersion and H-

DOI: 10.1021/acs.chemrev.5b00533
Chem. Rev. XXXX, XXX, XXX−XXX

Bonding Correction Terms Reliably Describes Various Types of Noncovalent Complexes. *J. Chem. Theory Comput.* **2009**, *5*, 1749−1760.
(157) Schwabe, T.; Grimme, S. Double-hybrid density functionals with long-range dispersion corrections: higher accuracy and extended applicability. *Phys. Chem. Chem. Phys.* **2007**, *9*, 3397−3406.
(158) Yousaf, K. E.; Brothers, E. N. Applications of Screened Hybrid Density Functionals with Empirical Dispersion Corrections to Rare Gas Dimers and Solids. *J. Chem. Theory Comput.* **2010**, *6*, 864−872.
(159) Swart, M.; Solà, M.; Bickelhaupt, F. M. A new all-round density functional based on spin states and SN2 barriers. *J. Chem. Phys.* **2009**, *131*, 094103.
(160) Barone, V.; Biczysko, M.; Pavone, M. The role of dispersion correction to DFT for modelling weakly bound molecular complexes in the ground and excited electronic states. *Chem. Phys.* **2008**, *346*, 247−256.
(161) Becke, A. D. Density-Functional Exchange-Energy Approximation with Correct Asymptotic Behaviour. *Phys. Rev. A: At., Mol., Opt. Phys.* **1988**, *38*, 3098−3100.
(162) Lee, C.; Yang, W.; Parr, R. G. Development of the Colle-Salvetti Correlation-Energy Formula into a Functional of the Electron Density. *Phys. Rev. B: Condens. Matter Mater. Phys.* **1988**, *37*, 785−789.
(163) Civalleri, B.; Zicovich-Wilson, C. M.; Valenzano, L.; Ugliengo, P. B3LYP augmented with an empirical dispersion term (B3LYP-D*) as applied to molecular crystals. *CrystEngComm* **2008**, *10*, 405−410.
(164) Steinmann, S. N.; Csonka, G.; Corminboeuf, C. Unified Inter- and Intramolecular Dispersion Correction Formula for Generalized Gradient Approximation Density Functional Theory. *J. Chem. Theory Comput.* **2009**, *5*, 2950−2958.
(165) Austin, A.; Petersson, G. A.; Frisch, M. J.; Dobek, F. J.; Scalmani, G.; Throssell, K. A Density Functional with Spherical Atom Dispersion Terms. *J. Chem. Theory Comput.* **2012**, *8*, 4989−5007.
(166) Pyykkö, P.; Atsumi, M. Molecular Single-Bond Covalent Radii for Elements 1−118. *Chem. - Eur. J.* **2009**, *15*, 186−197.
(167) Casida, M. E. In *Recent Advances In Density Functional Methods*; Chong, D. P., Ed.; World Scientific: Singapore, 1995; Vol. *1*; pp 155−192.
(168) Starkschall, G.; Gordon, R. G. Calculation of Coefficients in the Power Series Expansion of the Long-Range Dispersion Force between Atoms. *J. Chem. Phys.* **1972**, *56*, 2801−2806.
(169) Thakkar, A. J. Higher dispersion coefficients: Accurate values for hydrogen atoms and simple estimates for other systems. *J. Chem. Phys.* **1988**, *89*, 2092−2098.
(170) Axilrod, B. M.; Teller, E. Interaction of the van der Waals Type Between Three Atoms. *J. Chem. Phys.* **1943**, *11*, 299−300.
(171) Muto, Y. Force between nonpolar molecules. *Proc. Phys. Soc. Jpn.* **1943**, *17*, 629.
(172) Risthaus, T.; Grimme, S. Benchmarking of London Dispersion-Accounting Density Functional Theory Methods on Very Large Molecular Complexes. *J. Chem. Theory Comput.* **2013**, *9*, 1580−1591.
(173) Brandenburg, J. G.; Grimme, S. Dispersion Corrected Hartree-Fock and Density Functional Theory for Organic Crystal Structure Prediction. *Top. Curr. Chem.* **2013**, *345*, 1−23.
(174) Reilly, A. M.; Tkatchenko, A. Understanding the role of vibrations, exact exchange, and many-body van der Waals interactions in the cohesive properties of molecular crystals. *J. Chem. Phys.* **2013**, *139*, 024705.
(175) Ambrosetti, A.; Alfè, D.; DiStasio, R. A.; Tkatchenko, A. Hard Numbers for Large Molecules: Toward Exact Energetics for Supramolecular Systems. *J. Phys. Chem. Lett.* **2014**, *5*, 849−855.
(176) Kromann, J. C.; Christensen, A. S.; Steinmann, C.; Korth, M.; Jensen, J. H. A third-generation dispersion and third-generation hydrogen bonding corrected PM6 method: PM6-D3H+. *PeerJ* **2014**, *2*, e449.
(177) Grimme, S. Towards First Principles Calculation of Electron Impact Mass Spectra of Molecules. *Angew. Chem., Int. Ed.* **2013**, *52*, 6306−6312.
(178) Brandenburg, J. G.; Grimme, S. Accurate Modeling of Organic Molecular Crystals by Dispersion-Corrected Density Functional Tight Binding (DFTB). *J. Phys. Chem. Lett.* **2014**, *5*, 1785−1789.
(179) Brandenburg, J. G.; Hochheim, M.; Bredow, T.; Grimme, S. Low-Cost Quantum Chemical Methods for Non-Covalent Interactions. *J. Phys. Chem. Lett.* **2014**, *5*, 4275−4284.
(180) Grimme, S. A General Quantum Mechanically Derived Force Field (QMDFF) for Molecules and Condensed Phase Simulations. *J. Chem. Theory Comput.* **2014**, *10*, 4497−4514.
(181) Schröder, H.; Creon, A.; Schwabe, T. Reformulation of the D3(Becke-Johnson) Dispersion Correction without Resorting to Higher than C6 Dispersion Coefficients. *J. Chem. Theory Comput.* **2015**, *11*, 3163−3170.
(182) Ehrlich, S.; Moellmann, J.; Reckien, W.; Bredow, T.; Grimme, S. System-Dependent Dispersion Coefficients for the DFT-D3 Treatment of Adsorption Processes on Ionic Surfaces. *ChemPhysChem* **2011**, *12*, 3414−3420.
(183) Hansen, A.; Bannwarth, C.; Grimme, S.; Petrović, P.; Werlé, C.; Djukic, J.-P. The Thermochemistry of London Dispersion-Driven Transition Metal Reactions: Getting the 'Right Answer for the Right Reason'. *ChemistryOpen* **2014**, *3*, 177−189.
(184) Sulzer, D.; Norman, P.; Saue, T. Atomic C 6 dispersion coefficients: a four-component relativistic Kohn−Sham study. *Mol. Phys.* **2012**, *110*, 2535−2541.
(185) Unsöld, A. Beiträge zur Quantenmechanik der Atome. *Ann. Phys.* **1927**, *387*, 355−393.
(186) Chu, X.; Dalgarno, A. Linear response time-dependent density functional theory for van der Waals coefficients. *J. Chem. Phys.* **2004**, *121*, 4083−4088.
(187) Kannemann, F. O.; Becke, A. D. Atomic volumes and polarizabilities in density-functional theory. *J. Chem. Phys.* **2012**, *136*, 034109.
(188) Hirshfeld, F. Bonded-atom fragments for describing molecular charge densities. *Theor. chim. acta* **1977**, *44*, 129−138.
(189) Bondi, A. van der Waals volumes and radii. *J. Phys. Chem.* **1964**, *68*, 441−451.
(190) Bučko, T.; Lebègue, S.; Hafner, J.; Ángyán, J. G. Improved Density Dependent Correction for the Description of London Dispersion Forces. *J. Chem. Theory Comput.* **2013**, *9*, 4293−4299.
(191) Bultinck, P.; Van Alsenoy, C.; Ayers, P. W.; Carbó-Dorca, R. Critical analysis and extension of the Hirshfeld atoms in molecules. *J. Chem. Phys.* **2007**, *126*, 144111.
(192) Ferri, N.; DiStasio, R. A.; Ambrosetti, A.; Car, R.; Tkatchenko, A. Electronic Properties of Molecules and Surfaces with a Self-Consistent Interatomic van der Waals Density Functional. *Phys. Rev. Lett.* **2015**, *114*, 176802.
(193) Tang, K. T.; Karplus, M. Padé-Approximant Calculation of the Nonretarded van der Waals Coefficients for Two and Three Helium Atoms. *Phys. Rev.* **1968**, *171*, 70−74.
(194) Silvestrelli, P. L.; Ambrosetti, A. Including screening in van der Waals corrected density functional theory calculations: The case of atoms and small molecules physisorbed on graphene. *J. Chem. Phys.* **2014**, *140*, 124107.
(195) Donchev, A. G. Many-body effects of dispersion interaction. *J. Chem. Phys.* **2006**, *125*, 074713.
(196) Ambrosetti, A.; Reilly, A. M.; DiStasio, R. A.; Tkatchenko, A. Long-range correlation energy calculated from coupled atomic response functions. *J. Chem. Phys.* **2014**, *140*, 18A508.
(197) Langreth, D. C.; Perdew, J. P. Exchange-correlation energy of a metallic surface: Wave-vector analysis. *Phys. Rev. B* **1977**, *15*, 2884−2901.
(198) Grimme, S. Supramolecular binding thermodynamics by dispersion corrected density functional theory. *Chem. - Eur. J.* **2012**, *18*, 9955−9964.
(199) Scuseria, G. E.; Henderson, T. M.; Sorensen, D. C. The ground state correlation energy of the random phase approximation from a ring coupled cluster doubles approach. *J. Chem. Phys.* **2008**, *129*, 231101.
(200) Scuseria, G. E.; Henderson, T. M.; Bulik, I. W. Particle-particle and quasiparticle random phase approximations: Connections to coupled cluster theory. *J. Chem. Phys.* **2013**, *139*, 104113.

DOI: 10.1021/acs.chemrev.5b00533
Chem. Rev. XXXX, XXX, XXX−XXX

(201) Otero-de-la Roza, A.; Johnson, E. R. Predicting energetics of supramolecular systems using the XDM dispersion model. *J. Chem. Theory Comput.* **2015**, *11*, 4033−4040.
(202) Blood-Forsythe, M. A.; Markovich, T.; DiStasio, R. A.; Car, R.; Aspuru-Guzik, A. Analytical nuclear gradients for the range-separated many-body dispersion model of noncovalent interactions. *Chem. Sci.* **2016**, *7*, 1712−1728.
(203) Bučko, T.; Lebègue, S.; Gould, T.; Ángyán, J. G. Many-body dispersion corrections for periodic systems: an efficient reciprocal space implementation. *J. Phys.: Condens. Matter* **2016**, *28*, 045201.
(204) Silvestrelli, P. L. Van der Waals Interactions in Density Functional Theory Using Wannier Functions. *J. Phys. Chem. A* **2009**, *113*, 5224−5234.
(205) Ambrosetti, A.; Silvestrelli, P. L. van der Waals Interactions in density functional theory using Wannier Functions: Improved C_6 and C_3 coefficients by a different approach. *Phys. Rev. B: Condens. Matter Mater. Phys.* **2012**, *85*, 073101.
(206) Silvestrelli, P. L. Van der Waals interactions in density functional theory by combining the quantum harmonic oscillator-model with localized Wannier functions. *J. Chem. Phys.* **2013**, *139*, 054106.
(207) Silvestrelli, P. L. Van der Waals Interactions in DFT Made Easy by Wannier Functions. *Phys. Rev. Lett.* **2008**, *100*, 053002.
(208) Marzari, N.; Vanderbilt, D. Maximally localized generalized Wannier functions for composite energy bands. *Phys. Rev. B: Condens. Matter Mater. Phys.* **1997**, *56*, 12847−12865.
(209) Andersson, Y.; Langreth, D. C.; Lundqvist, B. I. van der Waals Interactions in Density-Functional Theory. *Phys. Rev. Lett.* **1996**, *76*, 102−105.
(210) Becke, A. D.; Johnson, E. R. Exchange-hole dipole moment and the dispersion interaction revisited. *J. Chem. Phys.* **2007**, *127*, 154108.
(211) Becke, A. D.; Johnson, E. R. Exchange-hole dipole moment and the dispersion interaction. *J. Chem. Phys.* **2005**, *122*, 154104.
(212) Becke, A. D.; Roussel, M. R. Exchange holes in inhomogeneous systems: A coordinate-space model. *Phys. Rev. A: At., Mol., Opt. Phys.* **1989**, *39*, 3761−3767.
(213) Kannemann, F. O.; Becke, A. D. Van der Waals Interactions in Density-Functional Theory: Intermolecular Complexes. *J. Chem. Theory Comput.* **2010**, *6*, 1081−1088.
(214) Cambi, R.; Cappelletti, D.; Liuti, G.; Pirani, F. Generalized correlations in terms of polarizability for van der Waals interaction potential parameter calculations. *J. Chem. Phys.* **1991**, *95*, 1852−1861.
(215) Lide, D. R., Haynes, W., Eds. *CRC Handbook of Chemistry and Physics*, 90th ed.; CRC Press: 2010.
(216) Becke, A. D.; Johnson, E. R. Exchange-hole dipole moment and the dispersion interaction: High-order dispersion coefficients. *J. Chem. Phys.* **2006**, *124*, 014104.
(217) Kong, J.; Gan, Z.; Proynov, E.; Freindorf, M.; Furlani, T. Efficient Computation of the Dispersion Interaction with Density-Functional Theory. *Phys. Rev. A: At., Mol., Opt. Phys.* **2009**, *79*, 042510.
(218) DiLabio, G. A.; Otero-de-la-Roza, A. Noncovalent Interactions in Density-Functional Theory. *ArXiv E-Prints* 2014; arXiv:1405.1771v2 (accessed on July 23, 2015).
(219) Ángyán, J. G. On the exchange-hole model of London dispersion forces. *J. Chem. Phys.* **2007**, *127*, 024108.
(220) Heßelmann, A. Derivation of the dispersion energy as an explicit density- and exchange-hole functional. *J. Chem. Phys.* **2009**, *130*, 084104.
(221) Ayers, P. W. A perspective on the link between the exchange(-correlation) hole and dispersion forces. *J. Math. Chem.* **2009**, *46*, 86−96.
(222) Heßelmann, A. Long-range correlation energies from frequency-dependent weighted exchange-hole dipole polarisabilities. *J. Chem. Phys.* **2012**, *136*, 014104.
(223) Steinmann, S. N.; Corminboeuf, C. A System-Dependent Density-Based Dispersion Correction. *J. Chem. Theory Comput.* **2010**, *6*, 1990−2001.
(224) Steinmann, S. N.; Corminboeuf, C. A generalized-gradient approximation exchange hole model for dispersion coefficients. *J. Chem. Phys.* **2011**, *134*, 044117.
(225) Mayer, I.; Salvador, P. Overlap populations, bond orders and valences for 'fuzzy' atoms. *Chem. Phys. Lett.* **2004**, *383*, 368−375.
(226) Steinmann, S. N.; Corminboeuf, C. Comprehensive Benchmarking of a Density-Dependent Dispersion Correction. *J. Chem. Theory Comput.* **2011**, *7*, 3567−3577.
(227) Corminboeuf, C. Minimizing Density Functional Failures for Non-Covalent Interactions Beyond van der Waals Complexes. *Acc. Chem. Res.* **2014**, *47*, 3217−3224.
(228) Brémond, E.; Golubev, N.; Steinmann, S. N.; Corminboeuf, C. How important is self-consistency for the dDsC density dependent dispersion correction? *J. Chem. Phys.* **2014**, *140*, 18A516.
(229) Sato, T.; Nakai, H. Density functional method including weak interactions: Dispersion coefficients based on the local response approximation. *J. Chem. Phys.* **2009**, *131*, 224104.
(230) Sato, T.; Nakai, H. Local Response Dispersion Method. II. Generalized Multicenter Interactions. *J. Chem. Phys.* **2010**, *133*, 194101.
(231) Dobson, J. F.; Dinte, B. P. Constraint Satisfaction in Local and Gradient Susceptibility Approximations: Application to a van der Waals Density Functional. *Phys. Rev. Lett.* **1996**, *76*, 1780−1783.
(232) Becke, A. D. A multicenter numerical integration scheme for polyatomic molecules. *J. Chem. Phys.* **1988**, *88*, 2547.
(233) Vydrov, O. A.; Van Voorhis, T. Improving the accuracy of the nonlocal van der Waals density functional with minimal empiricism. *J. Chem. Phys.* **2009**, *130*, 104105.
(234) Giese, T. J.; Audette, V. M.; York, D. M. *J. Chem. Phys.* **2003**, *119*, 2618−2622.
(235) Kamiya, M.; Tsuneda, T.; Hirao, K. A density functional study of van der Waals interactions. *J. Chem. Phys.* **2002**, *117*, 6010−6015.
(236) Tsuneda, T.; Suzumura, T.; Hirao, K. A new one-parameter progressive Colle-Salvetti-type correlation functional. *J. Chem. Phys.* **1999**, *110*, 10664−10678.
(237) Kar, R.; Song, J.-W.; Sato, T.; Hirao, K. Long-range corrected density functionals combined with local response dispersion: A promising method for weak interactions. *J. Comput. Chem.* **2013**, *34*, 2353−2359.
(238) Alves de Lima, N. Van der Waals density functional from multipole dispersion interactions. *J. Chem. Phys.* **2010**, *132*, 014110.
(239) Lundqvist, B. I.; Andersson, Y.; Shao, H.; Chan, S.; Langreth, D. Density functional theory including Van Der Waals forces. *Int. J. Quantum Chem.* **1995**, *56*, 247−255.
(240) Langreth, D.; Lundqvist, B. I.; Chakarova-Käck, S. D.; Cooper, V.; Dion, M.; Hyldgaard, P.; Kelkkanen, A.; Kleis, J.; Kong, L.; Li, S.; et al. A density functional for sparse matter. *J. Phys.: Condens. Matter* **2009**, *21*, 084203.
(241) Berland, K.; Cooper, V. R.; Lee, K.; Schröder, E.; Thonhauser, T.; Hyldgaard, P.; Lundqvist, B. I. van der Waals forces in density functional theory: a review of the vdW-DF method. *Rep. Prog. Phys.* **2015**, *78*, 066501.
(242) Zaremba, E.; Kohn, W. Van der Waals interaction between an atom and a solid surface. *Phys. Rev. B* **1976**, *13*, 2270.
(243) Rapcewicz, K.; Ashcroft, N. Fluctuation attraction in condensed matter: A nonlocal functional approach. *Phys. Rev. B: Condens. Matter Mater. Phys.* **1991**, *44*, 4032.
(244) Zangwill, A.; Soven, P. Density-functional approach to local-field effects in finite systems: Photoabsorption in the rare gases. *Phys. Rev. A: At., Mol., Opt. Phys.* **1980**, *21*, 1561.
(245) Andersson, Y.; Rydberg, H. Dispersion Coefficients for van der Waals Complexes, Including C_{60}−C_{60}. *Phys. Scr.* **1999**, *60*, 211.
(246) Gräfenstein, J.; Cremer, D. An efficient algorithm for the density-functional theory treatment of dispersion interactions. *J. Chem. Phys.* **2009**, *130*, 124105.
(247) Hult, E.; Rydberg, H.; Lundqvist, B. I.; Langreth, D. C. Unified treatment of asymptotic van der Waals forces. *Phys. Rev. B: Condens. Matter Mater. Phys.* **1999**, *59*, 4708.
(248) Rydberg, H.; Lundqvist, B. I.; Langreth, D. C.; Dion, M. Tractable nonlocal correlation density functionals for flat surfaces and slabs. *Phys. Rev. B: Condens. Matter Mater. Phys.* **2000**, *62*, 6997.
(249) Rydberg, H.; Dion, M.; Jacobson, N.; Schröder, E.; Hyldgaard, P.; Simak, S.; Langreth, D. C.; Lundqvist, B. I. Van der Waals Density Functional for Layered Structures. *Phys. Rev. Lett.* **2003**, *91*, 126402.

DOI: 10.1021/acs.chemrev.5b00533
Chem. Rev. XXXX, XXX, XXX−XXX

(250) Hyldgaard, P.; Berland, K.; Schröder, E. Interpretation of van der Waals density functionals. *Phys. Rev. B: Condens. Matter Mater. Phys.* **2014**, *90*, 075148.
(251) Dion, M.; Rydberg, H.; Schröder, E.; Langreth, D. C.; Lundqvist, B. I. Van der Waals Density Functional for General Geometries. *Phys. Rev. Lett.* **2004**, *92*, 246401.
(252) Dion, M.; Rydberg, H.; Schröder, E.; Langreth, D. C.; Lundqvist, B. I. Erratum: Van der Waals Density Functional for General Geometries [Phys. Rev. Lett. 92, 246401 (2004)]. *Phys. Rev. Lett.* **2005**, *95*, 109902.
(253) Thonhauser, T.; Cooper, V. R.; Li, S.; Puzder, A.; Hyldgaard, P.; Langreth, D. C. Van der Waals density functional: Self-consistent potential and the nature of the van der Waals bond. *Phys. Rev. B: Condens. Matter Mater. Phys.* **2007**, *76*, 125112.
(254) Vydrov, O. A.; Wu, Q.; Van Voorhis, T. Self-consistent implementation of a nonlocal van der Waals density functional with a Gaussian basis set. *J. Chem. Phys.* **2008**, *129*, 014106.
(255) Vydrov, O. A.; Van Voorhis, T. Benchmark Assessment of the Accuracy of Several Van der Waals Density Functionals. *J. Chem. Theory Comput.* **2012**, *8*, 1.
(256) Román-Pérez, G.; Soler, J. M. Efficient Implementation of a van der Waals Density Functional: Application to Double-Wall Carbon Nanotubes. *Phys. Rev. Lett.* **2009**, *103*, 096102.
(257) Gulans, A.; Puska, M. J.; Nieminen, R. M. Linear-scaling self-consistent implementation of the van der Waals density functional. *Phys. Rev. B: Condens. Matter Mater. Phys.* **2009**, *79*, 201105.
(258) Zhang, Y.; Yang, W. Comment on "Generalized Gradient Approximation Made Simple. *Phys. Rev. Lett.* **1998**, *80*, 890.
(259) Klimeš, J.; Bowler, D. R.; Michaelides, A. Chemical accuracy for the van der Waals density functional. *J. Phys.: Condens. Matter* **2010**, *22*, 022201.
(260) Murray, É D.; Lee, K.; Langreth, D. C. Investigation of Exchange Energy Density Functional Accuracy for Interacting Molecules. *J. Chem. Theory Comput.* **2009**, *5*, 2754−2762.
(261) Elliott, P.; Burke, K. Non-empirical derivation of the parameter in the B88 exchange functional. *Can. J. Chem.* **2009**, *87*, 1485−1491.
(262) Otero-de-la-Roza, A.; Johnson, E. R. A Benchmark for Non-Covalent Interactions in Solids. *J. Chem. Phys.* **2012**, *137*, 054103.
(263) Berland, K.; Hyldgaard, P. Exchange functional that tests the robustness of the plasmon description of the van der Waals density functional. *Phys. Rev. B: Condens. Matter Mater. Phys.* **2014**, *89*, 035412.
(264) Kresse, G.; Hafner, J. Ab initio molecular dynamics for liquid metals. *Phys. Rev. B: Condens. Matter Mater. Phys.* **1993**, *47*, 558.
(265) Kresse, G.; Furthmüller, J. Efficient iterative schemes for ab initio total-energy calculations using a plane-wave basis set. *Phys. Rev. B: Condens. Matter Mater. Phys.* **1996**, *54*, 11169.
(266) Kresse, G.; Furthmüller, J. Efficiency of ab-initio total energy calculations for metals and semiconductors using a plane-wave basis set. *Comput. Mater. Sci.* **1996**, *6*, 15.
(267) Giannozzi, P.; et al. QUANTUM ESPRESSO: a modular and open-source software project for quantum simulations of materials. *J. Phys.: Condens. Matter* **2009**, *21*, 395502.
(268) Soler, J. M.; Artacho, E.; Gale, J. D.; García, A.; Junquera, J.; Ordejón, P.; Sánchez-Portal, D. The SIESTA method for ab initio order-N materials simulation. *J. Phys.: Condens. Matter* **2002**, *14*, 2745.
(269) Shao, Y.; et al. Advances in methods and algorithms in a modern quantum chemistry program package. *Phys. Chem. Chem. Phys.* **2006**, *8*, 3172−3191.
(270) Vydrov, O. A.; Van Voorhis, T. Nonlocal van der Waals Density Functional Made Simple. *Phys. Rev. Lett.* **2009**, *103*, 063004.
(271) Langreth, D. C.; Lundqvist, B. I. Comment on "Nonlocal Van Der Waals Density Functional Made Simple. *Phys. Rev. Lett.* **2010**, *104*, 099303.
(272) Vydrov, O. A.; Van Voorhis, T. Vydrov and Van Voorhis Reply. *Phys. Rev. Lett.* **2010**, *104*, 099304.
(273) Vydrov, O. A.; Van Voorhis, T. Dispersion interactions from a local polarizability model. *Phys. Rev. A: At., Mol., Opt. Phys.* **2010**, *81*, 062708.
(274) Hujo, W.; Grimme, S. Performance of the van der Waals Density Functional VV10 and (hybrid)GGA Variants for Thermochemistry and Noncovalent Interactions. *J. Chem. Theory Comput.* **2011**, *7*, 3866−3871.
(275) Jurečka, P.; Šponer, J.; Černý, J.; Hobza, P. Benchmark database of accurate (MP2 and CCSD(T) complete basis set limit) interaction energies of small model complexes, DNA base pairs, and amino acid pairs. *Phys. Chem. Chem. Phys.* **2006**, *8*, 1985−1993.
(276) Řezáč, J.; Riley, K. E.; Hobza, P. S66: A Well-balanced Database of Benchmark Interaction Energies Relevant to Biomolecular Structures. *J. Chem. Theory Comput.* **2011**, *7*, 2427−2438.
(277) Aragó, J.; Ortí, E.; Sancho-García, J. C. Nonlocal van der Waals Approach Merged with Double-Hybrid Density Functionals: Toward the Accurate Treatment of Noncovalent Interactions. *J. Chem. Theory Comput.* **2013**, *9*, 3437−3443.
(278) Tran, F.; Hutter, J. Nonlocal van der Waals functionals: The case of rare-gas dimers and solids. *J. Chem. Phys.* **2013**, *138*, 204103.
(279) Björkman, T.; Gulans, A.; Krasheninnikov, A. V.; Nieminen, R. M. van der Waals Bonding in Layered Compounds from Advanced Density-Functional First-Principles Calculations. *Phys. Rev. Lett.* **2012**, *108*, 235502.
(280) Björkman, T.; Gulans, A.; Krasheninnikov, A.; Nieminen, R. Are we van der Waals ready? *J. Phys.: Condens. Matter* **2012**, *24*, 424218.
(281) Björkman, T. van der Waals density functional for solids. *Phys. Rev. B: Condens. Matter Mater. Phys.* **2012**, *86*, 165109.
(282) Hujo, W.; Grimme, S. Comparison of the performance of dispersion-corrected density functional theory for weak hydrogen bonds. *Phys. Chem. Chem. Phys.* **2011**, *13*, 13942−13950.
(283) Goerigk, L.; Grimme, S. Efficient and Accurate Double-Hybrid-Meta-GGA Density Functionals-Evaluation with the Extended GMTKN30 Database for General Main Group Thermochemistry, Kinetics, and Noncovalent Interactions. *J. Chem. Theory Comput.* **2011**, *7*, 291−309.
(284) Zhao, Y.; Truhlar, D. G. Design of Density Functionals That Are Broadly Accurate for Thermochemistry, Thermochemical Kinetics, and Nonbonded Interactions. *J. Phys. Chem. A* **2005**, *109*, 5656−5667.
(285) Sperger, T.; Sanhueza, I. A.; Kalvet, I.; Schoenebeck, F. Computational Studies of Synthetically Relevant Homogeneous Organometallic Catalysis Involving Ni, Pd, Ir, and Rh: An Overview of Commonly Employed DFT Methods and Mechanistic Insights. *Chem. Rev.* **2015**, *115*, 9532−9586.
(286) Petrović, P.; Djukic, J.-P.; Hansen, A.; Bannwarth, C.; Grimme, S. Non-covalent stabilization in transition metal coordination and organometallic complexes. In *Non-covalent Interactions in Synthesis and Design of New Compounds*; Maharromov, A. M., Mahmudov, K. T., Kopylovich, M. N., Eds.; Wiley-VCH: Weinheim, Germany, 2016; Chapter 7, ISBN 9781119109891, in press.
(287) Vydrov, O. A.; Van Voorhis, T. Implementation and assessment of a simple nonlocal van der Waals density functional. *J. Chem. Phys.* **2010**, *132*, 164113.
(288) Neese, F. The ORCA program system. *WIREs Comput. Mol. Sci.* **2012**, *2*, 73−78.
(289) Furche, F.; Ahlrichs, R.; Hättig, C.; Klopper, W.; Sierka, M.; Weigend, F. Turbomole. *WIREs Comput. Mol. Sci.* **2014**, *4*, 91−100.
(290) Feynman, R. P. Forces in Molecules. *Phys. Rev.* **1939**, *56*, 340−343.
(291) Hunt, K. L. C. Dispersion dipoles and dispersion forces: Proof of Feynman's "conjecture" and generalization to interacting molecules of arbitrary symmetry. *J. Chem. Phys.* **1990**, *92*, 1180−1187.
(292) Odbadrakh, T. T.; Jordan, K. D. Dispersion dipoles for coupled Drude oscillators. *J. Chem. Phys.* **2016**, *144*, 034111.
(293) von Lilienfeld, O. A.; Tavernelli, I.; Röthlisberger, U.; Sebastiani, D. Optimization of Effective Atom Centered Potentials for London Dispersion Forces in Density Functional Theory. *Phys. Rev. Lett.* **2004**, *93*, 153004.
(294) von Lilienfeld, O. A.; Tavernelli, I.; Rothlisberger, U.; Sebastiani, D. Performance of optimized atom-centered potentials for weakly bonded systems using density functional theory. *Phys. Rev. B: Condens. Matter Mater. Phys.* **2005**, *71*, 195119.

DOI: 10.1021/acs.chemrev.5b00533
Chem. Rev. XXXX, XXX, XXX−XXX

(295) Tapavicza, E.; Lin, I.-C.; von Lilienfeld, O. A.; Tavernelli, I.; Coutinho-Neto, M. D.; Rothlisberger, U. Weakly Bonded Complexes of Aliphatic and Aromatic Carbon Compounds Described with Dispersion Corrected Density Functional Theory. *J. Chem. Theory Comput.* **2007**, *3*, 1673−1679.
(296) Lin, I.-C.; von Lilienfeld, O. A.; Coutinho-Neto, M. D.; Tavernelli, I.; Rothlisberger, U. Predicting Noncovalent Interactions between Aromatic Biomolecules with London-Dispersion-Corrected DFT. *J. Phys. Chem. B* **2007**, *111*, 14346−14354.
(297) Arey, J. S.; Aeberhard, P. C.; Lin, I.-C.; Rothlisberger, U. Hydrogen Bonding Described Using Dispersion-Corrected Density Functional Theory. *J. Phys. Chem. B* **2009**, *113*, 4726−4732.
(298) Tkatchenko, A.; von Lilienfeld, O. A. Adsorption of Ar on graphite using London dispersion forces corrected Kohn-Sham density functional theory. *Phys. Rev. B: Condens. Matter Mater. Phys.* **2006**, *73*, 153406.
(299) Sun, Y. Y.; Kim, Y.-H.; Lee, K.; Zhang, S. B. Accurate and efficient calculation of van der Waals interactions within density functional theory by local atomic potential approach. *J. Chem. Phys.* **2008**, *129*, 154102.
(300) Mackie, I. D.; DiLabio, G. A. Accurate dispersion interactions from standard density-functional theory methods with small basis sets. *Phys. Chem. Chem. Phys.* **2010**, *12*, 6092−8.
(301) Torres, E.; DiLabio, G. A. A (Nearly) Universally Applicable Method for Modeling Noncovalent Interactions Using B3LYP. *J. Phys. Chem. Lett.* **2012**, *3*, 1738−1744.
(302) DiLabio, G. A.; Koleini, M.; Torres, E. Extension of the B3LYP-dispersion-correcting potential approach to the accurate treatment of both inter- and intra-molecular interactions. *Theor. Chem. Acc.* **2013**, *132*, 1389.
(303) van Santen, J. A.; DiLabio, G. A. Dispersion Corrections Improve the Accuracy of Both Noncovalent and Covalent Interactions Energies Predicted by a Density-Functional Theory Approximation. *J. Phys. Chem. A* **2015**, *119*, 6703−6713.
(304) Andrae, D.; Häußermann, U.; Dolg, M.; Stoll, H.; Preuss, H. Energy-adjusted ab initio pseudopotentials for the second and third row transition elements. *Theor. Chim. Acta* **1990**, *77*, 123−141.
(305) Peterson, K. A.; Figgen, D.; Goll, E.; Stoll, H.; Dolg, M. Systematically convergent basis sets with relativistic pseudopotentials. II. Small-core pseudopotentials and correlation consistent basis sets for the post-*d* group 16−18 elements. *J. Chem. Phys.* **2003**, *119*, 11113−11123.
(306) Perdew, J. P.; Zunger, A. Self-interaction correction to density-functional approximations for many-electron systems. *Phys. Rev. B: Condens. Matter Mater. Phys.* **1981**, *23*, 5048−5079.
(307) Baumeier, B.; Krüger, P.; Pollmann, J. Self-interaction-corrected pseudopotentials for silicon carbide. *Phys. Rev. B: Condens. Matter Mater. Phys.* **2006**, *73*, 195205.
(308) Segev, D.; Janotti, A.; Van de Walle, C. G. Self-consistent band-gap corrections in density functional theory using modified pseudopotentials. *Phys. Rev. B: Condens. Matter Mater. Phys.* **2007**, *75*, 035201.
(309) Lin, I.-C.; Coutinho-Neto, M. D.; Felsenheimer, C.; von Lilienfeld, O. A.; Tavernelli, I.; Rothlisberger, U. Library of dispersion-corrected atom-centered potentials for generalized gradient approximation functionals: Elements H, C, N, O, He, Ne, Ar, and Kr. *Phys. Rev. B: Condens. Matter Mater. Phys.* **2007**, *75*, 205131.
(310) Aeberhard, P. C.; Arey, J. S.; Lin, I.-C.; Rothlisberger, U. Accurate DFT Descriptions for Weak Interactions of Molecules Containing Sulfur. *J. Chem. Theory Comput.* **2009**, *5*, 23−28.
(311) Almbladh, C.-O.; von Barth, U. Exact results for the charge and spin densities, exchange-correlation potentials, and density-functional eigenvalues. *Phys. Rev. B: Condens. Matter Mater. Phys.* **1985**, *31*, 3231−3244.
(312) Katriel, J.; Davidson, E. R. Asymptotic behavior of atomic and molecular wave functions. *Proc. Natl. Acad. Sci. U. S. A.* **1980**, *77*, 4403−4406.
(313) Goerigk, L.; Kruse, H.; Grimme, S. Benchmarking Density Functional Methods against the S66 and S66 × 8 Datasets for Non-Covalent Interactions. *ChemPhysChem* **2011**, *12*, 3421−3433.
(314) Xu, X.; Goddard, W. A. The X3LYP extended density functional for accurate descriptions of nonbond interactions, spin states, and thermochemical properties. *Proc. Natl. Acad. Sci. U. S. A.* **2004**, *101*, 2673−2677.
(315) Xu, X.; Goddard, W. A. Bonding Properties of the Water Dimer: A Comparative Study of Density Functional Theories. *J. Phys. Chem. A* **2004**, *108*, 2305−2313.
(316) Černý, J.; Hobza, P. The X3LYP extended density functional accurately describes H- bonding but fails completely for stacking. *Phys. Chem. Chem. Phys.* **2005**, *7*, 1624−1626.
(317) Walsh, T. R. Exact exchange and Wilson−Levy correlation: a pragmatic device for studying complex weakly-bonded systems. *Phys. Chem. Chem. Phys.* **2005**, *7*, 443−451.
(318) Tao, J.; Perdew, J. P.; Staroverov, V. N.; Scuseria, G. E. Climbing the Density Functional Ladder: Nonempirical Meta Generalized Gradient Approximation Designed for Molecules and Solids. *Phys. Rev. Lett.* **2003**, *91*, 146401.
(319) Staroverov, V. N.; Scuseria, G. E.; Tao, J.; Perdew, J. P. Comparative assessment of a new nonempirical density functional: Molecules and hydrogen-bonded complexes. *J. Chem. Phys.* **2003**, *119*, 12129−12137.
(320) Ruzsinszky, A.; Perdew, J. P.; Csonka, G. I. Binding Energy Curves from Nonempirical Density Functionals II. van der Waals Bonds in Rare-Gas and Alkaline-Earth Diatomics. *J. Phys. Chem. A* **2005**, *109*, 11015−11021.
(321) Adamo, C.; Barone, V. Exchange functionals with improved long-range behavior and adiabatic connection methods without adjustable parameters: The mPW and mPW1PW models. *J. Chem. Phys.* **1998**, *108*, 664−675.
(322) Cohen, A. J.; Handy, N. C. Assessment of exchange correlation functionals. *Chem. Phys. Lett.* **2000**, *316*, 160−166.
(323) Boese, A. D.; Doltsinis, N. L.; Handy, N. C.; Sprik, M. New generalized gradient approximation functionals. *J. Chem. Phys.* **2000**, *112*, 1670−1678.
(324) Paverati, R.; Truhlar, D. G. The quest for a universal density functional: The accuracy of density functionals across a braod spectrum of databases in chemistry and physics. *Philos. Trans. R. Soc., A* **2013**, *327*, 20120476/1−51.
(325) Zhao, Y.; Schultz, N. E.; Truhlar, D. Exchange-Correlation Functional with Broad Accuracy for Metallic and Nonmetallic Compounds, Kinetics, and Noncovalent Interactions. *J. Chem. Phys.* **2005**, *123*, 161103.
(326) Zhao, Y.; Schultz, N. E.; Truhlar, D. G. Design of Density Functionals by Combining the Method of Constraint Satisfaction with Parametrization for Thermochemistry, Thermochemical Kinetics, and Noncovalent Interactions. *J. Chem. Theory Comput.* **2006**, *2*, 364−382.
(327) Zhao, Y.; Truhlar, D. G. Comparative DFT Study of van der Waals Complexes: Rare-Gas Dimers, Alkaline-Earth Dimers, Zinc Dimer, and Zinc-Rare-Gas Dimers. *J. Phys. Chem. A* **2006**, *110*, 5121.
(328) Becke, A. D. Simulation of Delocalized Exchange by Local Density Functionals. *J. Chem. Phys.* **2000**, *112*, 4020.
(329) Boese, A. D.; Martin, J. M. L. Development of density functionals for thermochemical kinetics. *J. Chem. Phys.* **2004**, *121*, 3405−3416.
(330) Becke, A. D. Density-functional thermochemistry. IV. A new dynamical correlation functional and implications for exact-exchange mixing. *J. Chem. Phys.* **1996**, *104*, 1040−1046.
(331) Zhao, Y.; Truhlar, D. G. A New Local Density Functional for Main-Group Thermochemistry, Transition Metal Bonding, Thermochemical Kinetics, and Noncovalent Interactions. *J. Chem. Phys.* **2006**, *125*, 194101.
(332) Zhao, Y.; Truhlar, D. G. The M06 Suite of Density Functionals for Main Group Thermochemistry, Thermochemical Kinetics, Noncovalent Interactions, Excited States, and Transition Elements: Two New Functionals and Systematic Testing of Four M06-Class Functionals and 12 Other Functionals. *Theor. Chem. Acc.* **2008**, *120*, 215.

DOI: 10.1021/acs.chemrev.5b00533
Chem. Rev. XXXX, XXX, XXX−XXX

(333) Zhao, Y.; Truhlar, D. G. Density Functional for Spectroscopy: no Long-Range Self-Interaction Error, Good Performance for Rydberg and Charge-Transfer States, and Better Performance on Average than B3LYP for Ground States. *J. Phys. Chem. A* **2006**, *110*, 13126.
(334) Van Voorhis, T.; Scuseria, G. E. A Novel Form for the Exchange-Correlation Energy Functional. *J. Chem. Phys.* **1998**, *109*, 400.
(335) Zhao, Y.; Truhlar, D. G. Exploring the Limit of Accuracy of the Global Hybrid Meta Density Functional for Main-Group Thermochemistry, Kinetics, and Noncovalent In- teractions. *J. Chem. Theory Comput.* **2008**, *4*, 1849.
(336) Peverati, R.; Truhlar, D. G. Improving the Accuracy of Hybrid Meta-GGA Density Functionals by Range Separation. *J. Phys. Chem. Lett.* **2011**, *2*, 2810.
(337) Peverati, R.; Truhlar, D. G. M11-L: A Local Density Functional That Provides Improved Accuracy for Electronic Structure Calculations in Chemistry and Physics. *J. Phys. Chem. Lett.* **2012**, *3*, 117.
(338) Peverati, R.; Truhlar, D. G. An Improved and Broadly Accurate Local Approximation to the Exchange Correlation Density Functional: The MN12-L Functional for Electronic Structure Calculations in Chemistry and Physics. *Phys. Chem. Chem. Phys.* **2012**, *14*, 13171.
(339) Peverati, R.; Truhlar, D. G. Exchange Correlation Functional with Good Accuracy for Both Structural and Energetic Properties while Depending Only on the Density and Its Gradient. *J. Chem. Theory Comput.* **2012**, *8*, 2310.
(340) Peverati, R.; Truhlar, D. G. Screened-Exchange Density Functionals with Broad Accuracy for Chemistry and Solid-State Physics. *Phys. Chem. Chem. Phys.* **2012**, *14*, 16187.
(341) Hammer, B.; Hansen, L. B.; Nørskov, J. K. Improved adsorption energetics within density-functional theory using revised Perdew-Burke-Ernzerhof functionals. *Phys. Rev. B: Condens. Matter Mater. Phys.* **1999**, *59*, 7413−7421.
(342) Goerigk, L.; Grimme, S. A General Database for Main Group Thermochemistry, Ki- netics, and Noncovalent Interactions - Assessment of Common and Reparameterized (meta-)GGA Density Functionals. *J. Chem. Theory Comput.* **2010**, *6*, 107−126.
(343) Kümmel, S.; Kronik, L. Orbital-dependent density functionals: Theory and applications. *Rev. Mod. Phys.* **2008**, *80*, 3−60.
(344) Arbuznikov, A. V.; Kaupp, M. The self-consistent implementation of exchange-correlation functionals depending on the local kinetic energy density. *Chem. Phys. Lett.* **2003**, *381*, 495−504.
(345) Mardirossian, N.; Head-Gordon, M. Characterizing and Understanding the Remarkably Slow Basis Set Convergence of Several Minnesota Density Functionals for Intermolecular Interaction Energies. *J. Chem. Theory Comput.* **2013**, *9*, 4453−4461.
(346) Johnson, E. R.; Mackie, I. D.; DiLabio, G. A. Dispersion Interactions in Density-Functional Theory. *J. Phys. Org. Chem.* **2009**, *22*, 1127.
(347) Goerigk, L. Treating London-Dispersion Effects with the Latest Minnesota Density Functionals: Problems and Possible Solutions. *J. Phys. Chem. Lett.* **2015**, *6*, 3891−3896.
(348) Sun, J.; Ruzsinszky, A.; Perdew, J. P. Strongly Constrained and Appropriately Normed Semilocal Density Functional. *Phys. Rev. Lett.* **2015**, *115*, 036402.
(349) Grimme, S. Comment on:"On the accuracy of DFT methods in reproducing ligand substitution energies for transition metal complexes in solution: the role of dispersive interactions" by H. Jacobsen and L. Cavallo. *ChemPhysChem* **2012**, *13*, 1407−1409.
(350) Kruse, H.; Goerigk, L.; Grimme, S. Why the Standard B3LYP/6-31G* Model Chemistry Should Not Be Used in DFT Calculations of Molecular Thermochemistry: Understanding and Correcting the Problem. *J. Org. Chem.* **2012**, *77*, 10824−10834.
(351) Grimme, S.; Brandenburg, J. G.; Bannwarth, C.; Hansen, A. Consistent structures and interactions by density functional theory with small atomic orbital basis sets. *J. Chem. Phys.* **2015**, *143*, 054107.
(352) Sure, R.; Brandenburg, J. G.; Grimme, S. Small Atomic Orbital Basis Set First-Principles Quantum Chemical Methods for Large Molecular and Periodic Systems: A Critical Analysis of Error Sources. *ChemistryOpen* **2015**, DOI: 10.1002/open.201500192.
(353) Sato, T.; Tsuneda, T.; Hirao, K. A density-functional study on π-aromatic interaction: Benzene dimer and naphthalene dimer. *J. Chem. Phys.* **2005**, *123*, 104307.
(354) Chai, J.-D.; Head-Gordon, M. Systematic optimization of long-range corrected hybrid density functionals. *J. Chem. Phys.* **2008**, *128*, 084106.
(355) Johnson, E. R.; Contreras-García, J.; Yang, W. Density-Functional Errors in Alkanes: A Real-Space Perspective. *J. Chem. Theory Comput.* **2012**, *8*, 2676−2681.
(356) Lin, Y.-S.; Li, G.-D.; Mao, S.-P.; Chai, J.-D. Long-Range Corrected Hybrid Density Functionals with Improved Dispersion Corrections. *J. Chem. Theory Comput.* **2013**, *9*, 263−272.
(357) Mardirossian, N.; Head-Gordon, M. ωB97X-V: A 10-parameter, range-separated hybrid, generalized gradient approximation density functional with nonlocal correlation, designed by a survival-of-the-fittest strategy. *Phys. Chem. Chem. Phys.* **2014**, *16*, 9904−9924.
(358) Tsuneda, T.; Hirao, K. Long-range correction for density functional theory. *WIREs Comput. Mol. Sci.* **2014**, *4*, 375−390.
(359) Jacob, C. R.; Neugebauer, J. Subsystem density-functional theory. *WIREs Comput. Mol. Sci.* **2014**, *4*, 325−362.
(360) Wesołowski, T. A.; Ellinger, Y.; Weber, J. Density functional theory with an approximate kinetic energy functional applied to study structure and stability of weak van der Waals complexes. *J. Chem. Phys.* **1998**, *108*, 6078−6083.
(361) Wesołowski, T. A.; Morgantini, P.-Y.; Weber, J. Intermolecular interaction energies from the total energy bifunctional: A case study of carbazole complexes. *J. Chem. Phys.* **2002**, *116*, 6411−6421.
(362) Schlüns, D.; Klahr, K.; Mück-Lichtenfeld, C.; Visscher, L.; Neugebauer, J. Subsystem-DFT potential-energy curves for weakly interacting systems. *Phys. Chem. Chem. Phys.* **2015**, *17*, 14323−14341.
(363) Klamt, A. The COSMO and COSMO-RS solvation models. *WIREs Comput. Mol. Sci.* **2011**, *1*, 699−709.
(364) Ewald, P. P. Die Berechnung optischer und elektrostatischer Gitterpotentiale. *Ann. Phys.* **1921**, *369*, 253−287.
(365) Darden, T.; York, D.; Pedersen, L. Particle mesh Ewald: An N log(N) method for Ewald sums in large systems. *J. Chem. Phys.* **1993**, *98*, 10089−10092.
(366) York, D. M.; Darden, T. A.; Pedersen, L. G. The effect of long-range electrostatic interactions in simulations of macromolecular crystals: A comparison of the Ewald and truncated list methods. *J. Chem. Phys.* **1993**, *99*, 8345−8348.
(367) Essmann, U.; Perera, L.; Berkowitz, M. L.; Darden, T.; Lee, H.; Pedersen, L. G. A smooth particle mesh Ewald method. *J. Chem. Phys.* **1995**, *103*, 8577−8593.
(368) Dovesi, R.; Orlando, R.; Erba, A.; Zicovich-Wilson, C. M.; Civalleri, B.; Casassa, S.; Maschio, L.; Ferrabone, M.; De La Pierre, M.; D'Arco, P.; Noël, Y.; Causá, M.; Rérat, M.; Kirtman, B. CRYSTAL14: A program for the ab initio investigation of crystalline solids. *Int. J. Quantum Chem.* **2014**, *114*, 1287−1317.
(369) Frisch, M. J., et al. *Gaussian 09, Revision D.01*; Gaussian Inc.: Wallingford, CT, 2009.
(370) te Velde, G.; Baerends, E. J. Precise density-functional method for periodic structures. *Phys. Rev. B: Condens. Matter Mater. Phys.* **1991**, *44*, 7888−7903.
(371) Blum, V.; Gehrke, R.; Hanke, F.; Havu, P.; Havu, V.; Ren, X.; Reuter, K.; Scheffler, M. Ab initio molecular simulations with numeric atom-centered orbitals. *Comput. Phys. Commun.* **2009**, *180*, 2175−2196.
(372) Lippert, G.; Hutter, J.; Parrinello, M. A hybrid Gaussian and plane wave density functional scheme. *Mol. Phys.* **1997**, *92*, 477−488.
(373) Thiel, W. Semiempirical quantum−chemical methods. *WIREs Comput. Mol. Sci.* **2014**, *4*, 145−157.
(374) Elstner, M.; Seifert, G. Density functional tight binding. *Philos. Trans. R. Soc., A* **2014**, *372*, 20120483.
(375) Yilmazer, N. D.; Korth, M. Enhanced semiempirical QM methods for biomolecular interactions. *Comput. Struct. Biotechnol. J.* **2015**, *13*, 169−175.
(376) Korth, M.; Pitoňák, M.; Řezáč, J.; Hobza, P. A Transferable H-Bonding Correction for Semiempirical Quantum-Chemical Methods. *J. Chem. Theory Comput.* **2010**, *6*, 344−352.

DOI: 10.1021/acs.chemrev.5b00533
Chem. Rev. XXXX, XXX, XXX−XXX

(377) Korth, M. Third-Generation Hydrogen-Bonding Corrections for Semiempirical QM Methods and Force Fields. *J. Chem. Theory Comput.* **2010**, *6*, 3808−3816.
(378) Stewart, J. Optimization of parameters for semiempirical methods VI: more modifications to the NDDO approximations and re-optimization of parameters. *J. Mol. Model.* **2013**, *19*, 1−32.
(379) Řezáč, J.; Hobza, P. Advanced Corrections of Hydrogen Bonding and Dispersion for Semiempirical Quantum Chemical Methods. *J. Chem. Theory Comput.* **2012**, *8*, 141−151.
(380) Bučko, T.; Lebégue, S.; Hafner, J.; Ángyán, J. G. Tkatchenko-Scheffler van der Waals correction method with and without self-consistent screening applied to solids. *Phys. Rev. B: Condens. Matter Mater. Phys.* **2013**, *87*, 064110.
(381) Moellmann, J.; Grimme, S. DFT-D3 Study of Some Molecular Crystals. *J. Phys. Chem. C* **2014**, *118*, 7615−7621.
(382) Mori-Sánchez, P.; Cohen, A. J.; Yang, W. Localization and Delocalization Errors in Density Functional Theory and Implications for Band-Gap Prediction. *Phys. Rev. Lett.* **2008**, *100*, 146401.
(383) Hostaš, J.; Řezáč, J.; Hobza, P. On the Performance of the Semiempirical Quantum Mechanical PM6 and PM7 methods for Noncovalent Interactions. *Chem. Phys. Lett.* **2013**, *568-569*, 161−166.
(384) Goerigk, L.; Grimme, S. Double-hybrid density functionals. *WIREs Comput. Mol. Sci.* **2014**, *4*, 576−600.
(385) Kennedy, M. R.; McDonald, A. R.; DePrince, A. E.; Marshall, M. S.; Podeszwa, R.; Sherrill, C. D. Communication: Resolving the Three-Body Contribution to the Lattice Energy of Crystalline Benzene: Benchmark Results from Coupled-Cluster Theory. *J. Chem. Phys.* **2014**, *140*, 121104.
(386) Gillan, M. J.; Alfé, D.; Bygrave, P. J.; Taylor, C. R.; Manby, F. R. Energy Benchmarks for Water Clusters and Ice Structures from an Embedded Many-Body Expansion. *J. Chem. Phys.* **2013**, *139*, 114101.
(387) Krishtal, A.; Vannomeslaeghe, K.; Geldof, D.; Van Alsenoy, C.; Geerlings, P. Importance of anisotropy in the evaluation of dispersion interactions. *Phys. Rev. A: At., Mol., Opt. Phys.* **2011**, *83*, 024501.
(388) The calculations have been conducted in the group of S. Grimme. Because of insufficient accuracy gain, the results were not published but may nevertheless be interesting for the chemical community.
(389) Xu, P.; Zahariev, F.; Gordon, M. S. The R^{-7} Dispersion Interaction in the General Effective Fragment Potential Method. *J. Chem. Theory Comput.* **2014**, *10*, 1576−1587.
(390) Guidez, E. B.; Xu, P.; Gordon, M. S. Derivation and Implementation of the Gradient of the R^{7} Dispersion Interaction in the Effective Fragment Potential Method. *J. Phys. Chem. A* **2016**, *120*, 639−647.
(391) Grimme, S. Seemingly Simple Stereoelectronic Effects in Alkane Isomers and the Implications for Kohn-Sham Density Functional Theory. *Angew. Chem., Int. Ed.* **2006**, *45*, 4460−4464.
(392) Schreiner, P. R.; Fokin, A. A.; Pascal, R. A.; de Meijere, A. Many Density Functional Theory Approaches Fail To Give Reliable Large Hydrocarbon Isomer Energy Differences. *Org. Lett.* **2006**, *8*, 3635−3638.
(393) Schreiner, P. R. Relative Energy Computations with Approximate Density Functional Theory-A Caveat! *Angew. Chem., Int. Ed.* **2007**, *46*, 4217−4219.
(394) Grimme, S. *n*-Alkane Isodesmic Reaction Energy Errors in Density Functional Theory Are Due to Electron Correlation Effects. *Org. Lett.* **2010**, *12*, 4670−4673.
(395) Kruse, H.; Mladek, A.; Gkionis, K.; Hansen, A.; Grimme, S.; Sponer, J. Quantum Chemical Benchmark Study on 46 RNA Backbone Families Using a Dinucleotide Unit. *J. Chem. Theory Comput.* **2015**, *11*, 4972−4991.
(396) Bannwarth, C.; Hansen, A.; Grimme, S. The Association of Two "Frustrated" Lewis Pairs by State-of-the-Art Quantum Chemical Methods. *Isr. J. Chem.* **2015**, *55*, 235−242.
(397) Grimme, S.; Kruse, H.; Goerigk, L.; Erker, G. The mechanism of dihydrogen activation by frustrated Lewis pairs revisited. *Angew. Chem., Int. Ed.* **2010**, *49*, 1402−1405.
(398) Weigend, F.; Furche, F.; Ahlrichs, R. Gaussian basis sets of quadruple zeta quality for atoms H to Kr. *J. Chem. Phys.* **2003**, *119*, 12753−12762.
(399) Weigend, F.; Ahlrichs, R. Balanced basis sets of split valence, triple zeta valence and quadruple zeta valence quality for H to Rn: Design and assessment of accuracy. *Phys. Chem. Chem. Phys.* **2005**, *7*, 3297−3305.
(400) Jiang, J.; Wu, Y.; Wang, Z.-X.; Wu, C. Assessing the Performance of Popular Quantum Mechanics and Molecular Mechanics Methods and Revealing the Sequence-Dependent Energetic Features Using 100 Tetrapeptide Models. *J. Chem. Theory Comput.* **2010**, *6*, 1199−1209.
(401) Goerigk, L.; Karton, A.; Martin, J. M. L.; Radom, L. Accurate quantum chemical energies for tetrapeptide conformations: why MP2 data with an insufficient basis set should be handled with caution. *Phys. Chem. Chem. Phys.* **2013**, *15*, 7028−7031.
(402) Price, S. L. Predicting Crystal Structures of Organic Compounds. *Chem. Soc. Rev.* **2014**, *43*, 2098−2111.
(403) Neumann, M. A.; Leusen, F. J. J.; Kendrick, J. A major advance in crystal structure prediction. *Angew. Chem., Int. Ed.* **2008**, *47*, 2427−2430.
(404) Pantelides, C. C.; Adjiman, C. S.; Kazantsev, A. V. General Computational Algorithms for Ab Initio Crystal Structure Prediction for Organic Molecules. *Top. Curr. Chem.* **2014**, *345*, 25−58.
(405) Block, S.; Weir, C. E.; Piermarini, G. J. Polymorphism in Benzene, Naphthalene, and Anthracene at High Pressure. *Science* **1970**, *169*, 586−587.
(406) van Eijck, B. P.; Spek, A. L.; Mooij, W. T. M.; Kroon, J. Hypothetical Crystal Structures of Benzene at 0 and 30 kbar. *Acta Crystallogr., Sect. B: Struct. Sci.* **1998**, *54*, 291−299.
(407) Schweizer, W. B.; Dunitz, J. D. Quantum Mechanical Calculations for Benzene Dimer Energies: Present Problems and Future Challenges. *J. Chem. Theory Comput.* **2006**, *2*, 288−291.
(408) Ringer, A.; Sherrill, C. First Principles Computation of Lattice Energies of Organic Solids: The Benzene Crystal. *Chem. - Eur. J.* **2008**, *14*, 2542−2547.
(409) Bludský, O.; Rubeš, M.; Soldán, P. *Ab initio* investigation of intermolecular interactions in solid benzene. *Phys. Rev. B: Condens. Matter Mater. Phys.* **2008**, *77*, 092103.
(410) Wen, S.; Beran, G. J. O. Accurate Molecular Crystal Lattice Energies from a Fragment QM/MM Approach with On-the-Fly Ab Initio Force Field Parametrization. *J. Chem. Theory Comput.* **2011**, *7*, 3733−3742.
(411) Podeszwa, R.; Rice, B. M.; Szalewicz, K. Predicting Structure of Molecular Crystals from First Principles. *Phys. Rev. Lett.* **2008**, *101*, 115503.
(412) Carter, D. J.; Rohl, A. L. Benchmarking Calculated Lattice Parameters and Energies of Molecular Crystals Using van der Waals Density Functionals. *J. Chem. Theory Comput.* **2014**, *10*, 3423−3437.
(413) Beran, G. J. O.; Nanda, K. Predicting Organic Crystal Lattice Energies with Chemical Accuracy. *J. Phys. Chem. Lett.* **2010**, *1*, 3480−3487.
(414) Brandenburg, J. G.; Alessio, M.; Civalleri, B.; Peintinger, M. F.; Bredow, T.; Grimme, S. Geometrical Correction for the Inter- and Intramolecular Basis Set Superposition Error in Periodic Density Functional Theory Calculations. *J. Phys. Chem. A* **2013**, *117*, 9282−9292.
(415) Raabe, G. The Use of Quantum-Chemical Semiempirical Methods to Calculate the Lattice Energies of Organic Molecular Crystals. *Z. Naturforsch., A: Phys. Sci.* **2004**, *59*, 609−614.
(416) Blöchl, P. E. Projector augmented-wave method. *Phys. Rev. B: Condens. Matter Mater. Phys.* **1994**, *50*, 17953.
(417) Kresse, G.; Joubert, J. From ultrasoft pseudopotentials to the projector augmented-wave method. *Phys. Rev. B: Condens. Matter Mater. Phys.* **1999**, *59*, 1758.
(418) Brandenburg, J. G.; Maas, T.; Grimme, S. Benchmarking DFT and Semiempirical Methods on Structures and Lattice Energies for Ten Ice Polymorphs. *J. Chem. Phys.* **2015**, *142*, 124104.
(419) Yang, J.; Hu, W.; Usvyat, D.; Matthews, D.; Schütz, M.; Chan, G. K.-L. Ab initio determination of the crystalline benzene lattice energy to sub-kilojoule/mol accuracy. *Science* **2014**, *345*, 640−643.

DOI: 10.1021/acs.chemrev.5b00533
Chem. Rev. XXXX, XXX, XXX−XXX

(420) Sorescu, D. C.; Byrd, E. F. C.; Rice, B. M.; Jordan, K. D. Assessing the Performances of Dispersion-Corrected Density Functional Methods for Predicting the Crystallographic Properties of High Nitrogen Energetic Salts. *J. Chem. Theory Comput.* **2014**, *10*, 4982−4994.
(421) Erba, A.; Maul, J.; Civalleri, B. Thermal properties of molecular crystals through dispersion-corrected quasi-harmonic ab initio calculations: the case of urea. *Chem. Commun.* **2016**, *52*, 1820−1823.
(422) Heit, Y. N.; Nanda, K. D.; Beran, G. J. O. Predicting finite-temperature properties of crystalline carbon dioxide from first principles with quantitative accuracy. *Chem. Sci.* **2016**, *7*, 246−255.
(423) The optimizations at the TPSS-D3 level and ZPVE and thermal correction at the DFTB3-D3 level have been conducted in the group of S. Grimme and compared to the ICSD entry 76418 and NIST entry 74-90-8.
(424) Witte, J.; Goldey, M.; Neaton, J. B.; Head-Gordon, M. Beyond Energies: Geometries of Nonbonded Molecular Complexes as Metrics for Assessing Electronic Structure Approaches. *J. Chem. Theory Comput.* **2015**, *11*, 1481−1492.
(425) Burow, A. M.; Bates, J. E.; Furche, F.; Eshuis, H. Analytical First-Order Molecular Properties and Forces within the Adiabatic Connection Random Phase Approximation. *J. Chem. Theory Comput.* **2014**, *10*, 180−194.
(426) Takatani, T.; Hohenstein, E. G.; Malagoli, M.; Marshall, M. S.; Sherrill, C. D. Basis set consistent revision of the S22 test set of noncovalent interaction energies. *J. Chem. Phys.* **2010**, *132*, 144104.
(427) Marshall, M. S.; Burns, L. A.; Sherrill, C. D. Basis set convergence of the coupled-cluster correction, $\delta_{MP2}^{CCSD(T)}$: Best practices for benchmarking non-covalent interactions and the attendant revision of the S22, NBC10, HBC6, and HSG databases. *J. Chem. Phys.* **2011**, *135*, 194102.
(428) Heßelmann, A.; Korona, T. Intermolecular symmetry-adapted perturbation theory study of large organic complexes. *J. Chem. Phys.* **2014**, *141*, 094107.
(429) Burkinshaw, P. M.; Mortimer, C. T. Enthalpies of sublimation of transition metal complexes. *J. Chem. Soc., Dalton Trans.* **1984**, 75−77.
(430) Goerigk, L. How Do DFT-DCP, DFT-NL, and DFT-D3 Compare for the Description of London-Dispersion Effects in Conformers and General Thermochemistry? *J. Chem. Theory Comput.* **2014**, *10*, 968−980.
(431) Antony, J.; Grimme, S. Is Spin-Component Scaled Second-Order Møller-Plesset Perturbation Theory an Appropriate Method for the Study of Noncovalent Interactions in Molecules? *J. Phys. Chem. A* **2007**, *111*, 4862−4868.
(432) Wen, S.; Beran, G. J. O. Accidental Degeneracy in Crystalline Aspirin: New Insights from High-Level ab Initio Calculations. *Cryst. Growth Des.* **2012**, *12*, 2169−2172.
(433) Marom, N.; DiStasio, R. A.; Atalla, V.; Levchenko, S.; Reilly, A. M.; Chelikowsky, J. R.; Leiserowitz, L.; Tkatchenko, A. Many-Body Dispersion Interactions in Molecular Crystal Polymorphism. *Angew. Chem., Int. Ed.* **2013**, *52*, 6629−6632.
(434) Reilly, A. M.; Tkatchenko, A. Role of Dispersion Interactions in the Polymorphism and Entropic Stabilization of the Aspirin Crystal. *Phys. Rev. Lett.* **2014**, *113*, 055701.
(435) Beran, G.; Wen, S.; Nanda, K.; Huang, Y.; Heit, Y. Accurate and Robust Molecular Crystal Modeling Using Fragment-Based Electronic Structure Methods. *Top. Curr. Chem.* **2013**, *345*, 59−93.
(436) See CCDC press release: https://www.ccdc.cam.ac.uk/News/List/post-43/ (Nov 2, 2015).
(437) Schweigert, I. V.; Lotrich, V. F.; Bartlett, R. J. *Ab initio* correlation functionals from second-order perturbation theory. *J. Chem. Phys.* **2006**, *125*, 104108.
(438) Ángyán, J. G.; Gerber, I. C.; Savin, A.; Toulouse, J. van der Waals forces in density functional theory: Perturbational long-range electron-interaction corrections. *Phys. Rev. A: At., Mol., Opt. Phys.* **2005**, *72*, 012510.

DOI: 10.1021/acs.chemrev.5b00533
Chem. Rev. XXXX, XXX, XXX−XXX